Status and prospects for rare B decays at Belle and Belle II

Gaetano de Marino*

Jozef Stefan Institute

on behalf of the Belle & Belle II collaborations

IP2I - LYON UNIVERSITY

May 29th, 2023

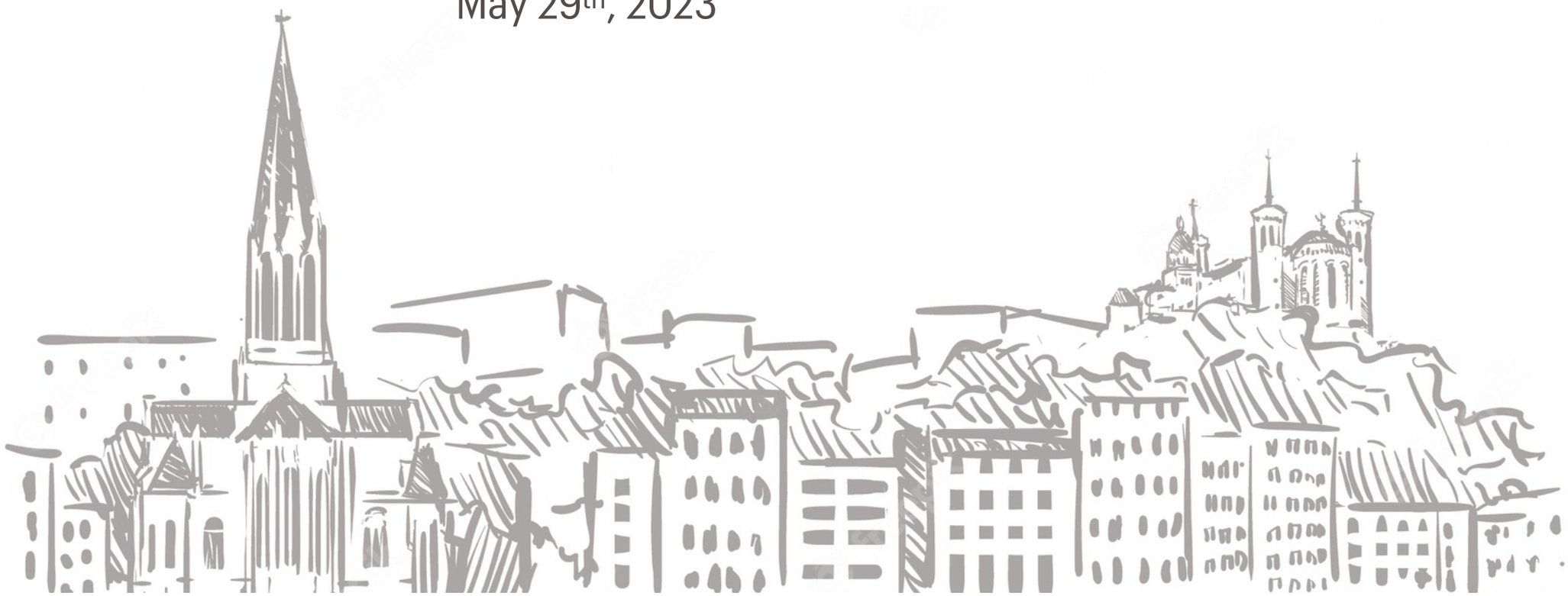

*gaetano.demarino@ijs.si

OUTLINE

Today's results are based on Belle dataset - 711 fb^{-1}@Υ(4S), 121 fb^{-1}@Υ(5S)
Belle II dataset - 63 fb^{-1}, 190 fb^{-1}@Υ(4S)

BF$_{SM}$

10^{-4} **Radiative -** not so rare

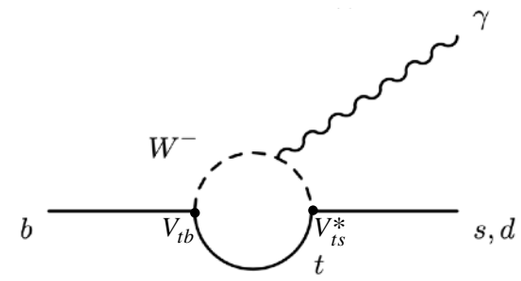

$10^{-7 \div -5}$ **Semileptonic -** rare

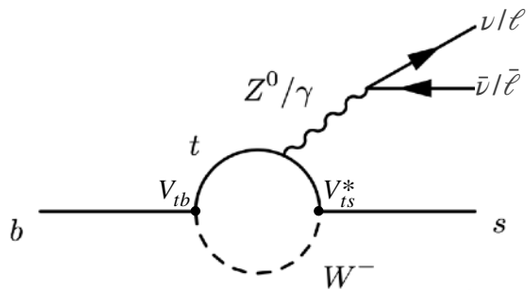

10^{-50} **LFV -** ultra rare!

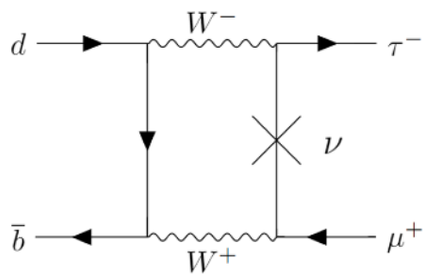

Suppression sources

CKM λ^2

GIM m_t, m_c, m_u

m_{ν_i}

Look for alterations/enhancements in FCNC due to BSM contributions

New interactions at 🌳 level

Weaker GIM cancellations due to new particles in 🔁 corrections

Different sensitivity to NP

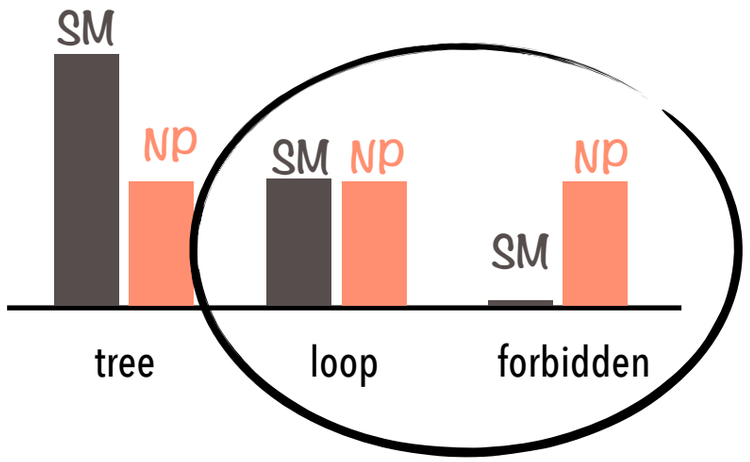

THE BELLE&BELLE II EXPERIMENTS

☞ talk on June 1st (4:50 p.m. @ Amphi Dirac)
"Future of Belle II" (J. Baudot)

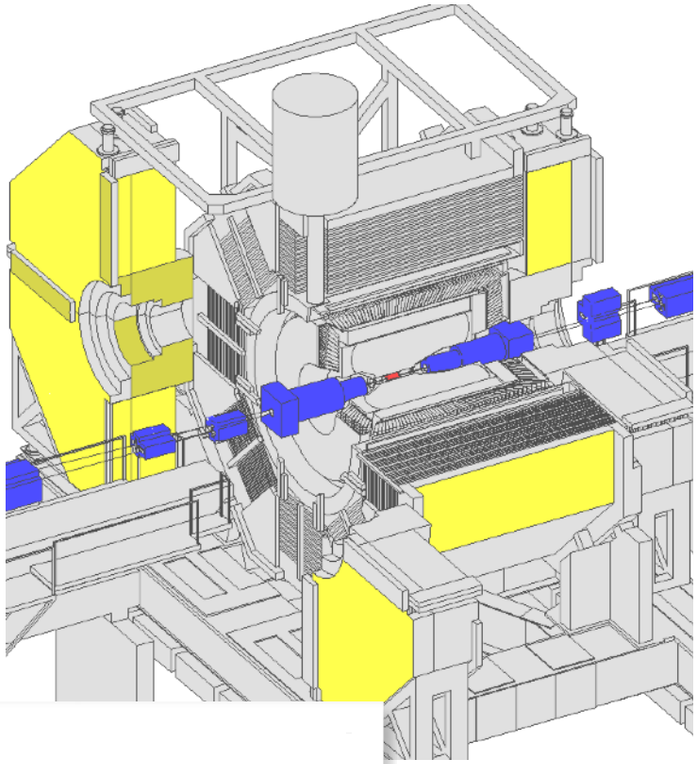

UPGRADE

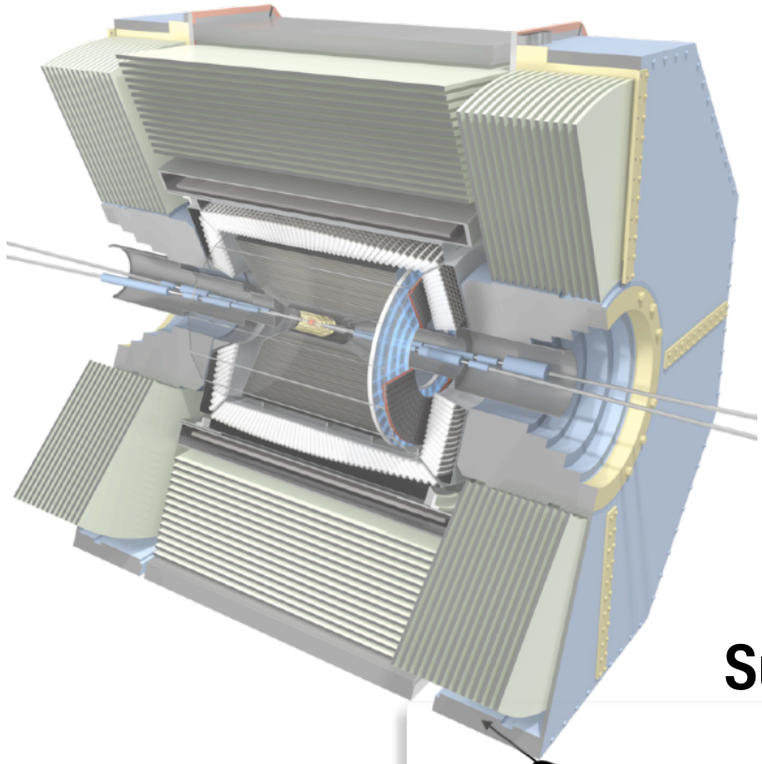

KEKB

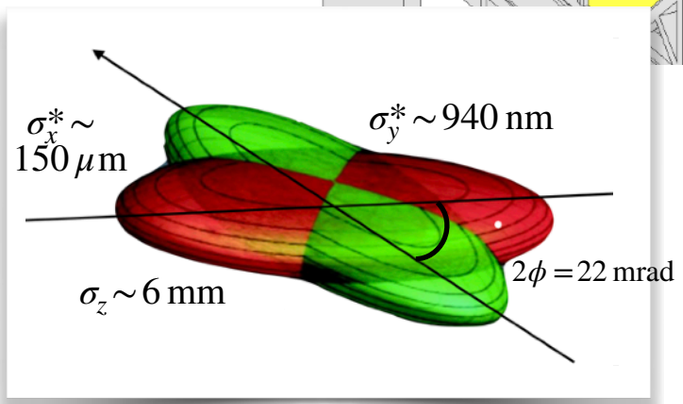

$\beta\gamma = 0.42$

SuperKEKB

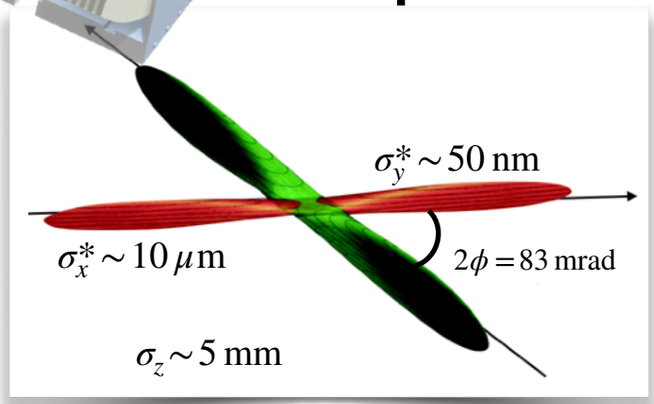

$\beta\gamma = 0.28$

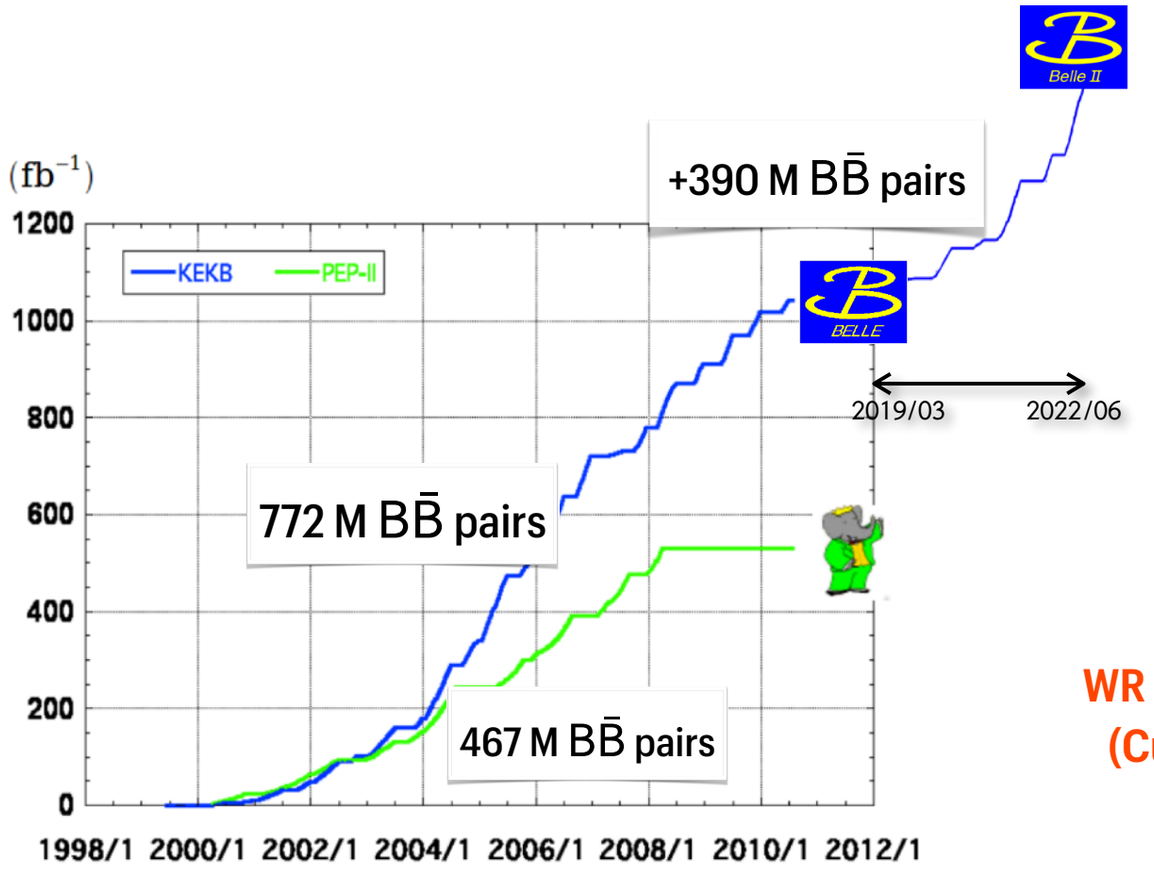

WR Luminosity of x 2.1×10^{34} cm^{-2} s^{-1} (Currents 1.2/1.6 A) (June 2009)

WR Luminosity of 4.7×10^{34} cm^{-2} s^{-1} (Currents 1.1/1.5 A) (June 2022)

Belle TDR, S0168-9002(01)02013-7

THE PERFORMANCES

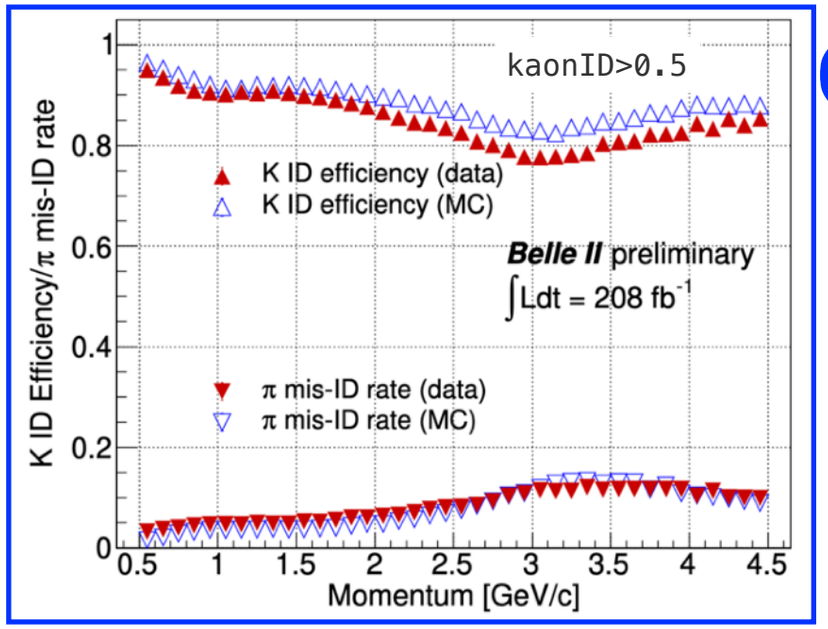

K ID

$\varepsilon \sim 90\,\%$

$\pi \to K \sim 6\,\%$

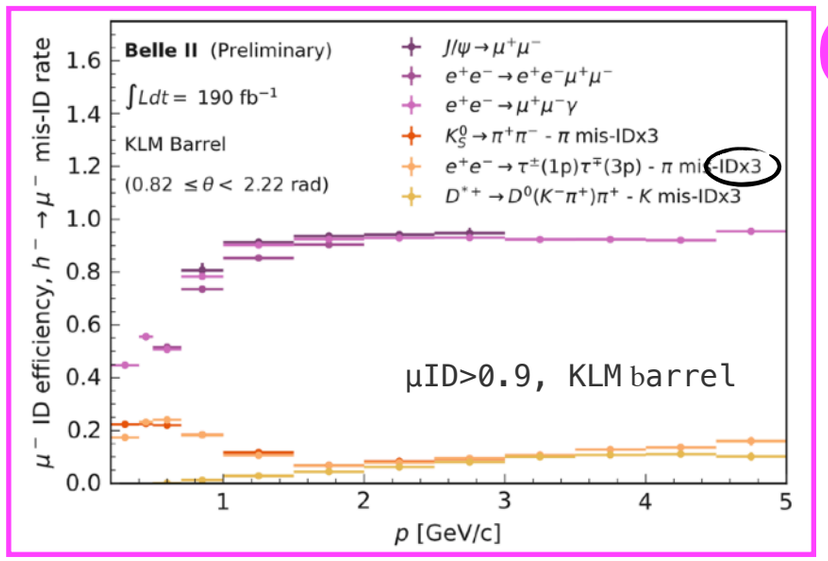

μ ID [1]

$\varepsilon \sim 90\,\%$

$\pi \to \mu \sim 5 - 10\,\%$

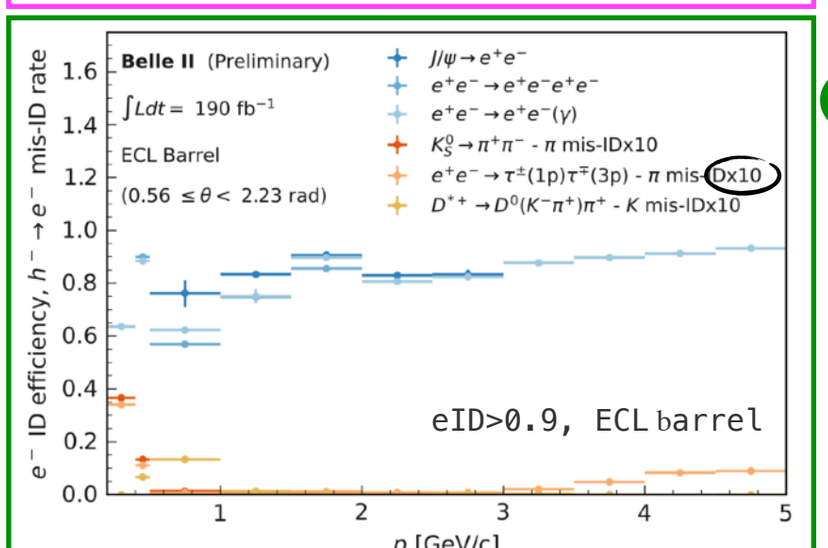

e ID [1]

$\varepsilon \sim 86\,\%$

$\pi \to e \sim 0.4\,\%$

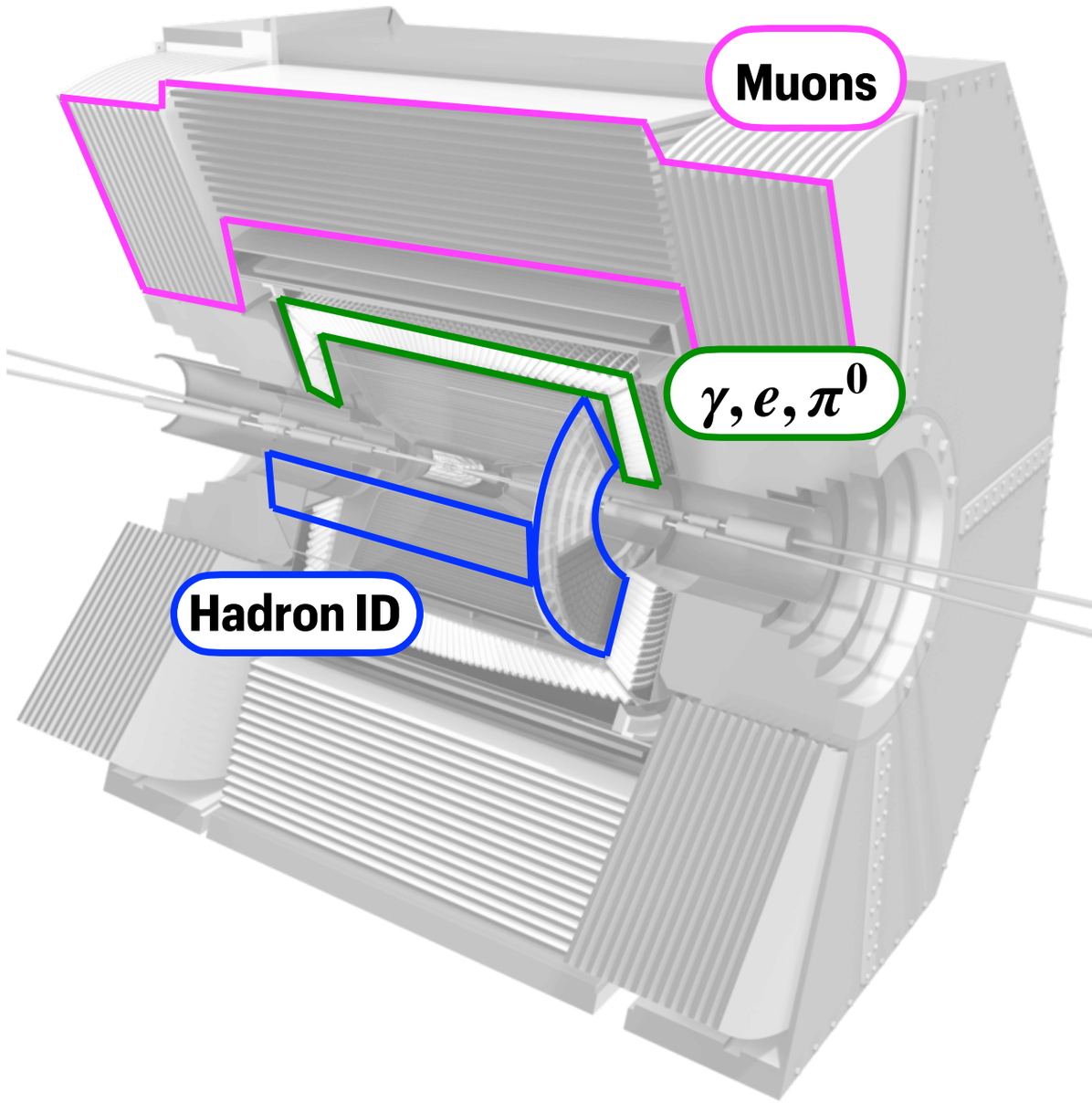

pID performance ~ Belle

Improvements in progress!

More info
☞ BACKUP

[1] BELLE2-CONF-PH-2022-003

B-TAGGING ALGORITHMS *at B-factories*

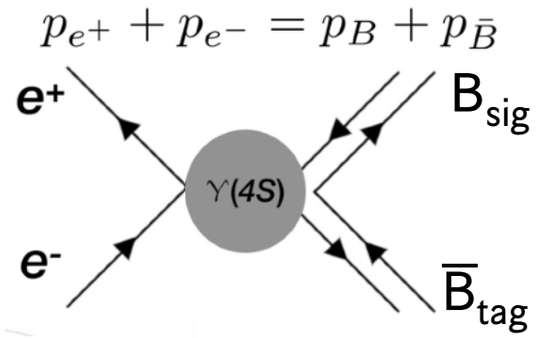

Typical B$\bar{B}$ events:
10 tracks and ~10 photons

- The reconstruction of the B_{tag} allows to infer the properties of the signal-side with missing energy - $B_{sig} \to D\tau\nu$, $K\nu\bar{\nu}$... and to have a handle on backgrounds

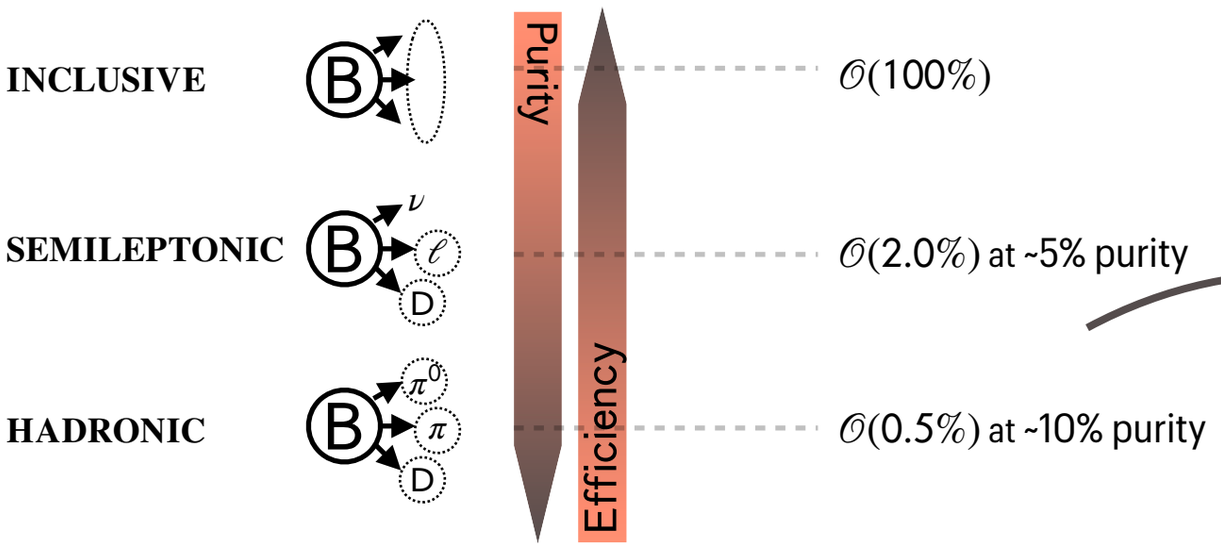

Full **E**vent **I**nterpretation (**FEI**)

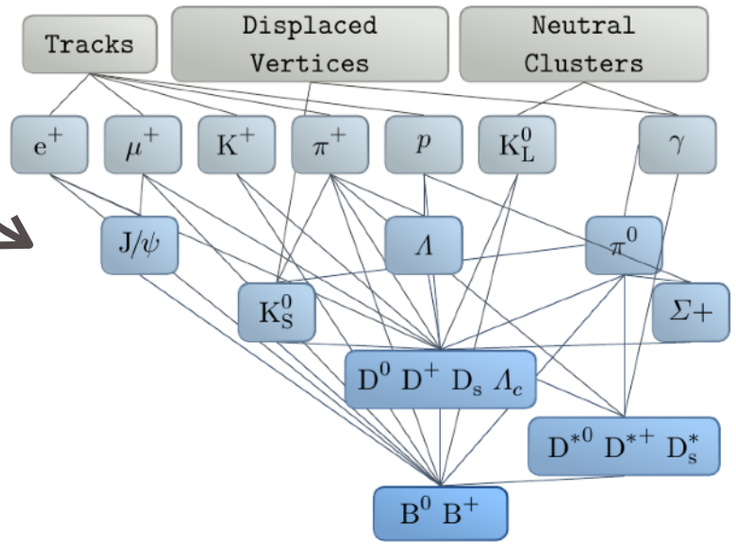

36 (32) hadronic $B^+(B^0)$-modes

- FEI is the algorithm for HAD/SL B_{tag} reconstruction at Belle II [1]
  - **~2x higher efficiency wrt previous algorithms [2]**
  - Employs BDTs trained on MC $\Upsilon(4S) \to B\bar{B}$ events
  - $\mathscr{P}_{FEI}$ used to select best B_{tag}

[1] Comput Softw Big Sci 3, 6 (2019) [2] Nucl.Instrum.Meth.A 654 (2011) 432-440

RADIATIVE DECAYS

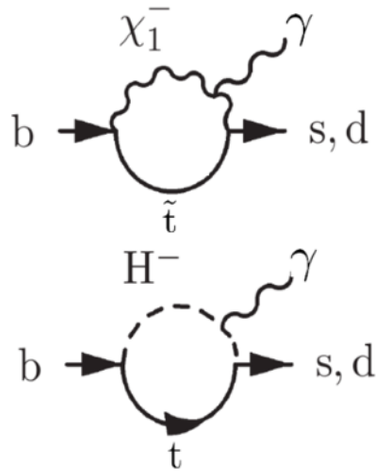

$\mathcal{B}(B \to X_s\gamma)$ measurement as the most effective way to search for or constrain NP in $b \to s\gamma$

- Only possible in the clean environment of B factories

Possible experimental approaches

1. Sum of exclusive $X_s \equiv K + K\pi + K\pi\pi + ...$

PROS High purity and X_s / X_d separation

CONS Large uncertainty in MC for contributions from non-reconstructed X_s states

Highest-energy photon

2. Inclusive approach

PROS High efficiency

CONS Large background, simulation reliant

Belle (605 fb^{-1}) [1]

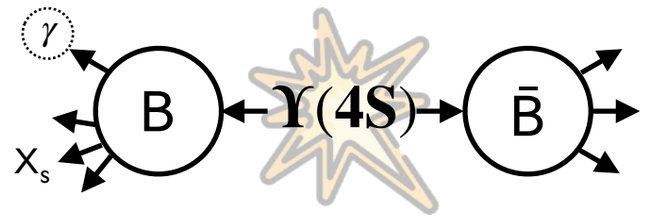

$$\mathcal{B}(B \to X_s\gamma) = (3.45 \pm 0.15 \pm 0.40) \times 10^{-4} \, (E_\gamma > 1.7\,\text{GeV})$$

3. Hadronic B-tagging

PROS Lower background, well-defined X_s, access to E_γ^B

CONS Reduced statistics (efficiency < 1%)

Belle II (190 fb^{-1})

Presented today [2]

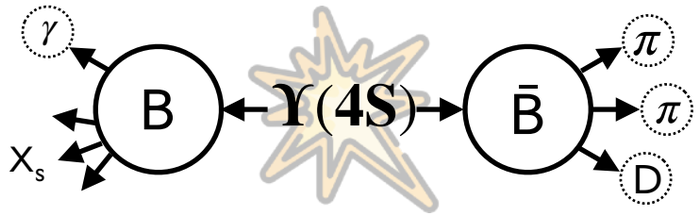

[1] PRL 103 (2009) 241801 [2] 2210.10220

$B \to X_s\gamma$ BF MEASUREMENT AT BELLE II

- Dominant $e^+e^- \to q\bar{q}$ **backgrounds are suppressed** with
  - Signal: π^0/η veto
  - Tag: BDT classifier
    (properties with small correlations with E^B_γ and M_{bc})

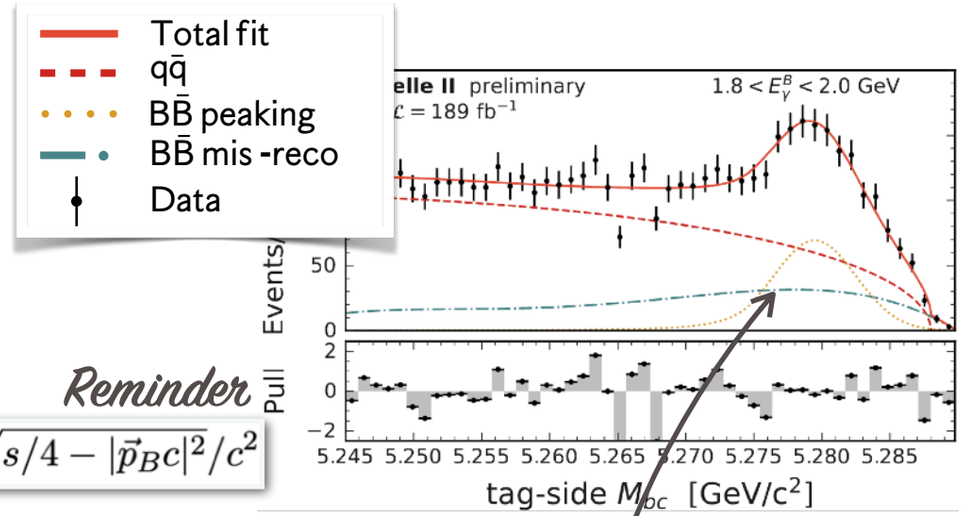

Reminder

$$M_{\rm bc} \equiv \sqrt{s/4 - |\vec{p}_B c|^2/c^2}$$

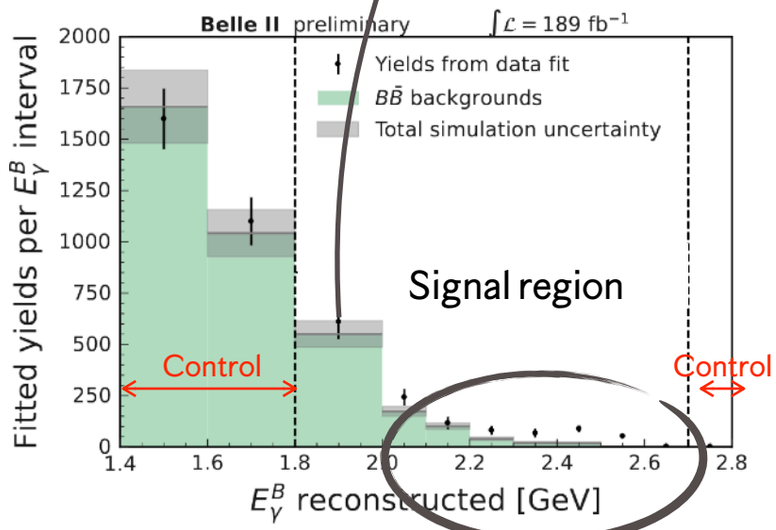

- **Simultaneous likelihood fits** to the M_{bc} distributions in the E^B_γ bins
- Leftover **background is subtracted** in each E^B_γ bin using MC expectation
- $b \to d\gamma$ contribution removed assuming
  - Same shape and selection efficiency as $B \to X_s\gamma$
  - $(|V_{td}|/|V_{ts}|)^2 \sim 4.3\,\%$

- **Unfolding**: the measured spectrum is corrected for the smearing effects
- Simulation based on the "Hybrid" model:
  - BTOXSGAMMA Evtgen [1,2]
  - Resonant $B \to K^*(892)\gamma$ sample [3]

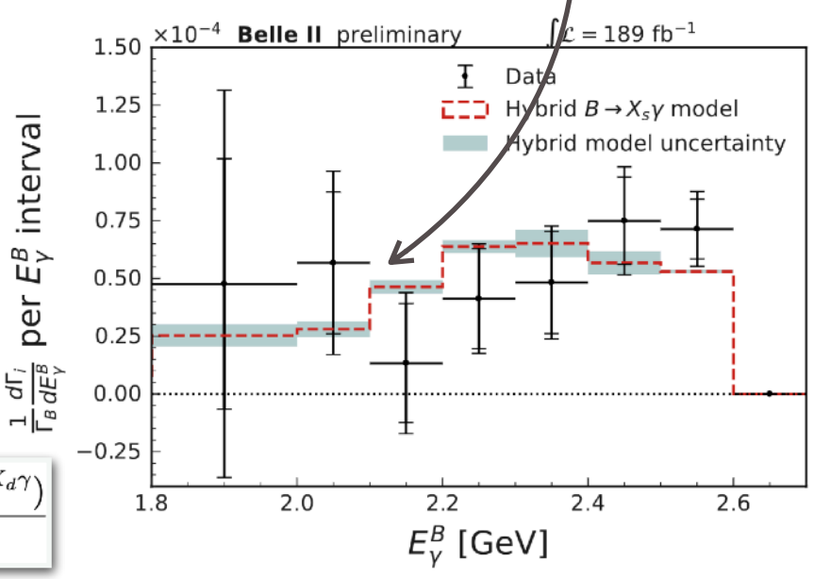

$$\frac{1}{\Gamma_B}\frac{d\Gamma_i}{dE^B_\gamma} = \frac{\mathcal{U}_i \times (N_i^{\rm DATA} - N_i^{\rm BKG,\ MC} - N_i^{B\to X_d\gamma})}{\varepsilon_i \times N_B}$$

[1] 9805303 [2] 2007.04320 [3] PhysRevD.41.1496

$B \to X_s\gamma$ BF MEASUREMENT AT BELLE II

2210.10220

E_γ^B threshold [GeV]	$\mathcal{B}(B \to X_s\gamma)$ $[10^{-4}]$
1.8	3.54 ± 0.78 (stat.) $\pm$ 0.83 (syst.)
2.0	3.06 ± 0.56 (stat.) $\pm$ 0.47 (syst.)
2.1	2.49 ± 0.46 (stat.) $\pm$ 0.35 (syst.)

Unfolded result

- Consistent with theoretical expectations
- Uncertainty is comparable with other had-tagged measurement

[BaBar 210 fb^{-1} (E_0=1.9 GeV), PRD.77.051103]

Updated γ spectrum prediction, 2211.07663

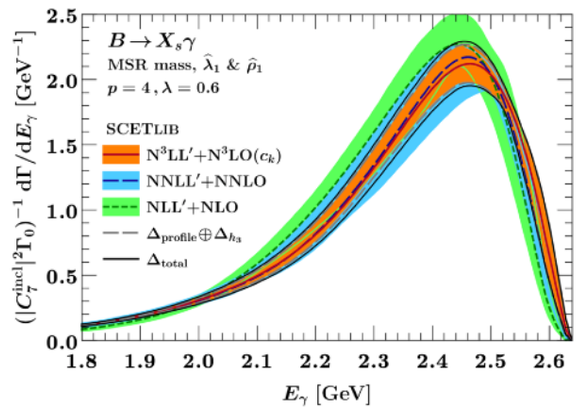

Reminder (For $E_\gamma > 1.6$ GeV)

$$\mathcal{B}_{\rm TH}(b \to s\gamma) = (3.40 \pm 0.17) \times 10^{-4}$$
$$\mathcal{B}_{\rm EX}(b \to s\gamma) = (3.49 \pm 0.19) \times 10^{-4}$$

JHEP06(2020)175

HFLAV-10/2022
All tagging approaches

Improved scenario relies on ongoing studies of $\pi^0/\eta \to \gamma\gamma$ veto modelling

Prospects 2207.06307

Lower E_γ^B threshold	Statistical uncertainty				Baseline (improved)
	1 ab^{-1}	5 ab^{-1}	10 ab^{-1}	50 ab^{-1}	syst. uncertainty
1.4 GeV	10.7%	6.4%	4.7%	2.2%	10.3% (5.2%)
1.6 GeV	9.9%	6.1%	4.5%	2.1%	8.5% (4.2%)
1.8 GeV	9.3%	5.7%	4.2%	2.0%	6.5% (3.2%)
2.0 GeV	8.3%	5.1%	3.8%	1.7%	3.7% (1.8%)

Background

Theory unc.

Lower E_γ^B thresholds ⇔ more challenging analysis due to larger $B\bar{B}$ backgrounds

$B \to K^{(*)} \ell\ell$ DECAYS AT BELLE II

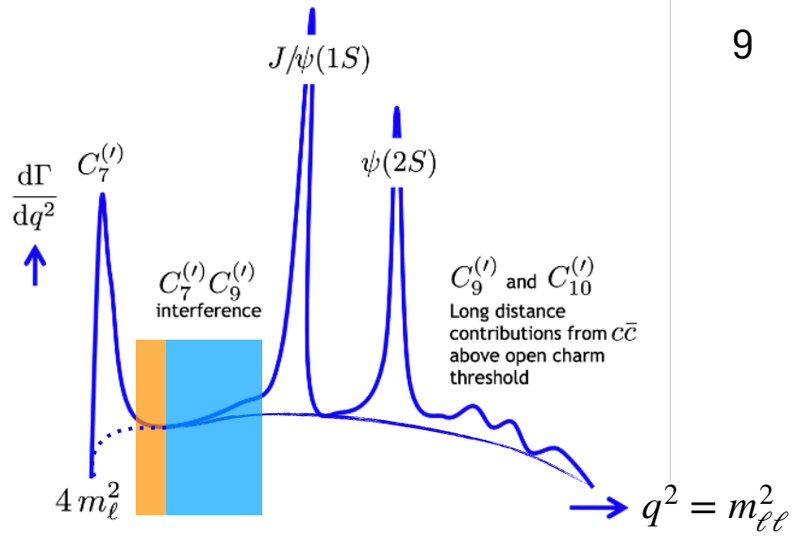

$q^2 \in [0.1, 1.1]\,\mathrm{GeV}^2/c^4$

$q^2 \in [1.1, 6.0]\,\mathrm{GeV}^2/c^4$

- $B \to K\ell\ell$: so far the control channel $B \to KJ/\psi(\ell\ell)$ was measured 2207.11275
- $\mathcal{B}(B \to K^*\ell\ell)$ with 189 fb^{-1}

  $B^0 \to K^{*0}(892)(K^+\pi^-)\ell^+\ell^-$

  $B^+ \to K^{*+}(892)(K^0_S\pi^+, K^+\pi^0)\ell^+\ell^-$

  2206.05946

☞ BACKUP

Belle II

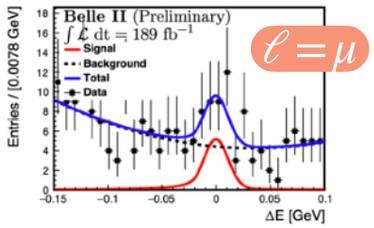

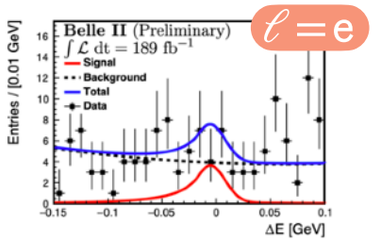

Enjoy good and similar performance for electrons and muons

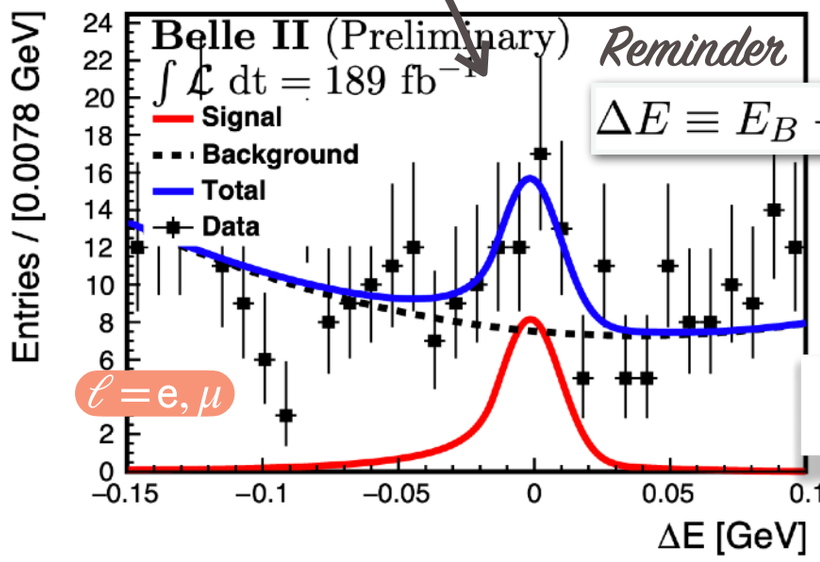

q^2 vetoed regions compatible with

$B \to K^*\{J/\psi, \psi(2S)\}$

$B \to K^*\gamma$

$\mathcal{B}(B \to K^*\ell^+\ell^-) = (1.25 \pm 0.30^{+0.08}_{-0.07}) \times 10^{-6}$

Belle(II) can be relevant in

- $B \to K^*ee$ (low q^2) - $C_7^{(\prime)}$ constraints (redundancy with LHCb)
- **Inclusive $\mathcal{B}(B \to X_s\ell\ell)$ - 10% accuracy @ 5 ab^{-1} expected** 1808.10567

$B \to K^{(*)} \ell\ell$ DECAYS AT BELLE II

- $B \to K \ell\ell$: so far the control channel $B \to K J/\psi(\ell\ell)$ was measured 2207.11275
- $\mathcal{B}(B \to K^* \ell\ell)$ with 189 fb^{-1}

  $B^0 \to K^{*0}(892)(K^+\pi^-)\ell^+\ell^-$

  $B^+ \to K^{*+}(892)(K^0_S\pi^+, K^+\pi^0)\ell^+\ell^-$

  2206.05946

☞ BACKUP

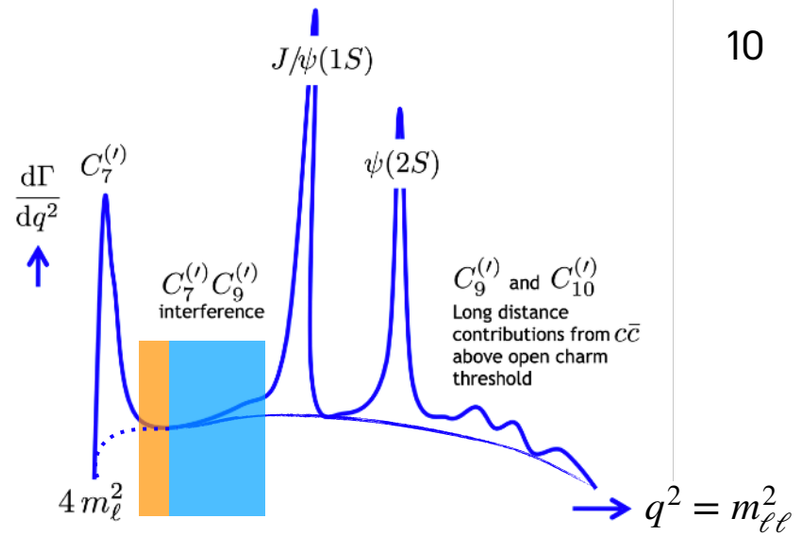

$q^2 \in [0.1, 1.1]\,\mathrm{GeV}^2/c^4$

$q^2 \in [1.1, 6.0]\,\mathrm{GeV}^2/c^4$

LFU tests: status and prospects

JHEP03(2021)10

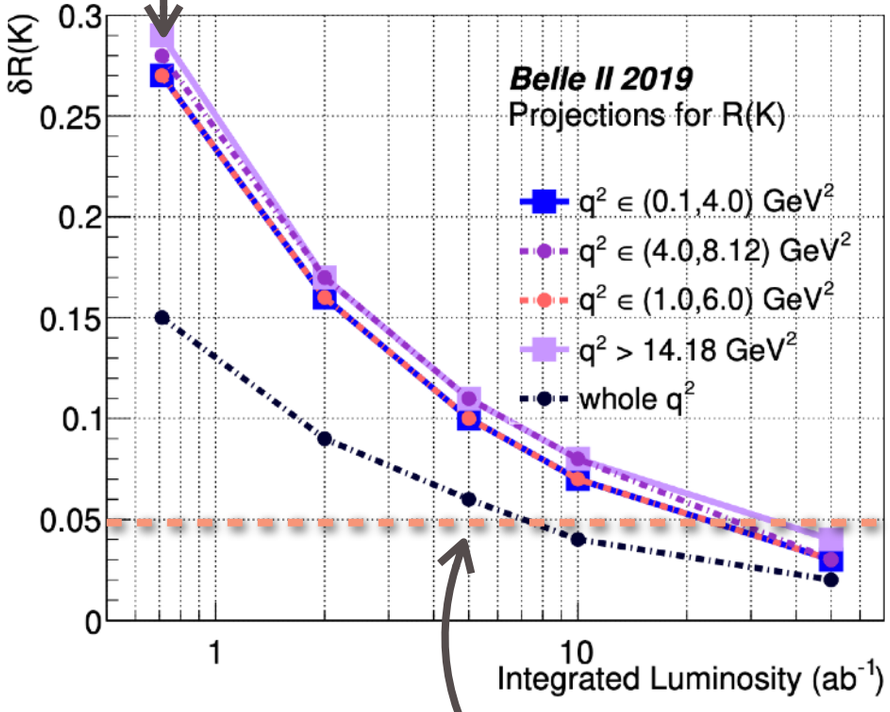

⇢ Current LHCb precision for $q^2 \in [1, 6]\,\mathrm{GeV}^2$ (9fb^{-1}) 202212.09152 (stat dominated)

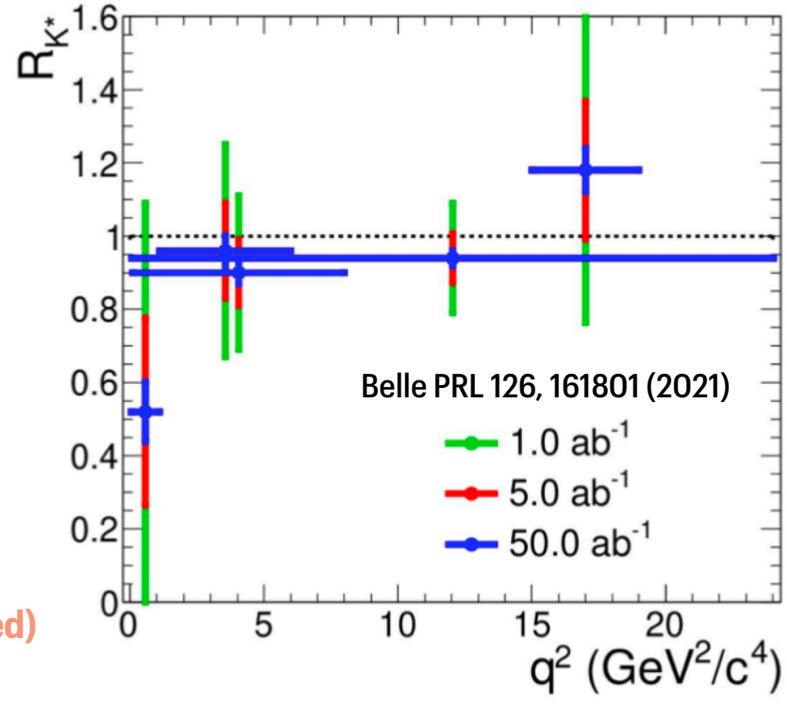

Independent measurement of $R_{K^{(*)}}$ at Belle II with 5-10 ab^{-1}, 3% precision at 50 ab^{-1}

$b \to s\tau\tau$ SEARCHES - OVERVIEW

- SM Expected BF $\mathcal{O}(10^{-7})$ [1]
- **Correlation with $R_{D^{(*)}}$ [2]**
- **Large enhancements to SM BF $\mathcal{O}(10^2 - 10^3)$**

$$C_9^{\tau\tau} = C_{10}^{\tau\tau} \sim -\frac{2\pi}{\alpha}\frac{V_{cb}}{V_{tb}V_{ts}^*}\left(\sqrt{\frac{R_{D^{(*)}}}{R_{D^{(*)}}^{SM}}} - 1\right) \text{ [3]}$$

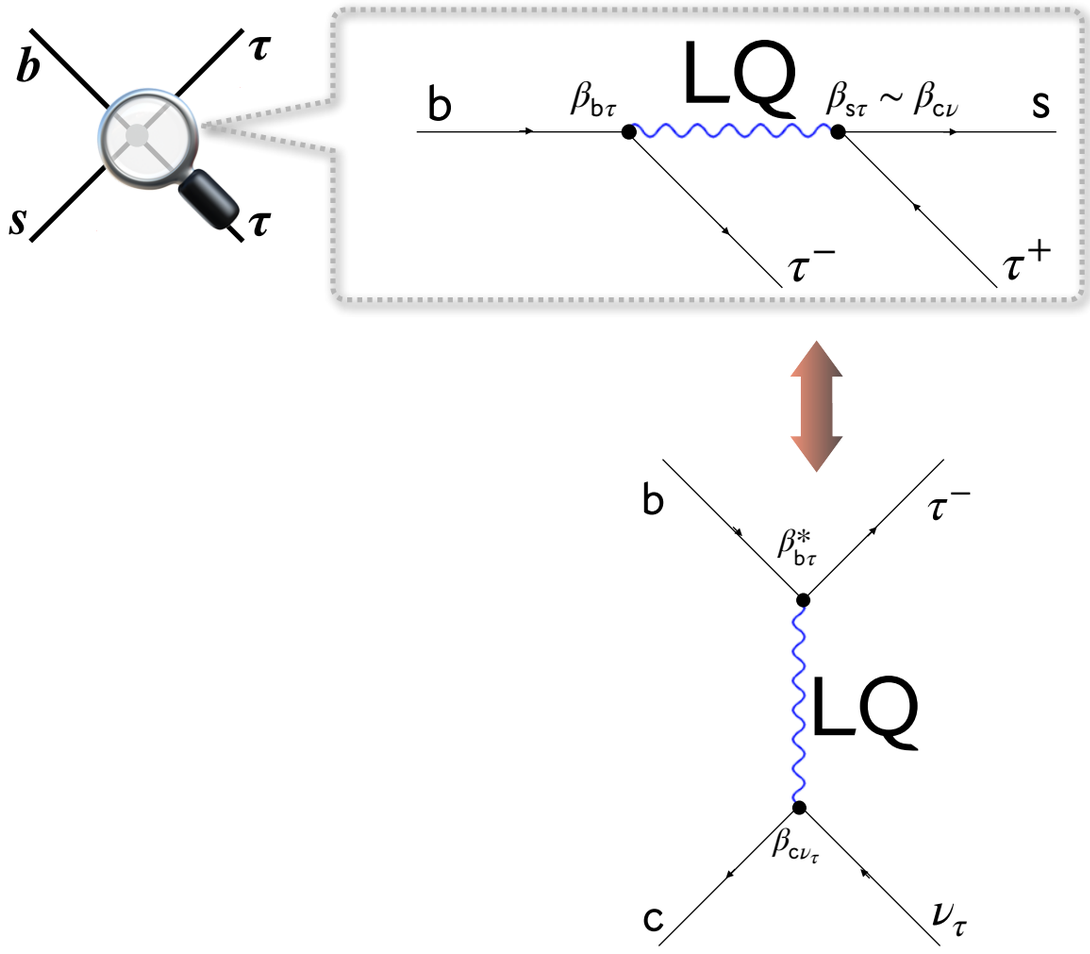

Decay	BF U.L. @ 90% CL		
$B_s \to \tau\tau$	5.2x10^{-3}	$3\,\text{fb}^{-1}$	PRL 118.251802 (2017)
$B^+ \to K^+\tau\tau$	2.3x10^{-3}	$424\,\text{fb}^{-1}$	PRL 118.031802 (2017)
$B^0 \to K^{*0}\tau\tau$	3.1x10^{-3}	$711\,\text{fb}^{-1}$	2110.03871

Current sensitivity far from $\mathcal{B}_{SM}$!

[1] PRL 120.181802 (2018) [2] PRL120.181802(2018) [3] PRD 105.113007 (2022)

$B \to K^{*0}\tau\tau$ SEARCHES AT BELLE (II)

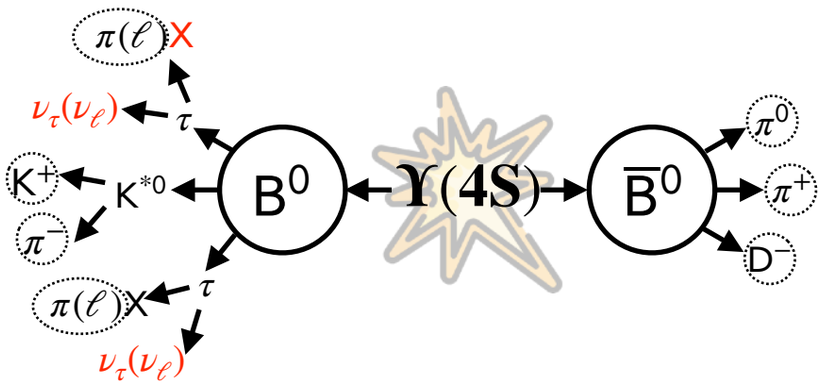

Search at Belle (711 fb^{-1})

- Hadronic B-tagging Belle algorithm (Neurobayes FR)
- $\tau \to \ell\nu\bar{\nu}, \pi\nu$ modes considered
- Cut&count analysis
- $\mathcal{B}(B^0 \to K^{*0}\tau\tau) < 3.1 \times 10^{-3}$ (90 % CL)

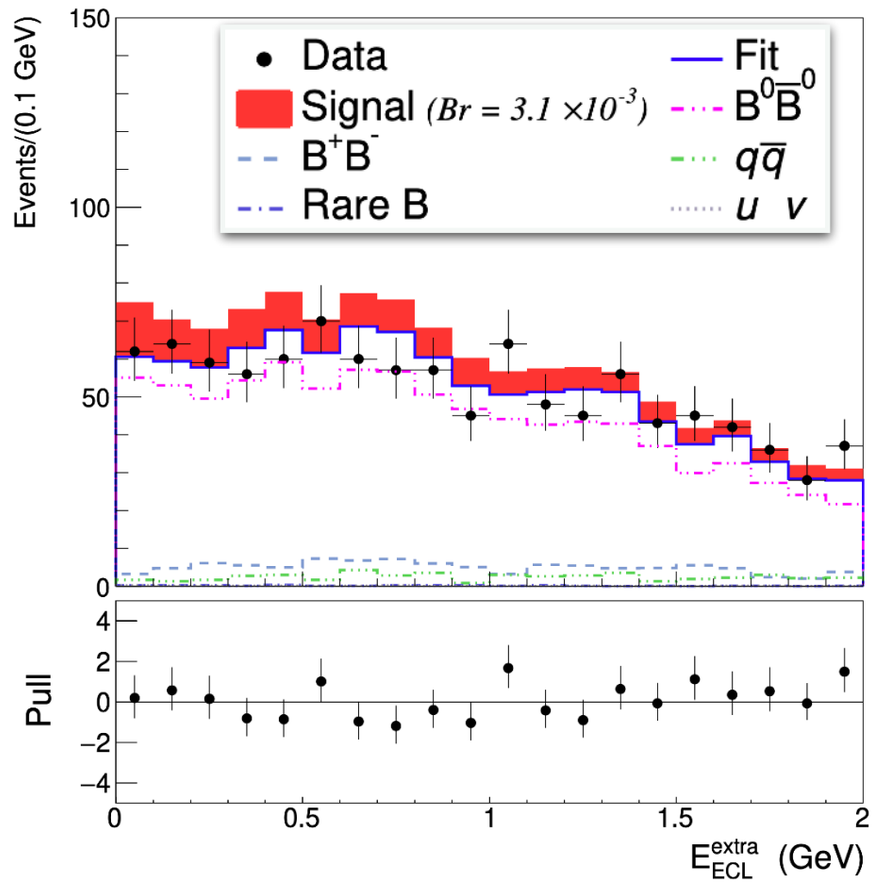

Belle II projections 2207.06307

ab^{-1}	$\mathcal{B}(B^0 \to K^{*0}\tau\tau)$ (had tag) "Baseline" scenario	"Improved" scenario
1	$< 3.2 \times 10^{-3}$	$< 1.2 \times 10^{-3}$
5	$< 2.0 \times 10^{-3}$	$< 6.8 \times 10^{-4}$
10	$< 1.8 \times 10^{-3}$	$< 6.5 \times 10^{-4}$
50	$< 1.6 \times 10^{-3}$	$< 5.3 \times 10^{-4}$

Increased signal efficiency while assuming same syst. unc. as Belle
(Total 9%: MC sample size 4%, B_{tag} eff. correction 5%, track eff. 4%)

Improvement @ Belle II

- ~2x hadronic B-tagging efficiency: **FR → FEI**
- **Multivariate analysis**
- **Add $\tau \to \rho\nu$ modes**

Will offer unprecedented sensitivity in $B \to K\tau\tau$ decays

$B \to K\nu\bar{\nu}$ - STATUS&PROSPECTS

- **The BF can be measured at B-factories because of the clean event environment and the well-defined initial state**
- Belle II result with inclusive B-tagging obtained with 10% of Belle data (1/6 of current Belle II dataset)
  - **20% better precision/lumi (wrt SL B-tagging)**

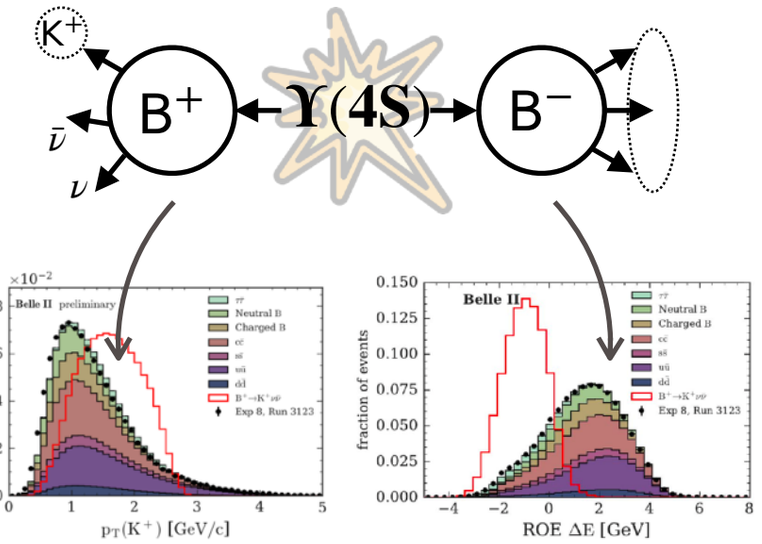

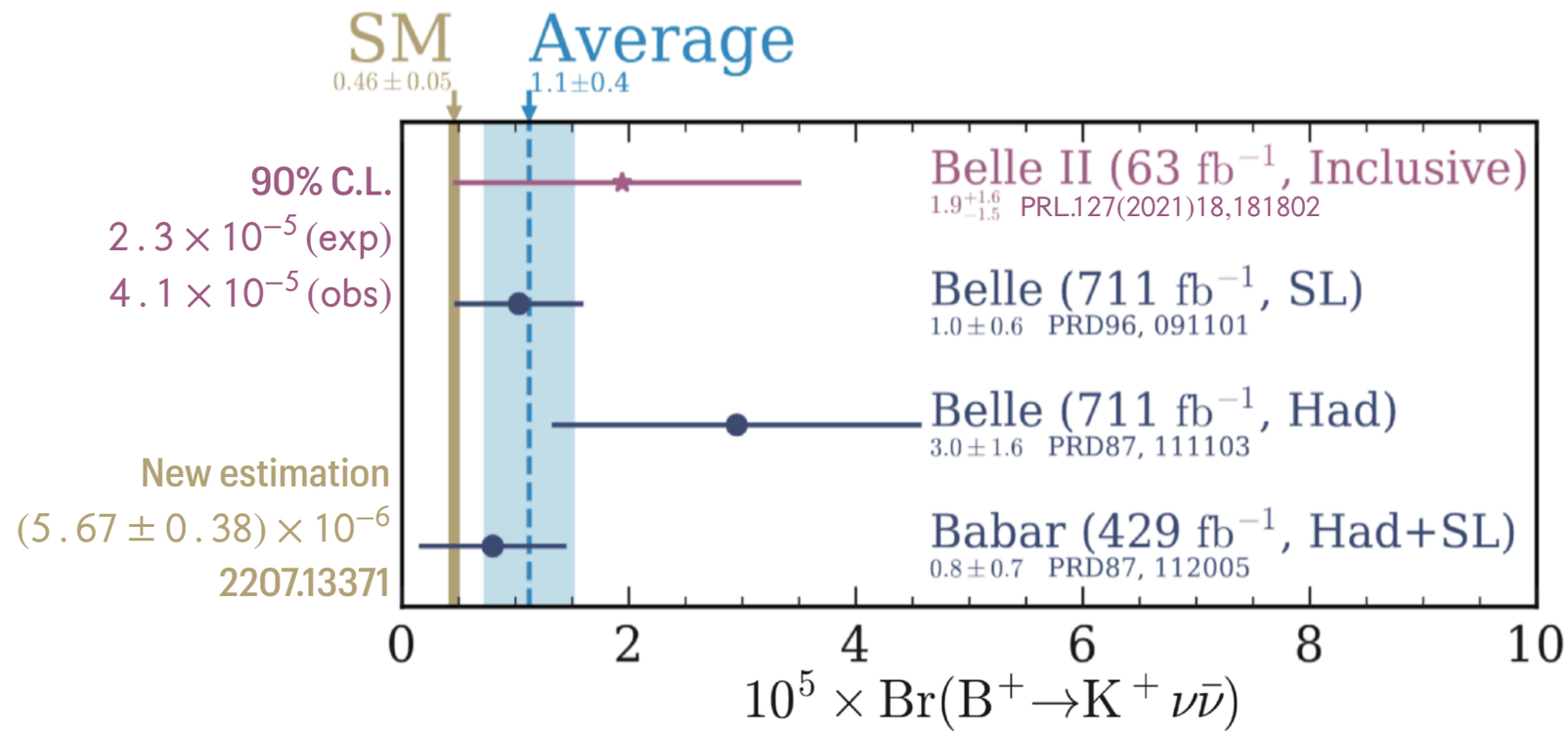

Decay	$1\,\mathrm{ab}^{-1}$	$5\,\mathrm{ab}^{-1}$	$10\,\mathrm{ab}^{-1}$
$B^+ \to K^+\nu\bar{\nu}$	0.55 (0.37)	0.28 (0.19)	0.21 (0.14)
$B^0 \to K^0_S\nu\bar{\nu}$	2.06 (1.37)	1.31 (0.87)	1.05 (0.70)
$B^+ \to K^{*+}\nu\bar{\nu}$	2.04 (1.45)	1.06 (0.75)	0.83 (0.59)
$B^0 \to K^{*0}\nu\bar{\nu}$	1.08 (0.72)	0.60 (0.40)	0.49 (0.33)

Exp. uncertainty on signal strength ($\mathscr{B}_{OBS}/\mathscr{B}_{SM}$)

- BASELINE scenario
- (IMPROVED) scenario

$B \to K\nu\bar{\nu}$ search dominated by Belle II. Current sensitivity allows to confirm SM prediction soon

EXPERIMENTAL STATUS ON LFV $b \to s\ell\ell'$

- $b \to s\ell\ell'$ probed at B-factories and LHCb
- $B \to K\tau\ell$ more interesting ($R_{K^{(*)}}$ & $R_{D^{(*)}}$ anomalies) but experimentally more challenging

  - Sensitivity is entering now the 10^{-6} regime

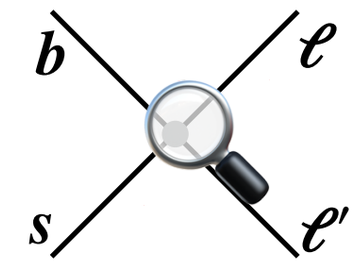

$\ell, \ell' = \{e, \mu, \tau\}$

LHCb (3 fb^{-1})
$B_s \to \tau\mu$: 3.4×10^{-5}
$B^+ \to K^+\mu e$: $(6\text{-}7)\times10^{-9}$
Belle (711 fb^{-1})
$B^{+/0} \to K^{+/0}\mu e$: $(4\text{-}9)\times10^{-8}$

BaBar (429 fb^{-1})
$B^+ \to K^+\tau\ell$: $(1.5\text{-}4.5)\times10^{-5}$

LHCb (9 fb^{-1})
$B^+ \to K^+\tau^+\mu^-$: 3.9×10^{-5}

NEW **Belle** (711 fb^{-1})
$B^+ \to K^+\tau\ell$: $(0.6\text{-}2.5)\times10^{-5}$

1999 — 2010 — 2012 — 2018 — **2022**

Belle: 711 fb^{-1}

BaBar: 429 fb^{-1}

LHCb: 3 fb^{-1}

LHCb: 6 fb^{-1}

Belle (711 fb^{-1})
$B^0 \to K^{*0}\mu e$: 1.8×10^{-7}

Belle II: 362 fb^{-1}

LHCb (9 fb^{-1})
$B^0 \to K^{*0}\mu e$: 1.0×10^{-8}
$B^0 \to K^{*0}\tau\mu$: $(0.8\text{-}1.0)\times10^{-5}$
$B_s \to \phi e\mu$: 1.6×10^{-8}

KEY-ELEMENTS FOR THE $B^+ \to K^+\tau\ell$ SEARCH

2 charge configurations x 2 flavors (e,μ)
⇔ different BSM models and backgrounds

$B^+ \to K^+\tau^+\ell^-$

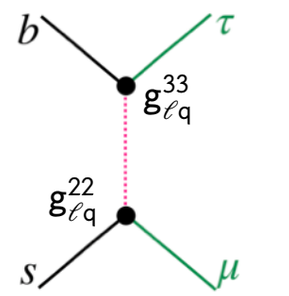

$B^+ \to K^+\tau^-\ell^+$

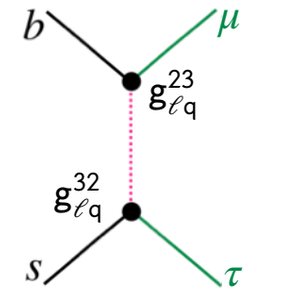

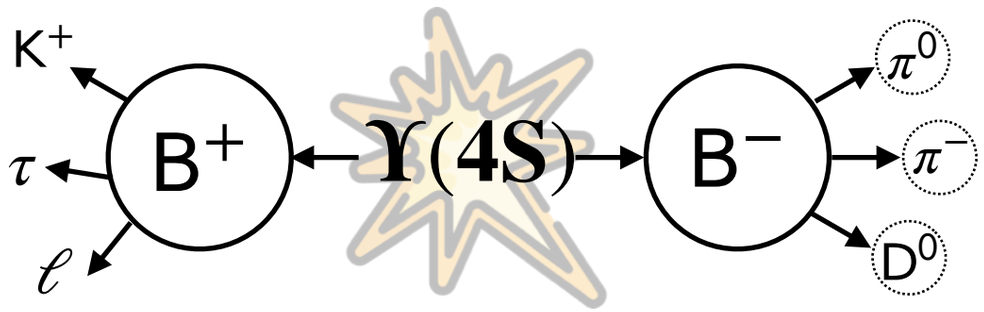

1. B_{tag} reconstruction
Hadronic FEI

KEY-ELEMENTS FOR THE $B^+ \to K^+\tau\ell$ SEARCH

2 charge configurations x 2 flavors (e,μ)
⇔ different BSM models and backgrounds

$B^+ \to K^+\tau^+\ell^-$

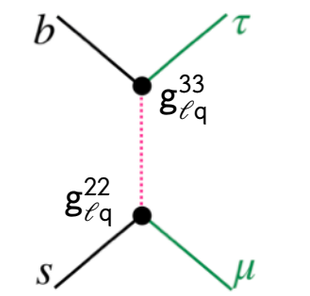

$B^+ \to K^+\tau^-\ell^+$

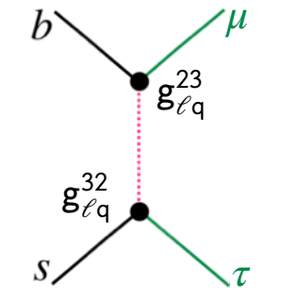

2. B_{sig} reconstruction

Kaon
Lepton {e,μ}

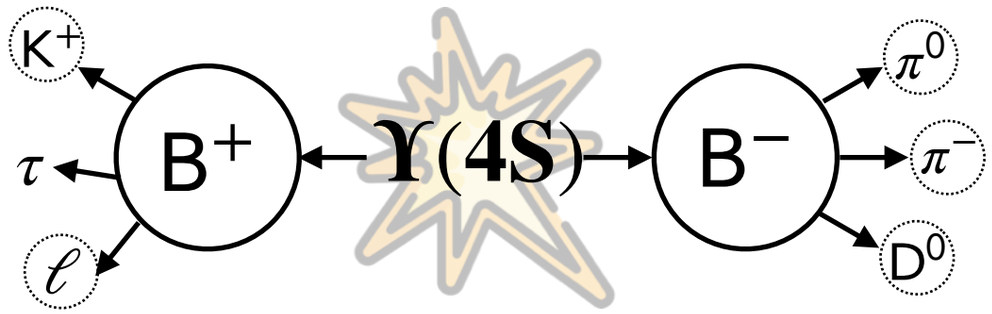

1. B_{tag} reconstruction

Hadronic FEI

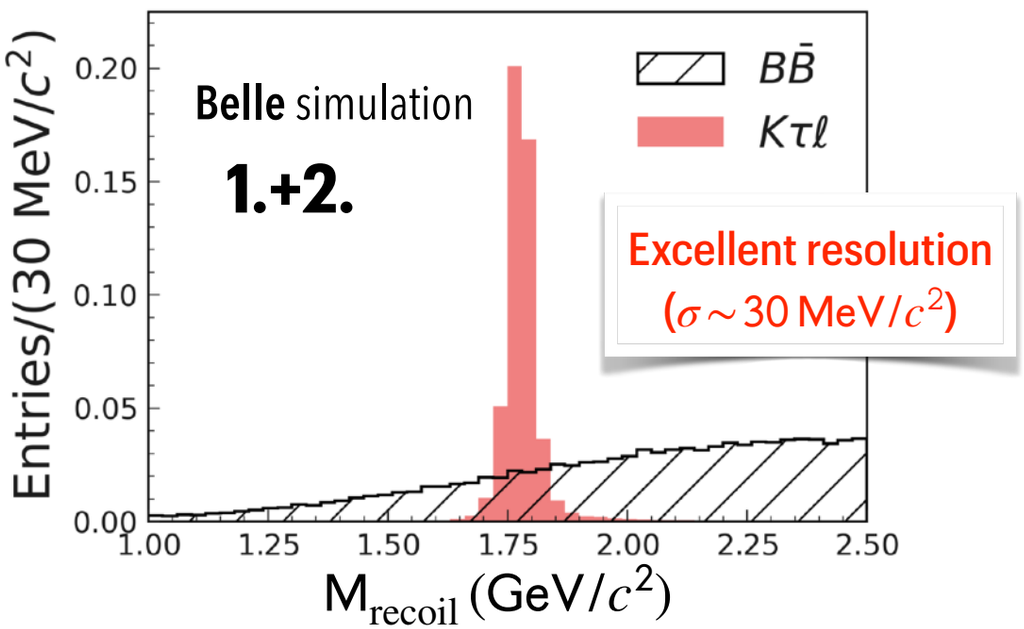

Signal is extracted fitting the

$$M_{recoil} = [m_B^2 + m_{K\ell}^2 - 2(\sqrt{s}E^*_{K\ell}/2 + |\vec{p}^{\,*}_{B_{tag}}||\vec{p}^{\,*}_{K\ell}|\cos\theta)]^{\frac{1}{2}}$$

$E^*_{B_{tag}} \to \sqrt{s}/2$

θ: $\angle(\vec{p}^{\,*}_{B_{tag}}, \vec{p}^{\,*}_{K\mu})$

KEY-ELEMENTS FOR THE $B^+ \to K^+\tau\ell$ SEARCH

2 charge configurations x 2 flavors (e,μ)
⇔ different BSM models and backgrounds

$B^+ \to K^+\tau^+\ell^-$

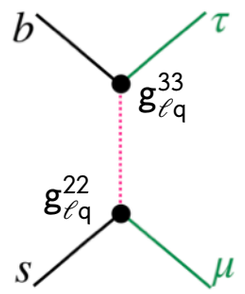

$B^+ \to K^+\tau^-\ell^+$

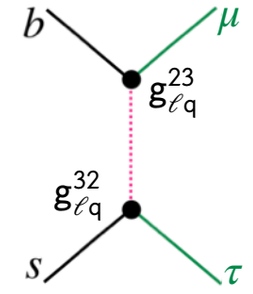

3. Additional requirements

$\tau \to \ell\nu\nu, \pi^+(n\pi^0)\nu$
No extra tracks

2. B_{sig} reconstruction

Kaon
Lepton {e,μ}

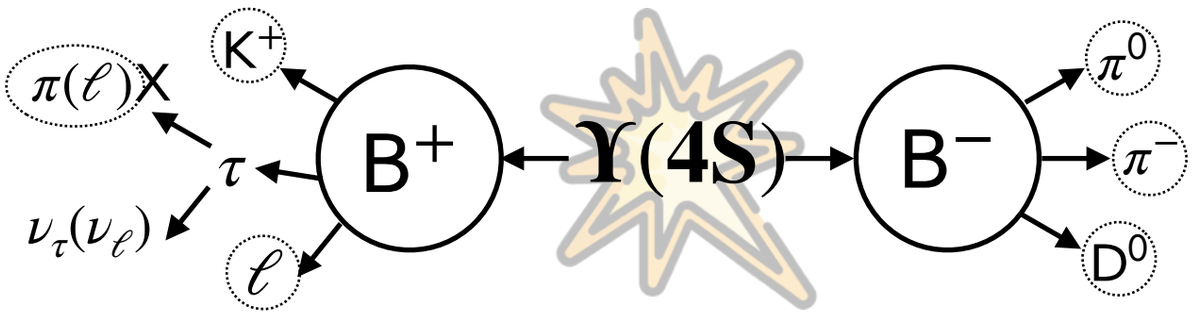

1. B_{tag} reconstruction

Hadronic FEI

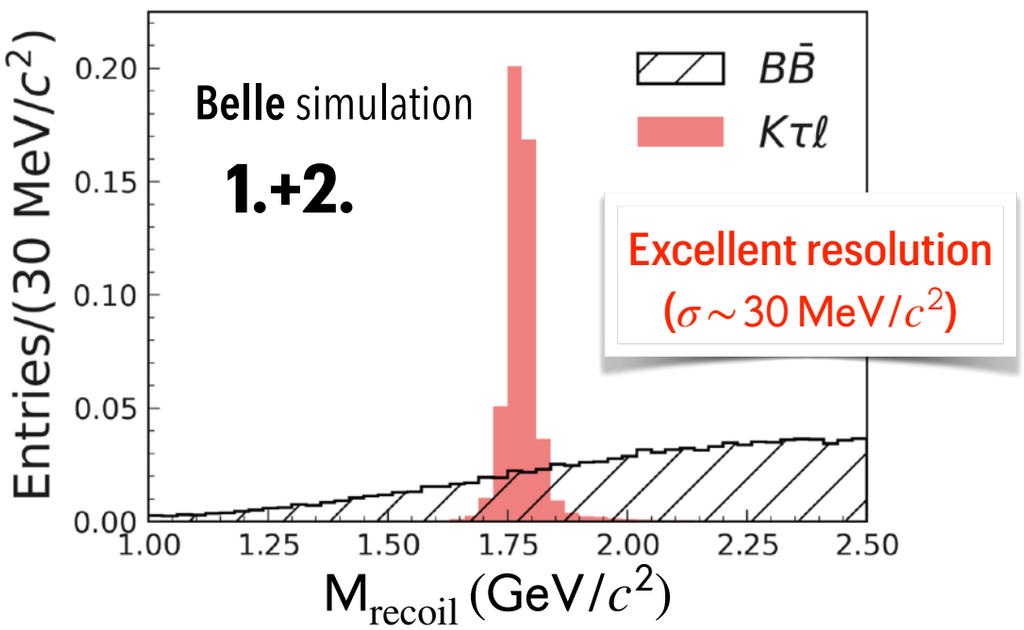

Signal is extracted fitting the

$$M_{recoil} = [m_B^2 + m_{K\ell}^2 - 2(\sqrt{s}E^*_{K\ell}/2 + |\vec{p}^*_{B_{tag}}||\vec{p}^*_{K\ell}|\cos\theta)]^{\frac{1}{2}}$$

$E^*_{B_{tag}} \to \sqrt{s}/2$

θ: $\angle(\vec{p}^*_{B_{tag}}, \vec{p}^*_{K\mu})$

$B^+ \to K^+ \tau \ell$ AT BELLE

MVA is adopted for

1. $B\bar{B}$ **bg suppression**

- $M(K^+_{sig} X^-_{sig})$
- ROE properties
- Decay topology
- B_{tag} quality

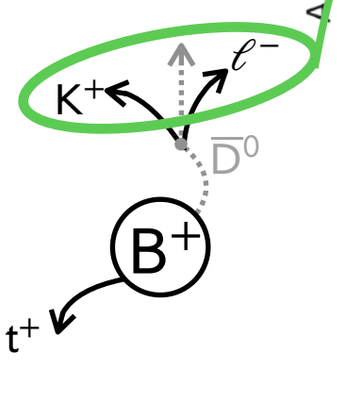

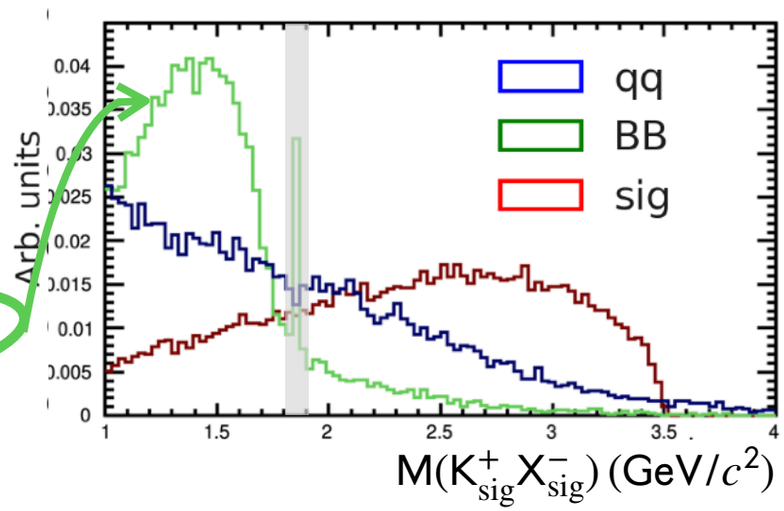

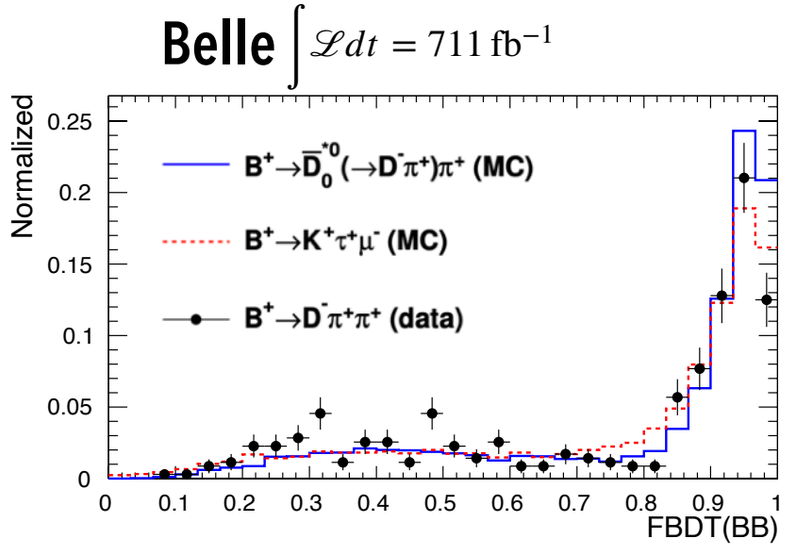

2. $q\bar{q}$ **bg suppression**

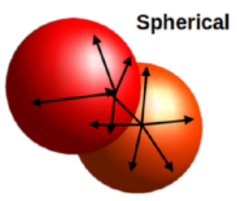

$e^- e^+ \to B\bar{B}$

$p(B) \approx 0.3\,\mathrm{GeV/c}$

$e^- e^+ \to q\bar{q}$

$p(q) \approx 5\,\mathrm{GeV/c}$

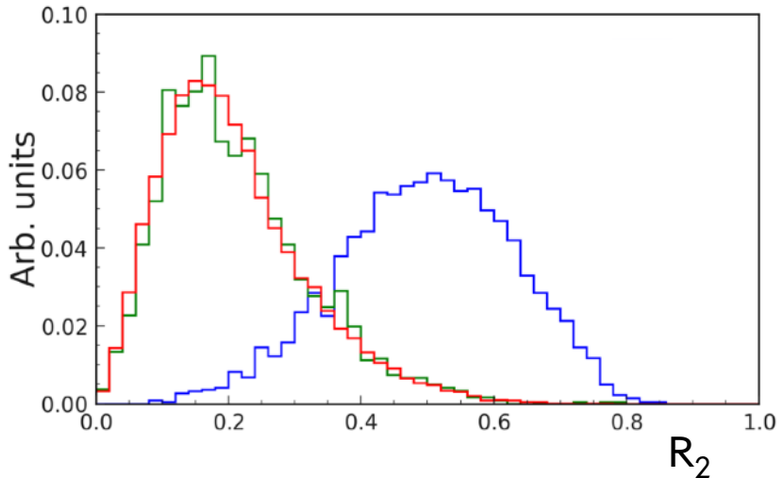

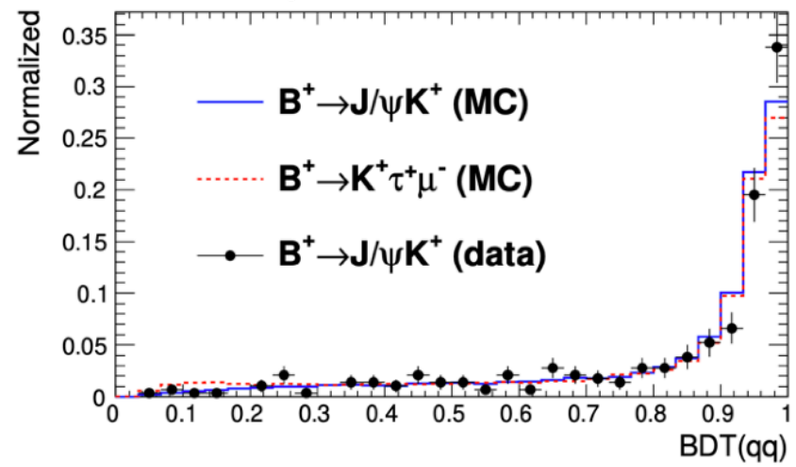

☞ *More details in BACKUP*

$B^+ \to K^+ \tau \ell$ AT BELLE - RESULTS

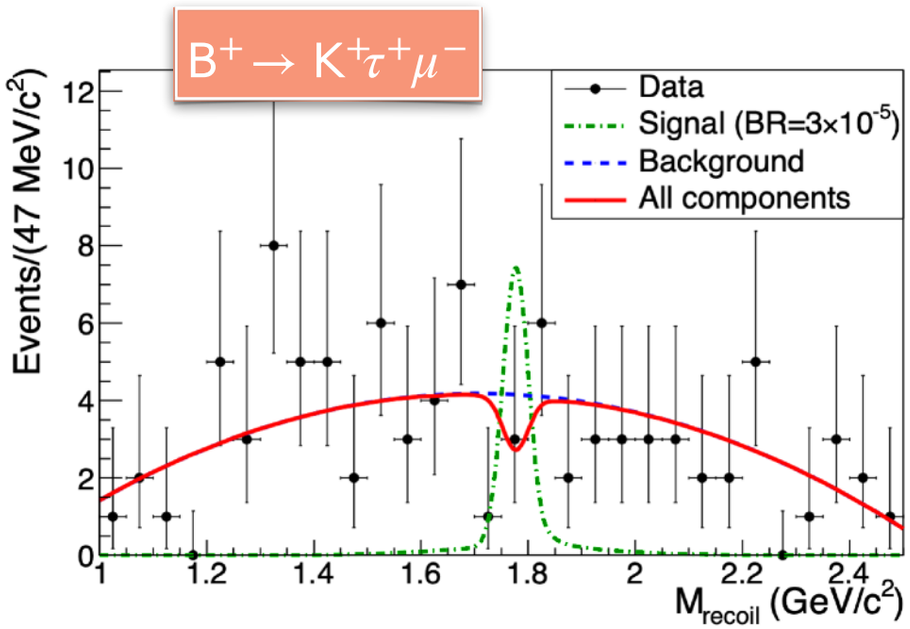

No significant signal is observed for any of the 4 modes

Mode	$\varepsilon(\%)$	$N_{\rm sig}$	$\mathcal{B}^{\rm UL}(10^{-5})$ @90 % CL
$B^+ \to K^+ \tau^+ \mu^-$	0.064	-2.1 ± 2.9	0.59
$B^+ \to K^+ \tau^+ e^-$	0.084	1.5 ± 5.5	1.51
$B^+ \to K^+ \tau^- \mu^+$	0.046	2.3 ± 4.1	2.45
$B^+ \to K^+ \tau^- e^+$	0.079	-1.1 ± 7.4	1.53

$$\mathcal{B}^{\rm UL} = \frac{N^{\rm UL}_{\rm sig}}{\varepsilon \times 2N_{B\bar{B}} \times f^{+-}}$$

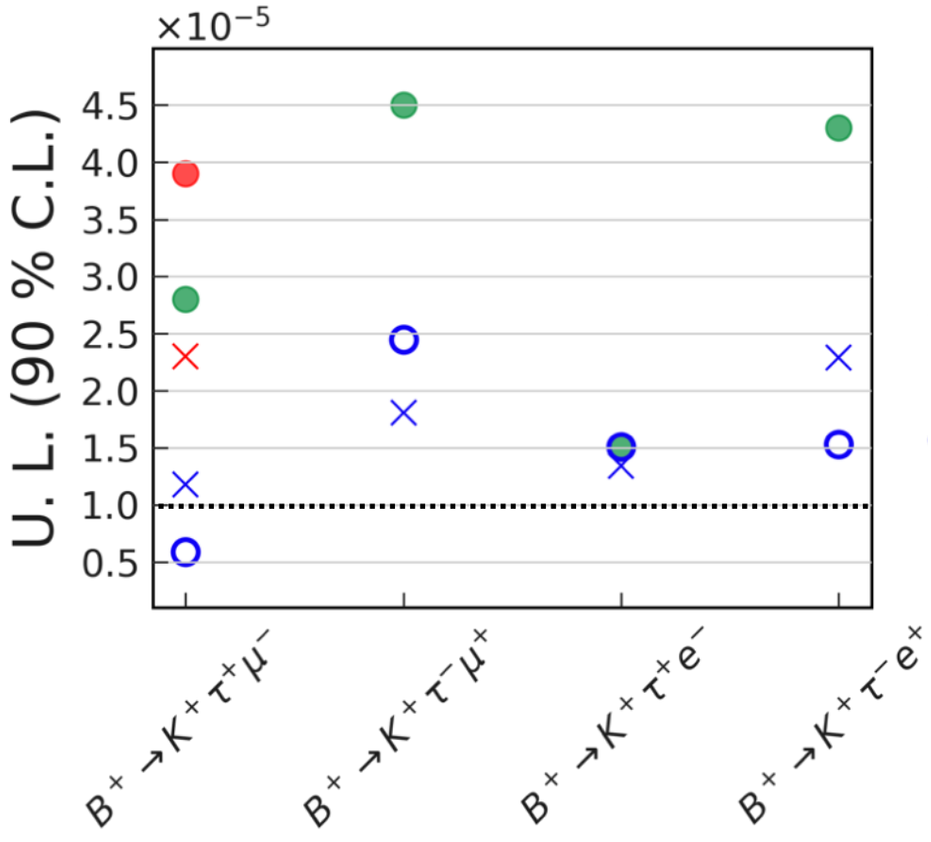

- BaBar (429 fb^{-1}) — Hadronic B-tagging
- LHCb (9 fb^{-1}) - expected
- LHCb (9 fb^{-1}) — $B^{*0}_{s2} \to B^+ K^-$ tagged
- Belle (711 fb^{-1}) - expected
- Belle (711 fb^{-1}) — Hadronic B-tagging

Best limits for the $B^+ \to K^+ \tau \ell$ modes!

$B^+ \to K^+ \tau \ell$ AT BELLE - RESULTS

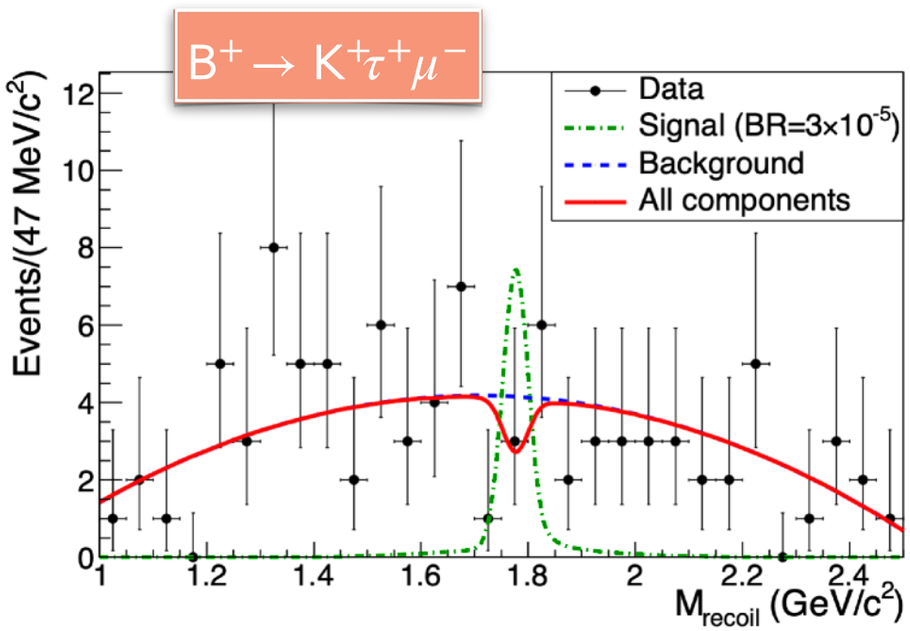

Mode	$\varepsilon(\%)$	$N_{\rm sig}$	$\mathcal{B}^{\rm UL}(10^{-5})$	
$B^+ \to K^+ \tau^+ \mu^-$	0.064	-2.1 ± 2.9	0.59	(0.65)
$B^+ \to K^+ \tau^+ e^-$	0.084	1.5 ± 5.5	1.51	(1.71)
$B^+ \to K^+ \tau^- \mu^+$	0.046	2.3 ± 4.1	2.45	(2.97)
$B^+ \to K^+ \tau^- e^+$	0.079	-1.1 ± 7.4	1.53	(2.08)

↑ PHSP ↑ $C_{S,P}$

- Efficiency map to recast the efficiency to any NP scenarios
- Quoted the most `unfavourable' scenario corresponding to (pseudo)scalar LFV mediator (signal efficiency drop ~20%)

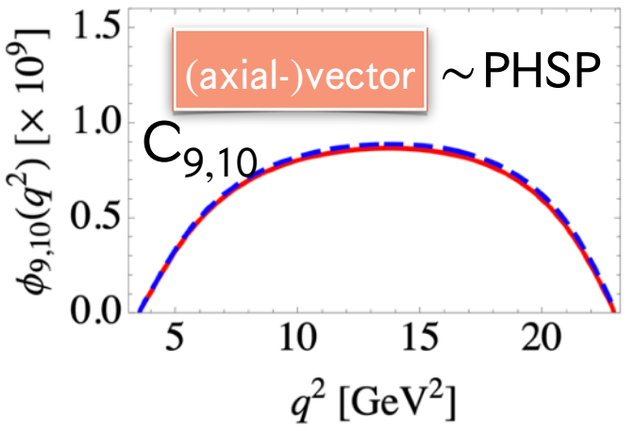

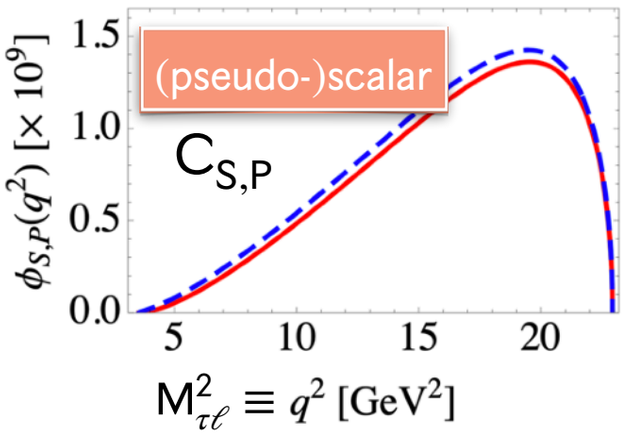

1602.00881

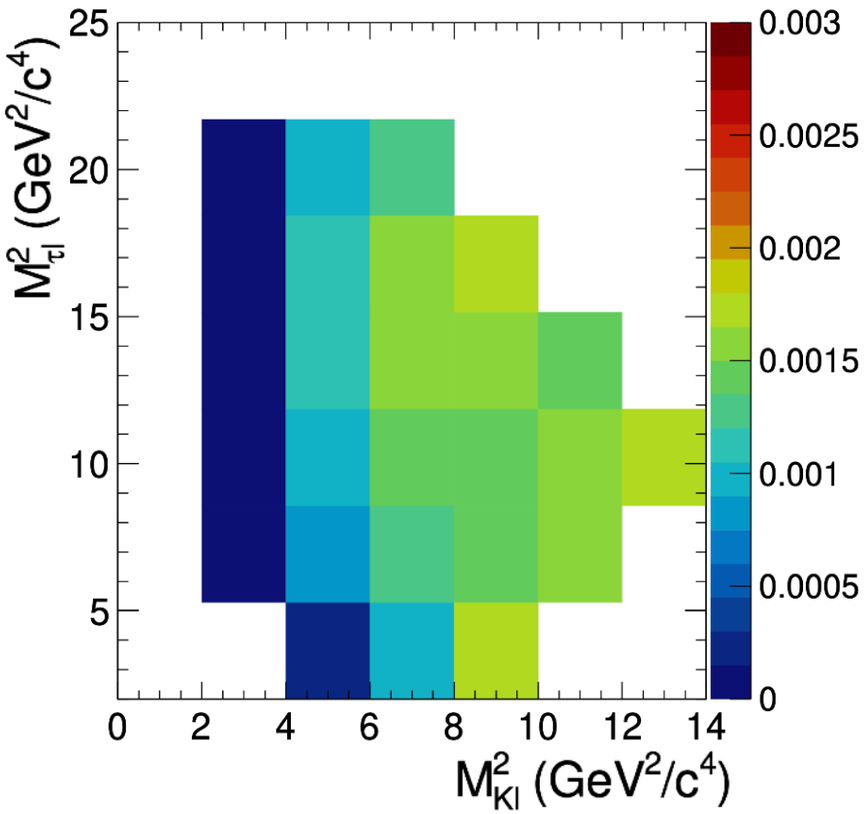

$B^0_{d,s} \to \tau\ell$ SEARCHES AT BELLE

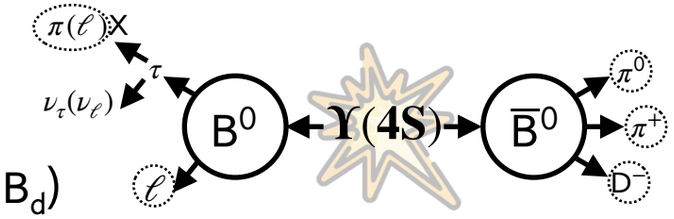

- $\Upsilon(4S) \to B^0\bar{B}^0$ events (700M B_d)
- Hadronic B^0 tagging
- $B^0_{tag}\ell^\pm$ with $M_{miss} \in [1.4, 2.2]\ \mathrm{GeV}/c^2$
- Unbinned extended ML fit to M_{miss} distribution

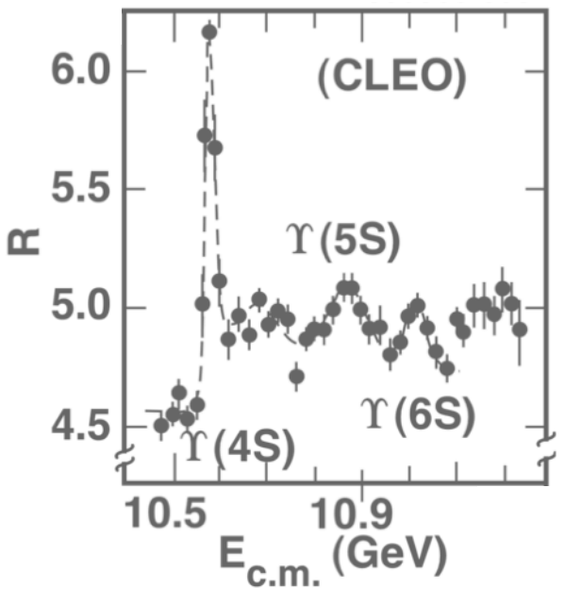

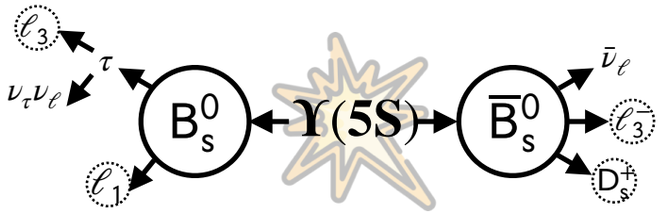

- $\Upsilon(5S) \to B_s^{(*)0}\bar{B}_s^{(*)0}$events (17M B_s)
- Semileptonic B^0_s tagging
- BDT classifier for background suppression
- U.L. estimation based on N_{sig} in $p_1^* \in [2.1, 2.7]\ \mathrm{GeV}/c^2$ [1]

121 fb^{-1}@$\Upsilon(5S)$

PRD 104, L091105 (2021)

$B^0 \to \tau\mu$

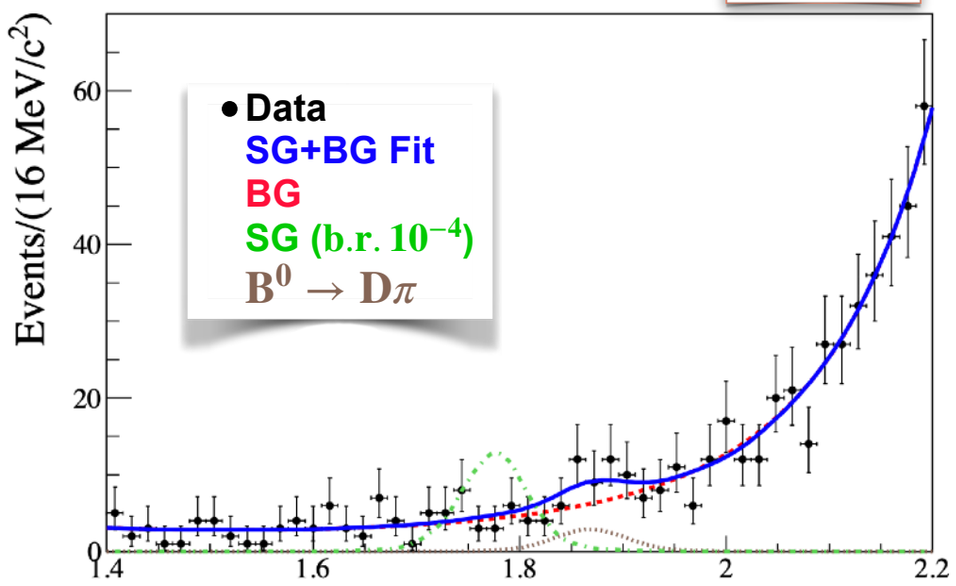

$M^2_{miss} = [(\sqrt{s}, \mathbf{0}) - (E^*_B, \vec{\mathbf{p}}^*_B) - (E^*_\ell, \vec{\mathbf{p}}^*_\ell)]^2$

2301.10989, submitted to JHEP

$B^0_s \to \tau e$

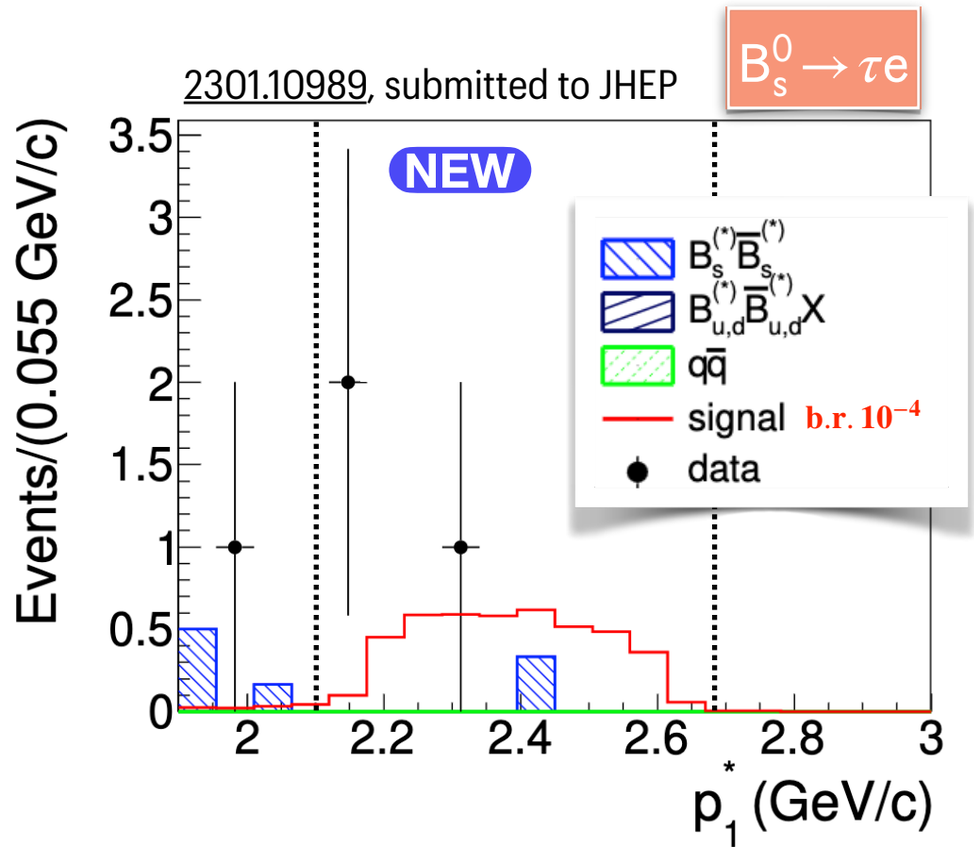

[1] PRD.67.012002

$B^0_{(s)} \to \tau\ell$ SEARCHES AT BELLE

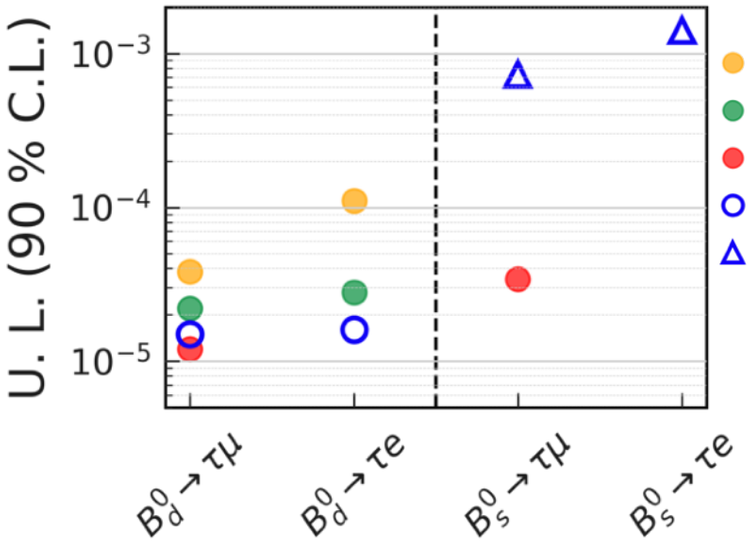

PRL 93, 241802 (2004)
PRD 77, 091104(R) (2008)
PRL 123, 211801 (2019)
PRD 104, L091105 (2021)
arxiv:2301.10989

Decay	BF U.L. @ 90% CL
$B_d \to \tau e$	1.6×10^{-5}
$B_d \to \tau\mu$	1.5×10^{-5}
$B_s \to \tau e$	14.1×10^{-4}
$B_s \to \tau\mu$	7.3×10^{-4}

- U.L. for $B \to e\mu$ are $\mathcal{O}(10^{-9})$ and are dominated by LHCb
- $B_d \to \tau\mu$: Belle ~ LHCb
- $B_{d(s)} \to \tau e$: Best (first) U.L.

HFLAV-10/2022

Main syst. unc. breakdown

$B_d \to \tau\ell$	$B_s \to \tau\ell$
Tagging (4.5%)	N_{Bs} (16.1%)
Lepton ID (1.6%)	Tagging (15%)
N_{BB} (1.4%)	Lepton ID (4.3%)

- BDT classifier for background suppression
- U.L. estimation based on N_{sig} in the p_1^* signal region [1]

[1] PRD.67.012002

SUMMARY

Rare *B* decays offer unique search opportunities at Belle(II)

First Belle II measurement of $\mathcal{B}(B \to X_s\gamma)$ with hadronic B-tagging (190 fb^{-1})

$B^+ \to K^+\nu\nu$ - Powerful inclusive B-tagging approach. Ongoing analysis with 362 fb^{-1}
Consistency with SM will be established at Belle II

Clarifications of $B \to K^{(*)}\ell\ell$, $R_{K^{(*)}}$ require more data (longer term, 5-10 ab^{-1}), healthy redundancy with LHCb

$B \to K\tau\tau$ **more challenging, expected world leading sensitivity**

Belle still has the largest $\Upsilon(4,5S)$ datasets - searches for LFV processes

$B_s^0 \to \ell\tau$: first U.L. for $\ell = e$

$B^+ \to K^+\ell\tau$: **the most stringent UL's to-date** - Benefit from software improvements in Belle II (e.g. FEI)

Do not miss tomorrow's talk
(2 p.m. @ Amphi Dirac)

"Recent Belle II results on radiative and electroweak penguin decays" (J. Cerasoli)

Thank you for your attention

ADDITIONAL MATERIAL

THE UPGRADE

Belle II TDR, arXiv: 1011.0352

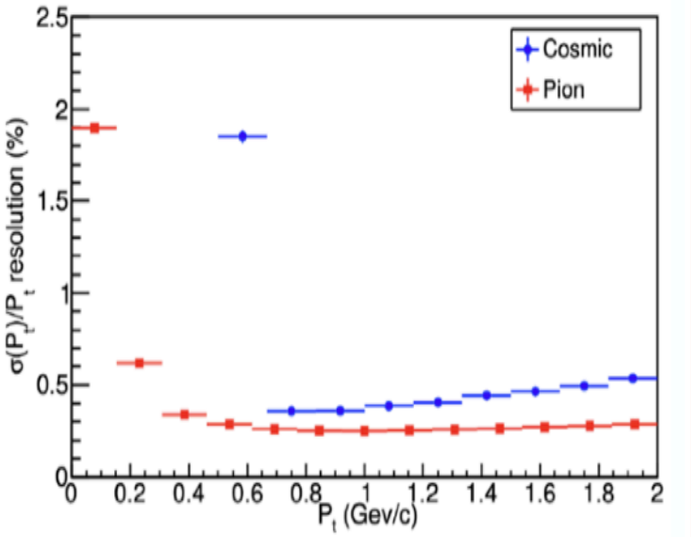

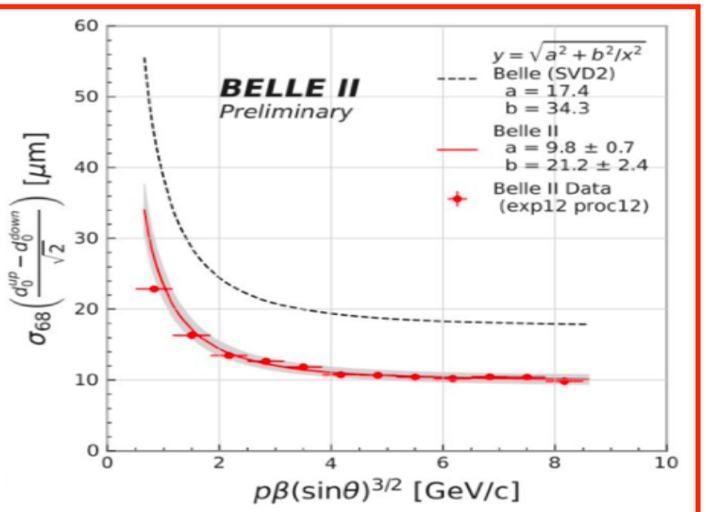

Momentum resolution 20% better than Belle

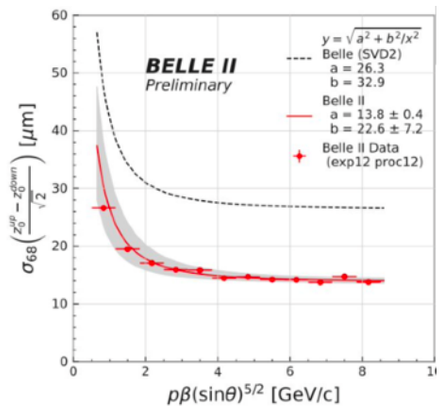

x2 improved resolution on impact parameter (d0,z0)

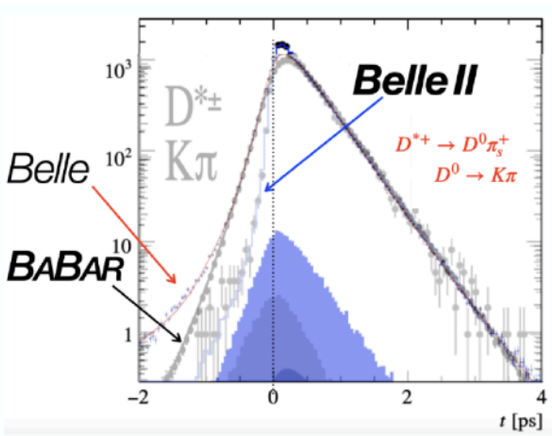

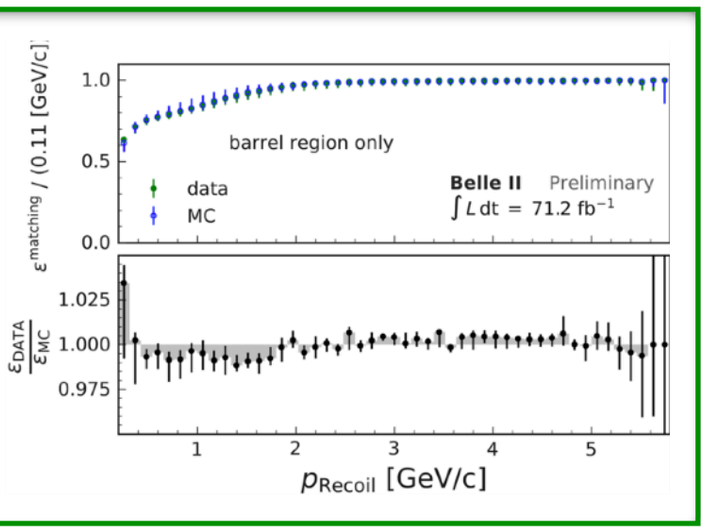

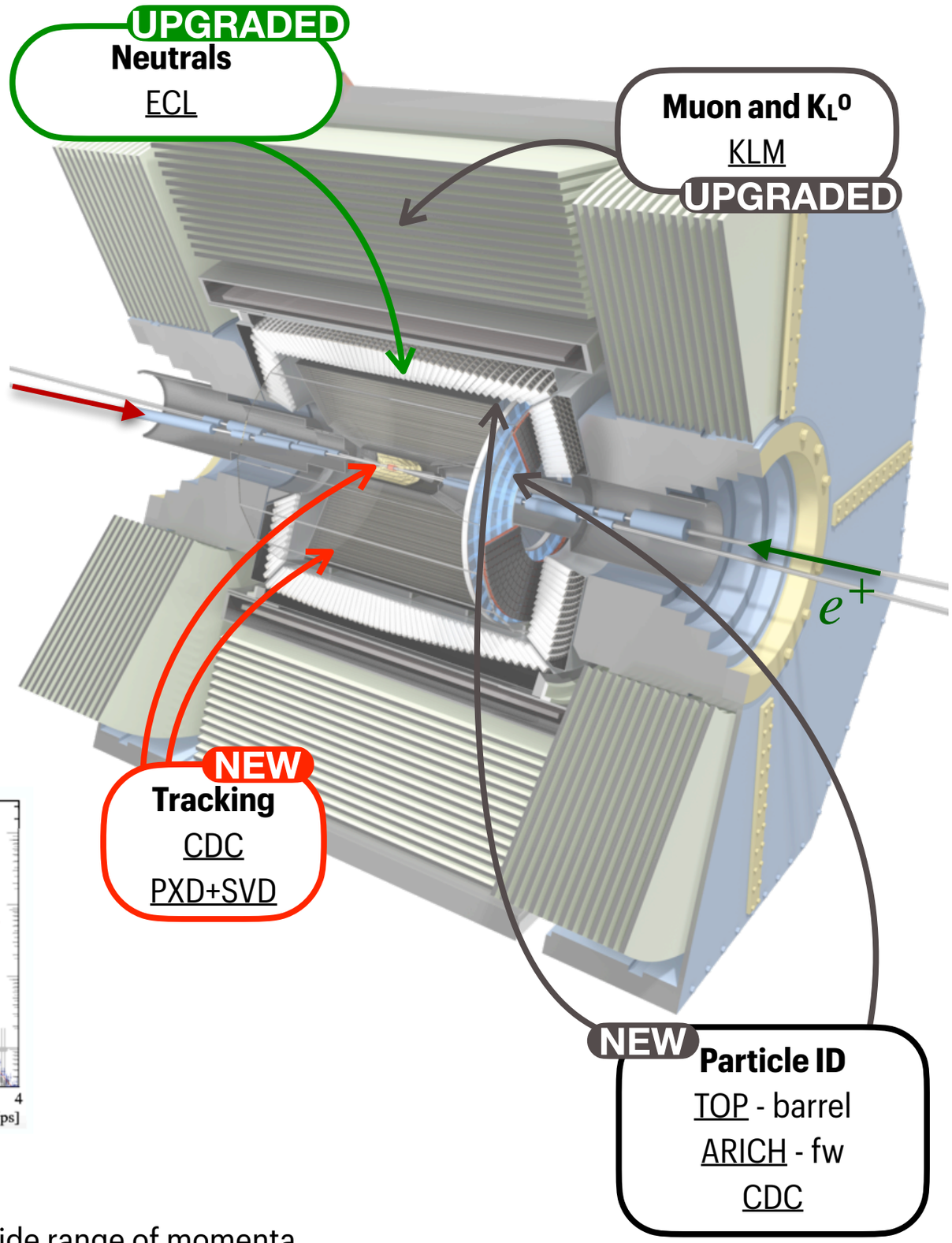

BELLE2-NOTE-PL-2021-008

High photon efficiency on a wide range of momenta

Belle-like resolution on π^0 mass

PARTICLE ID

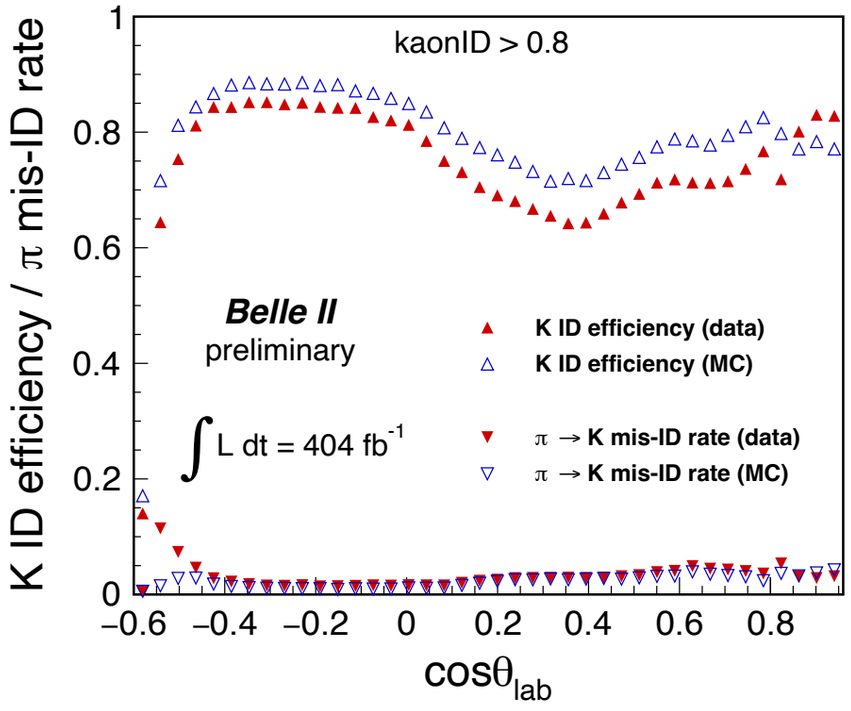

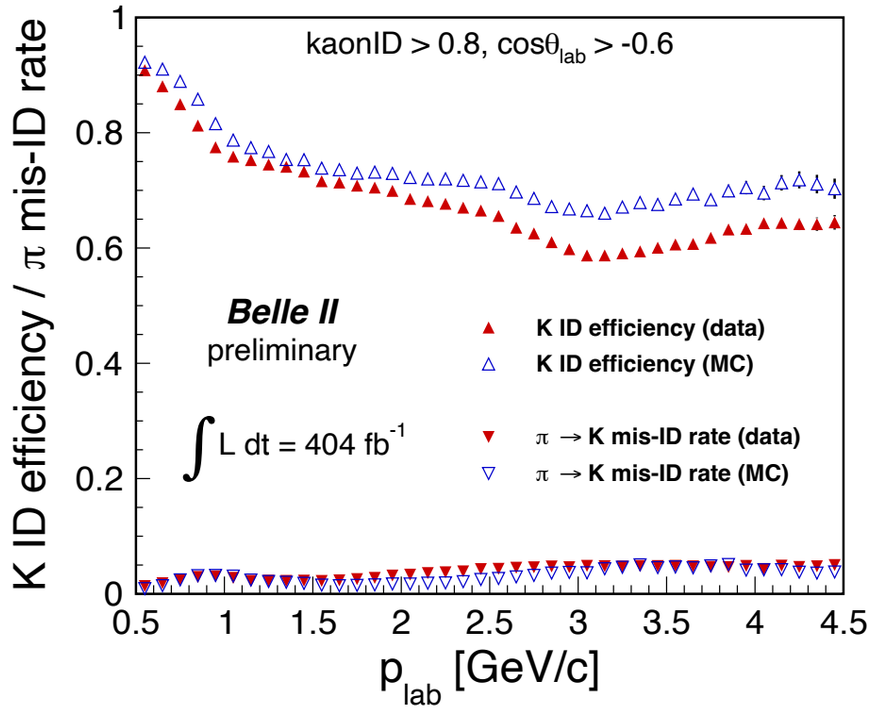

BELLE

	Definition	Cut	Range	Efficiency	Fake rate
e	$L_{\text{eid}} = \frac{\Pi_{i=1}^{N} L_e^i}{\Pi_{i=1}^{N} L_e^i + \Pi_{i=1}^{N} L_{\bar{e}}^i}$	> 0.5	$p \in (1,3)\,\text{GeV}/c$	$(92.4 \pm 0.4)\%$	$\pi: (0.25 \pm 0.02)\%$ $K: (0.43 \pm 0.07)\%$
μ	$\mathcal{L}_\mu = \frac{prob_\mu}{prob_\mu + prob_\pi + prob_K}$	> 0.9	$p \in (1,3)\,\text{GeV}/c$	$(88.8 \pm 0.9)\%$	$\pi: (1.35 \pm 0.07)\%$ $K: (1.7 \pm 0.4)\%$
K	$\text{Prob}(K:\pi)$	> 0.6	$p \in (0.5, 4.0)\,\text{GeV}/c$	$(87.99 \pm 0.12)\%$	$\pi: (8.53 \pm 0.10)\%$

https://doi.org/10.1016/S0168-9002(02)01510-3

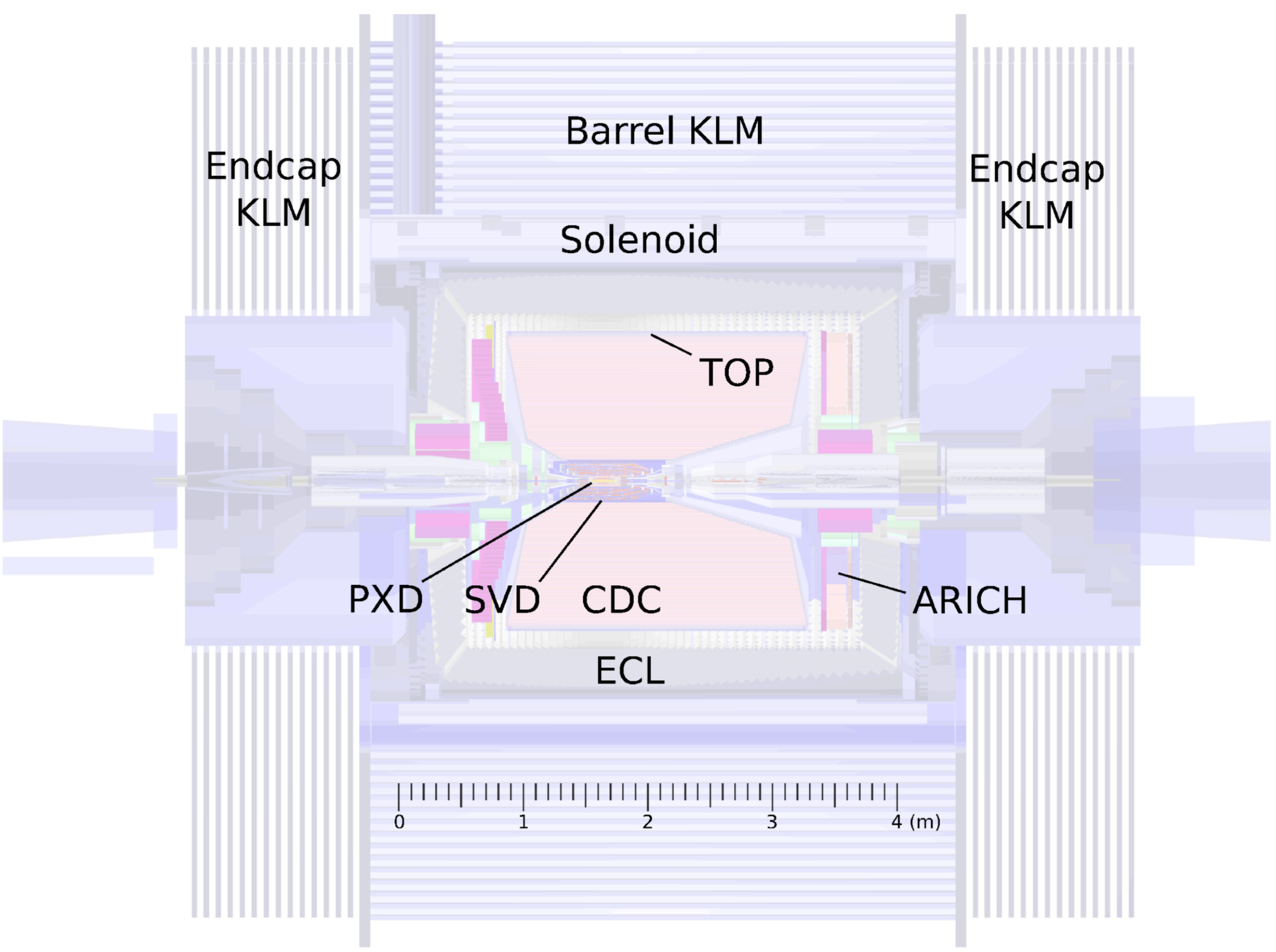
Endcap
KLM
Barrel KLM
Endcap
KLM
Solenoid
TOP
PXD
SVD
CDC
ARICH
ECL
0
1
2
3
4 (m)

BELLE II ECL

- Made up of 8736 CsI(Tl) ~ 30cm crystals, equivalent to 16 radiation lengths (X_0) for electrons and photons

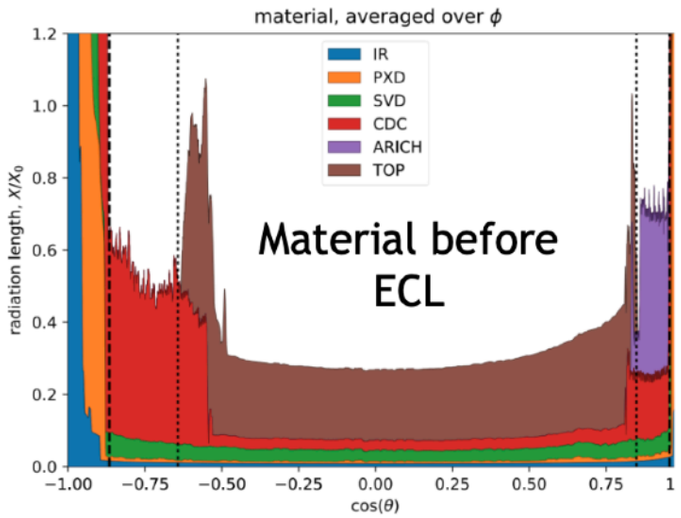

Compared to $2.5X_0$ before LHCB's ECAL

Belle II: $\frac{E}{E_0} = e^{-X/X_0} \approx e^{-0.3} = 74\%$

LHCb: $\frac{E}{E_0} = e^{-2.5} = 8\%$

Better timing resolution at Belle (II) also allows for better bremsstrahlung recovery

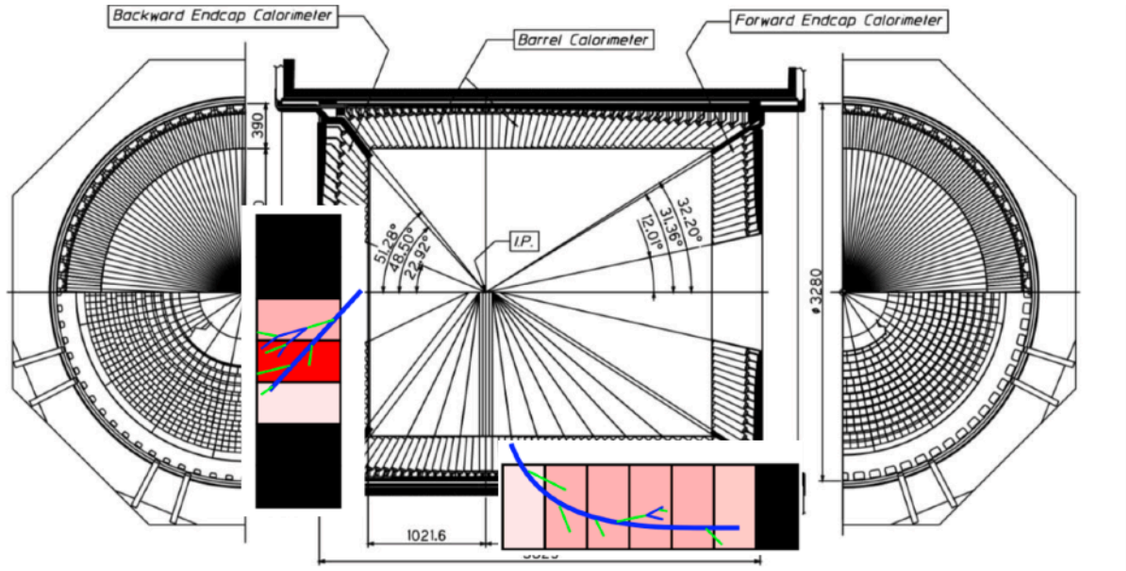

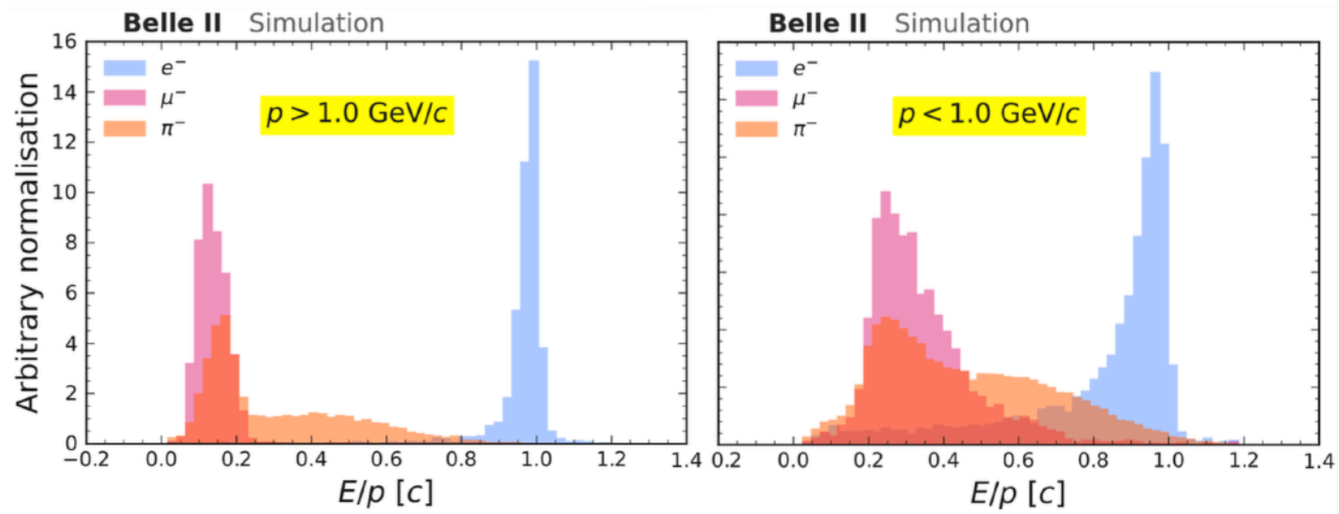

DATA TAKING SCHEDULE

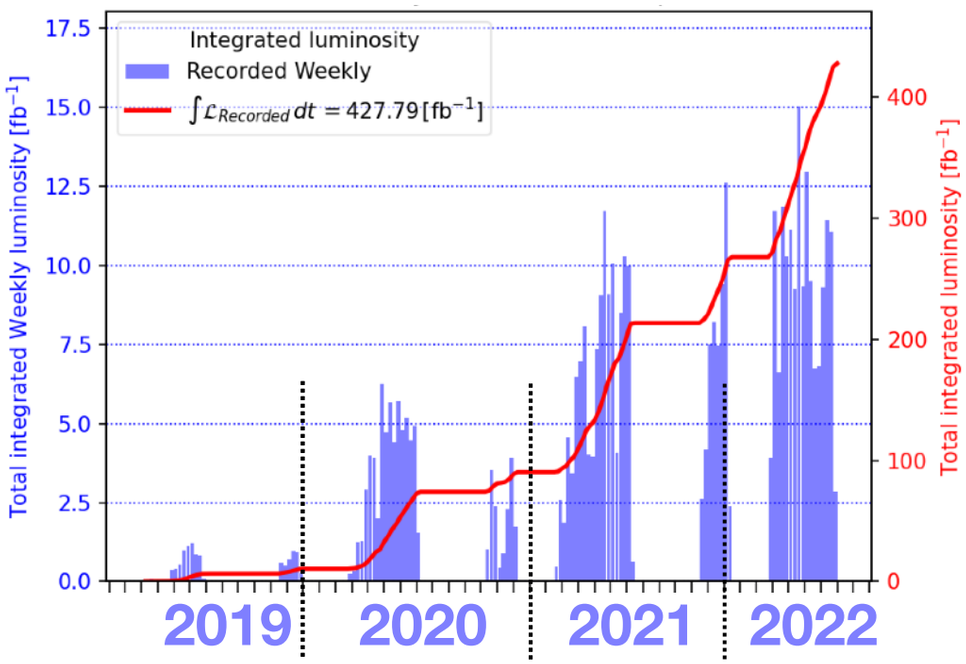

Recorded 424 fb^{-1}

- 362 fb^{-1} at $\Upsilon(4S)$
  cf. BaBar: 424 fb^{-1} at $\Upsilon(4S)$
- 42 fb^{-1} at $\Upsilon(4S)$ – 60 MeV
- 19 fb^{-1} around 10.75 GeV in 2021 autumn to study new structure $\Upsilon(10753)$ observed by Belle in $\pi^+\pi^-\Upsilon(nS)$ transition

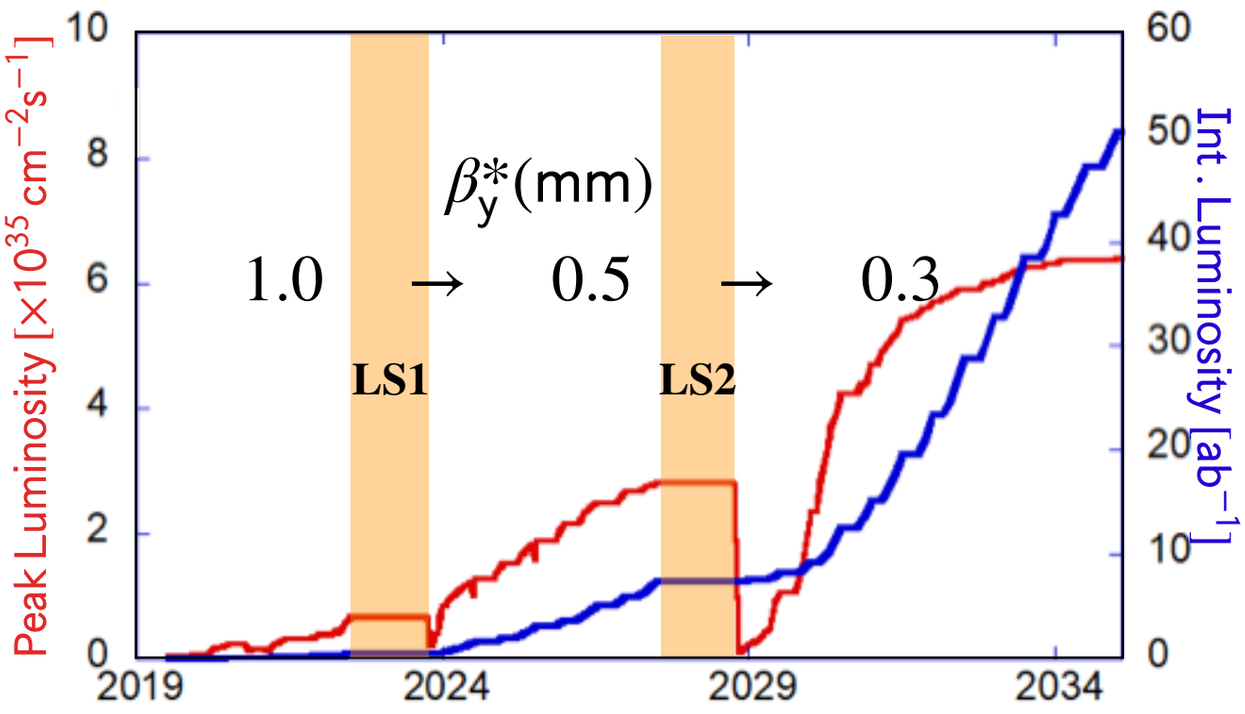

LS1: July 2022 – October 2023

Belle II detector upgrade

- Exchange of PXD (pixel detector) with the full 2nd layer
- TOP conventional MCP-PMT replacement (TBD)
- Migration to new back-end readout (COPPER → PCIe40)

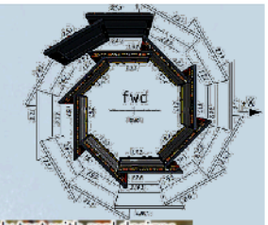

Beam background mitigation

- Additional shield on the QCS(*) bellows
- Additional shield for neutron background
- Installation of a non-linear collimator

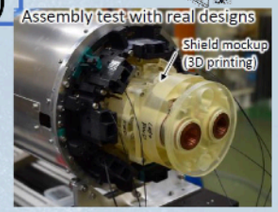

Protection of machine and Belle II

- Collimator heads of more robust material
- Faster beam abort system

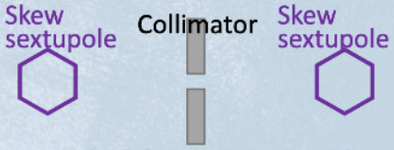

Improvement of beam injection

- Enlarged beam pipe at the HER injection
- Pulse-by-pulse beam control for Linac

Beam kick by skew sextupole:
$\Delta p_y = \frac{SK_2}{2}(y^2 - x^2),\ \Delta p_x = SK_2 xy$

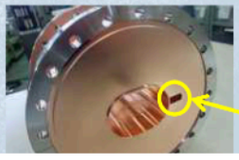

QCS: Final focusing system

SUPERKEKB PERFORMANCE

The world smallest vertical β function ($\beta_y^* = 0.8$ mm) and beam size ($\sigma_y^* \approx 200$ nm) at the interaction point with the "nano-beam scheme".

$$L = \frac{\gamma_\pm}{2er_e}\left(1 + \frac{\sigma_y^*}{\sigma_x^*}\right)\frac{I_\pm \xi_{y\pm}}{\beta_{y\pm}^*}\frac{R_L}{R_{\xi_y}}$$

(cf. KEKB 5.9 mm)

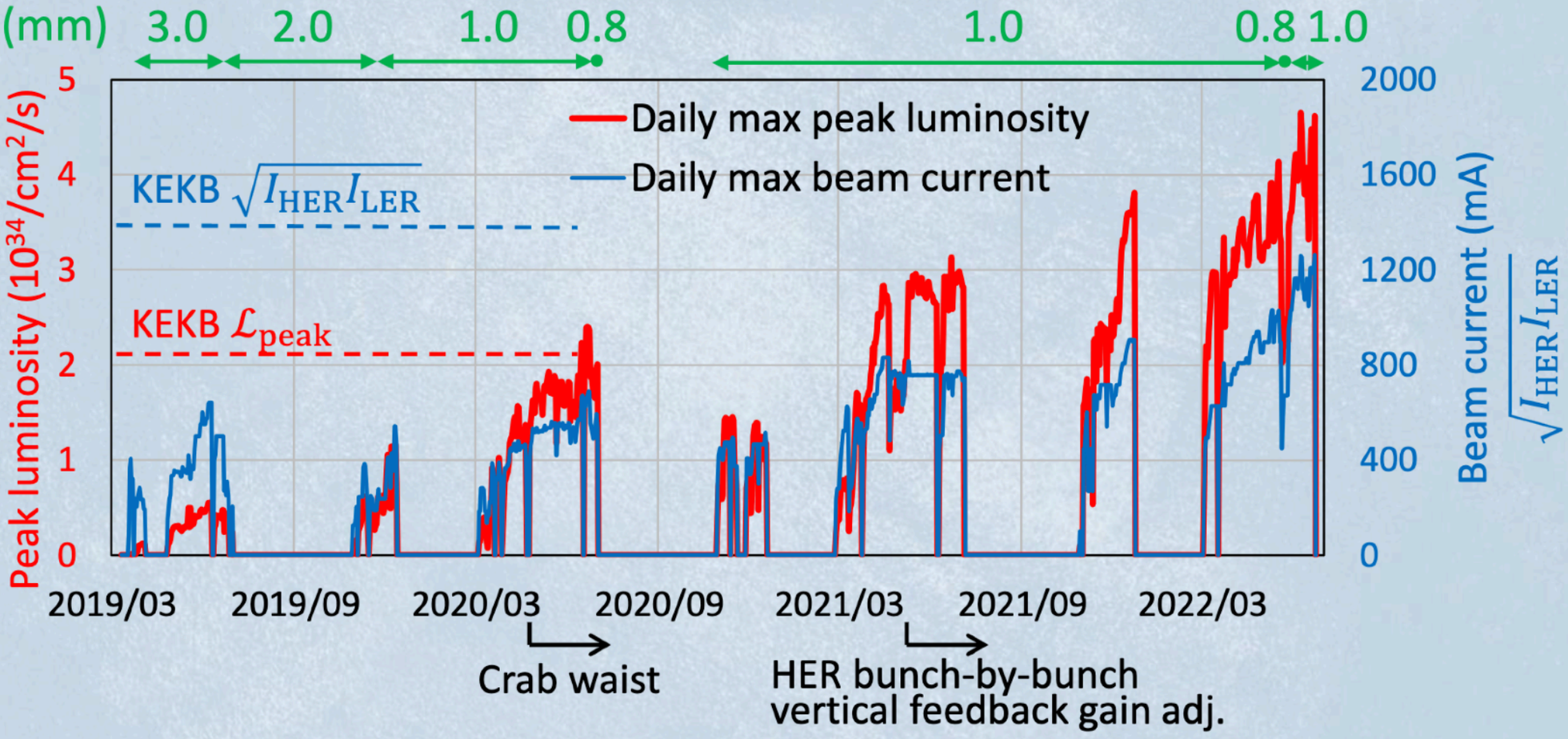

Keep updating the world record of the peak luminosity.

e^+e^- COLLISIONS AT $\sqrt{s} = 10.58$ GEV

2023.01.24 - G*d*M

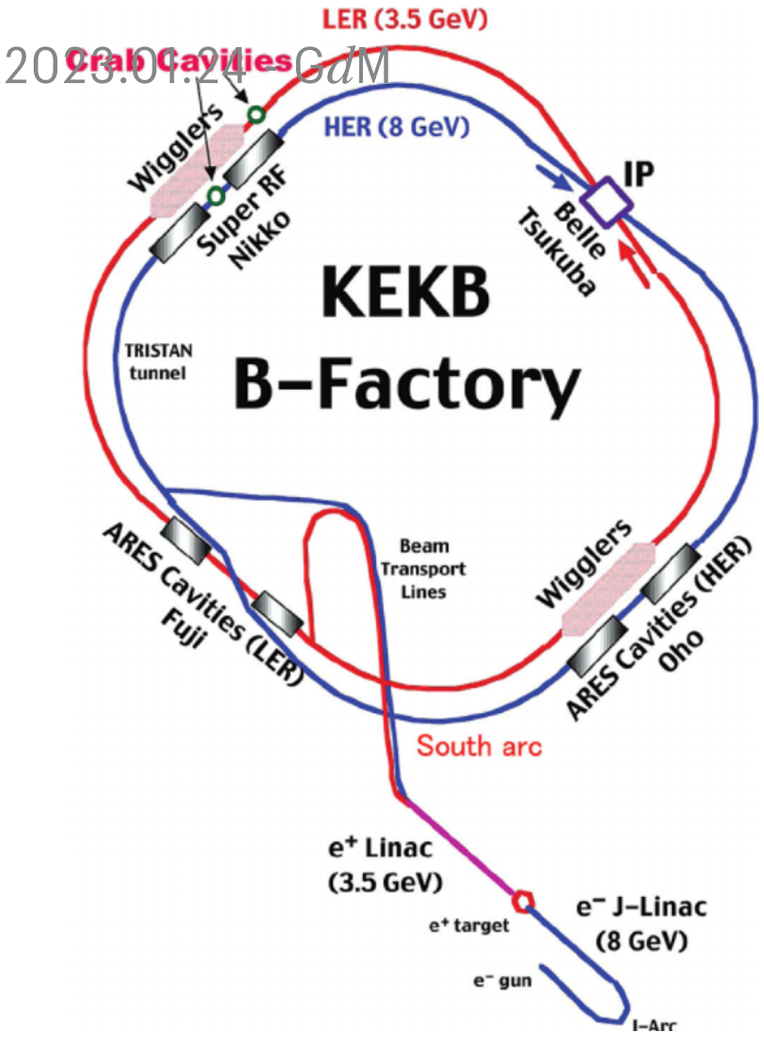

- KEKB: Asymmetric e^+e^- collider
- $\sigma_{\mathrm{tot}} = 143$ nb: Mostly bhabha, $\gamma\gamma$, $e^+e^-(\ell^+\ell^-)$
- Only a small fraction for hadron $q\bar{q}$ production: $\sigma_{\mathrm{tot}}^{\mathrm{had}} \sim 5$ nb

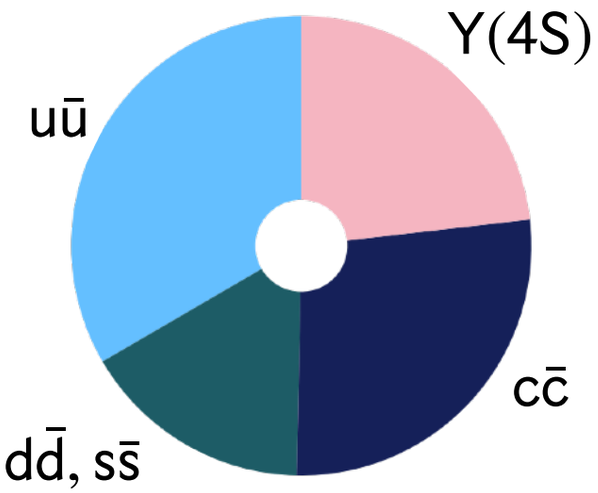

`continuum'
$q\bar{q}$

$\mathcal{B}(\Upsilon(4S) \to B\bar{B}) > 96\,\%$
$(\sigma_{\Upsilon(4S)} = 1.1$ nb$)$

Two B-mesons and nothing else!

$\Upsilon(4S)$ $J^{PC} = 1^{--}$
$\sqrt{s} = m_{\Upsilon(4S)}c^2 = 10.58$ GeV/c^2

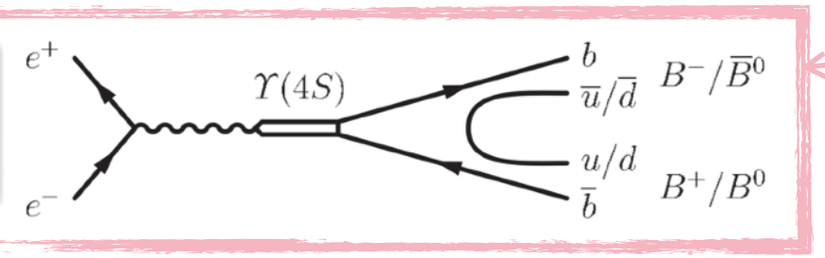

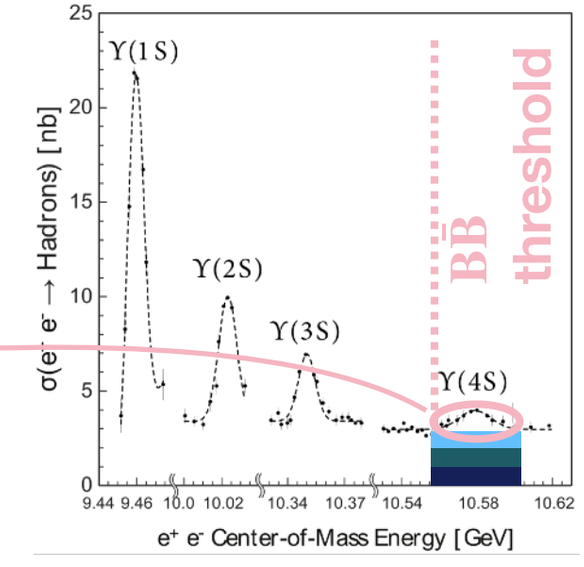

$R_K(J/\psi)$ **TOWARDS** $B \to K\ell\ell$

- Measurement of the tree-level $B \to KJ/\psi$ in preparation for the penguin $B \to K\ell\ell$
- Result with 189 fb^{-1} data
- Signal extracted from a 2-D fit to (M_{bc}, ΔE)

$$R_K(J/\psi) = \frac{\Gamma\left(B \to KJ/\psi(\mu^+\mu^-)\right)}{\Gamma\left(B \to KJ/\psi(e^+e^-)\right)}$$

ΔE fit projections

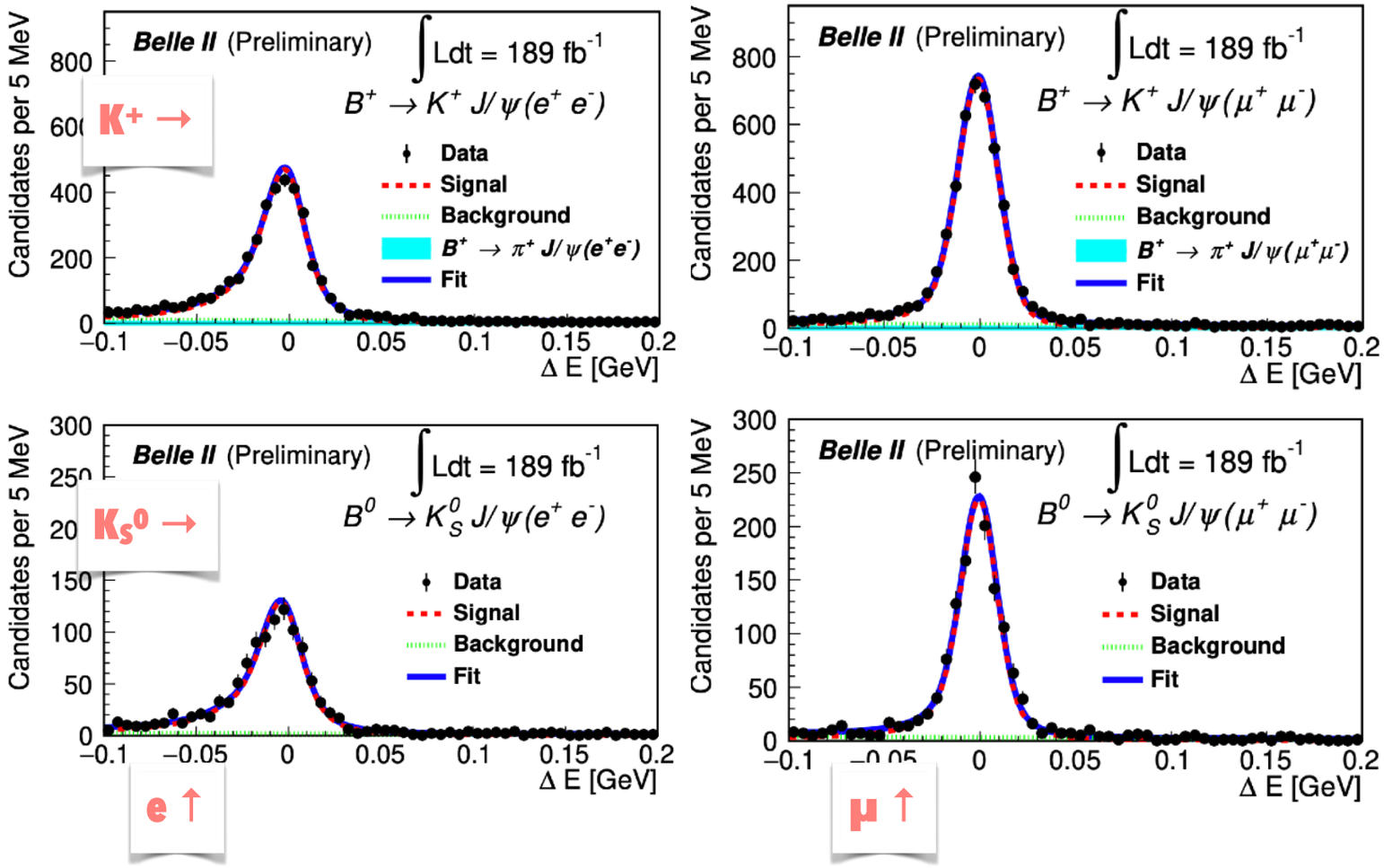

$R_{K^+}(J/\psi) = 1.009 \pm 0.022 \pm 0.008$
$R_{K^0}(J/\psi) = 1.042 \pm 0.042 \pm 0.008$

Belle (2021) JHEP 03 (2021) 105

$R_{K^+}(J/\psi) = 0.994 \pm 0.011 \pm 0.010$
$R_{K^0}(J/\psi) = 0.993 \pm 0.015 \pm 0.010$

Improved syst uncertainty related to lepton-ID

Reminder

$$M_{bc} = \sqrt{E^{*2}_{beam} - p^{*2}_B}$$
$$\Delta E = E^*_B - E^*_{beam}$$
$$E^*_{beam} = \sqrt{s}/2$$

Analysis for $B \to K\ell\ell$ BF measurement on pre-LS1 dataset ongoing!

$B \to X_s\gamma$ INCLUSIVE APPROACH

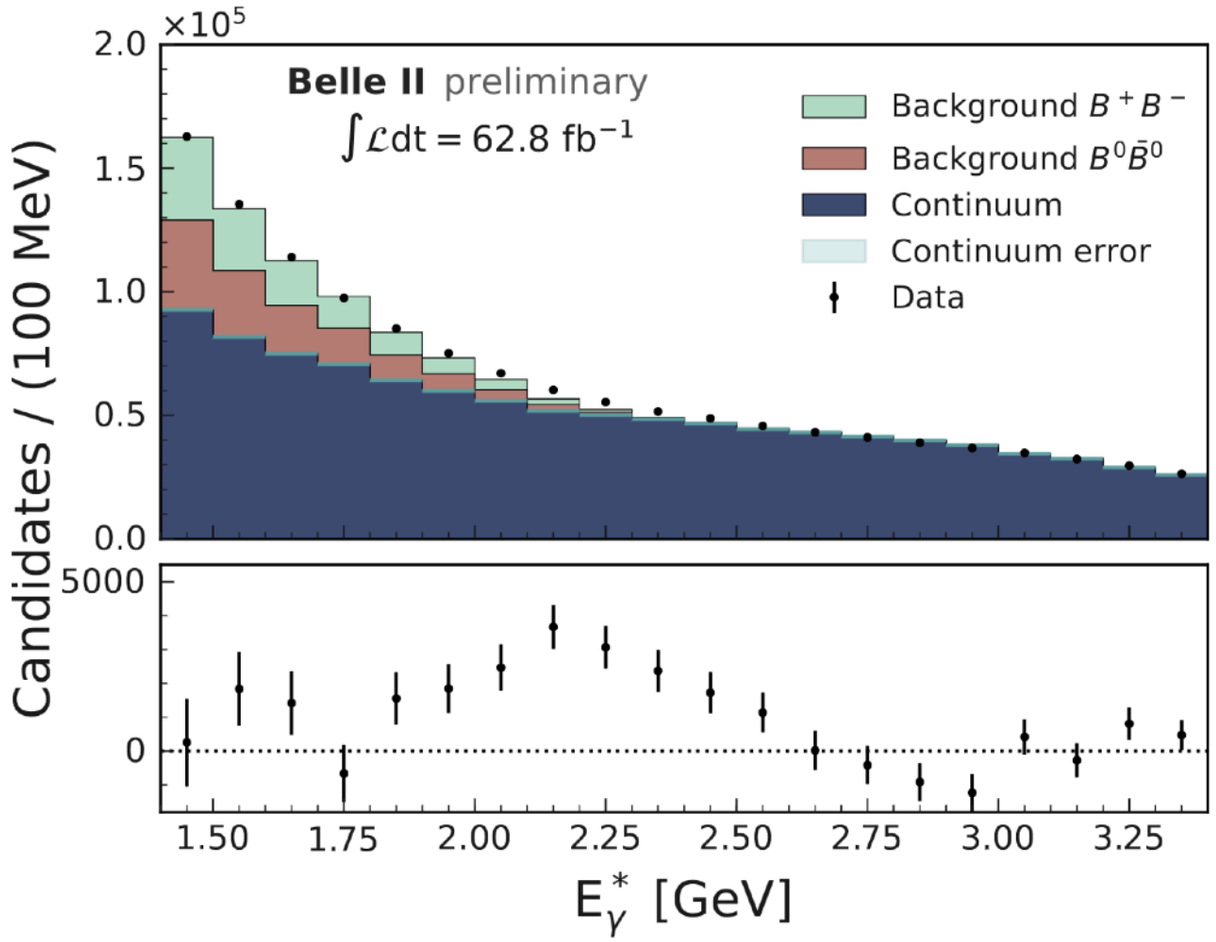

FIG. 1. Photon energy spectrum of selected $b \to (s,d)\gamma$ candidates measured in the $\Upsilon(4S)$ rest frame overlaid with expectations for continuum events and background $B\bar{B}$ events. The data points come from the dataset collected by the Belle II experiment in 2019 and 2020 with integrated luminosity of 62.8 fb^{-1}. The dataset with integrated luminosity of 9.2 fb^{-1} collected below the $\Upsilon(4S)$ resonance is used as a model for the continuum ($e^+e^- \to q\bar{q}$, $q = u,d,s,c$) background: the continuum spectrum are the off-resonance data scaled to match the on-resonance luminosity. The shape of the $B\bar{B}$ background component is obtained from simulation. The $B\bar{B}$ contribution is scaled so that sum of the expectations from $B\bar{B}$ background, continuum, and signal components in the first bin matches the number of observed events in this bin (the expected number of signal events is taken from simulations). The bottom plot shows the difference between the observed number of candidates and the sum of expected number of background candidates for each bin. Bottom plot indicates the evidence for an inclusive $B \to X_{(s,d)}\gamma$ signal. The shown uncertainties are statistical only.

BELLE2-NOTE-PL-2021-004

RADIATIVE DECAYS - 1808.10567

Table 60: Observables accessible in $B \to X_q\gamma$ and the corresponding reconstruction methods. The table uses abbreviations for reconstruction (reco.), hadronic (had.), semi-leptonic and leptonic (SL and L), efficiency (effi.), signal to background ratio (S/B), if the spectator quark may be specified (q), and if the momentum of the signal B meson is measured (p_B).

reco. method	tagging	effi.	S/B	q	p_B	A_{CP}	Δ_{0+}	ΔA_{CP}
sum-of-exclusive	none	high	moderate	s or d	yes	yes	yes	yes
fully-inclusive	had. B	very low	very good	s and d	yes	yes	yes	yes
	SL B	very low	very good	s and d	no	yes	yes	yes
	L	moderate	good	s and d	no	yes	no	no
	none	very high	very bad	s and d	no	no	no	no

Observables	Belle 0.71 ab^{-1} (0.12 ab^{-1})	Belle II 5 ab^{-1}	Belle II 50 ab^{-1}
$\Delta_{0+}(B \to K^*\gamma)$	2.0%	0.70%	0.53%
$A_{CP}(B^0 \to K^{*0}\gamma)$	1.7%	0.58%	0.21%
$A_{CP}(B^+ \to K^{*+}\gamma)$	2.4%	0.81%	0.29%
$\Delta A_{CP}(B \to K^*\gamma)$	2.9%	0.98%	0.36%
$S_{K^{*0}\gamma}$	0.29	0.090	0.030
$\mathrm{Br}(B^0 \to \rho^0\gamma)$	24%	7.6%	4.5%
$\mathrm{Br}(B^+ \to \rho^+\gamma)$	30%	9.6%	5.0%
$\mathrm{Br}(B^0 \to \omega\gamma)$	50%	14%	5.8%
$\Delta_{0+}(B \to \rho\gamma)$	18%	5.4%	1.9%
$A_{CP}(B^0 \to \rho^0\gamma)$	44%	12%	3.8%
$A_{CP}(B^+ \to \rho^+\gamma)$	30%	9.6%	3.0%
$A_{CP}(B^0 \to \omega\gamma)$	91%	23%	7.7%
$\Delta A_{CP}(B \to \rho\gamma)$	53%	16%	4.8%
$S_{\rho^0\gamma}$	0.63	0.19	0.064
$\lvert V_{td}/V_{ts}\rvert_{\rho/K^*}$	12%	8.2%	7.6%
$\mathrm{Br}(B_s^0 \to \phi\gamma)$	23%	6.5%	–
$\mathrm{Br}(B^0 \to K^{*0}\gamma)/\mathrm{Br}(B_s^0 \to \phi\gamma)$	23%	6.7%	–
$\mathrm{Br}(B_s^0 \to K^{*0}\gamma)$	–	15%	–
$A_{CP}(B_s^0 \to K^{*0}\gamma)$	–	15%	–
$\mathrm{Br}(B_s^0 \to K^{*0}\gamma)/\mathrm{Br}(B_s^0 \to \phi\gamma)$	–	15%	–
$\mathrm{Br}(B^0 \to K^{*0}\gamma)/\mathrm{Br}(B_s^0 \to K^{*0}\gamma)$	–	15%	–

HFLAV AVERAGE

$\mathcal{B}(B \to X_s\gamma)$

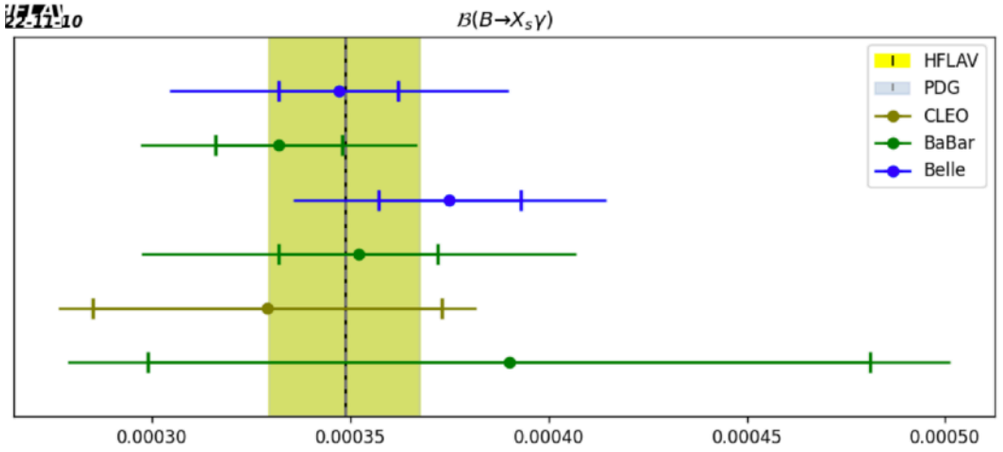

Experiment	Measurement [10^{-4}]	$\Delta\chi^2$	Reference	Comments
Average	3.49 ± 0.19	0.96	$p = 0.97$ (ndf=5)	
PDG	3.49 ± 0.19		pdgLive	
Belle	$3.47 \pm 0.15 \pm 0.40$	0.00	Phys.Rev.Lett. **103**,241801 (2009)	Measurement extrapolated to $E_\gamma > 1.6$ GeV using the met
BaBar	$3.32 \pm 0.16 \pm 0.31$	0.23	Phys.Rev.Lett. **109**,191801 (2012)	Measurement extrapolated to $E_\gamma > 1.6$ GeV using the met
Belle	$3.75 \pm 0.18 \pm 0.35$	0.45	Phys.Rev.D **91**,052004 (2015)	Measurement extrapolated to $E_\gamma > 1.6$ GeV using the met
BaBar	$3.52 \pm 0.20 \pm 0.51$	0.00	Phys.Rev.D **86**,052012 (2012)	Measurement extrapolated to $E_\gamma > 1.6$ GeV using the met
CLEO	$3.29 \pm 0.44 \pm 0.29$	0.14	Phys.Rev.Lett. **87**,251807 (2001)	Measurement extrapolated to $E_\gamma > 1.6$ GeV using the met
BaBar	$3.90 \pm 0.91 \pm 0.64$	0.14	Phys.Rev.D **77**,051103 (2008)	Measurement extrapolated to $E_\gamma > 1.6$ GeV using the met

$\mathcal{B}(B \to X_s\gamma)$

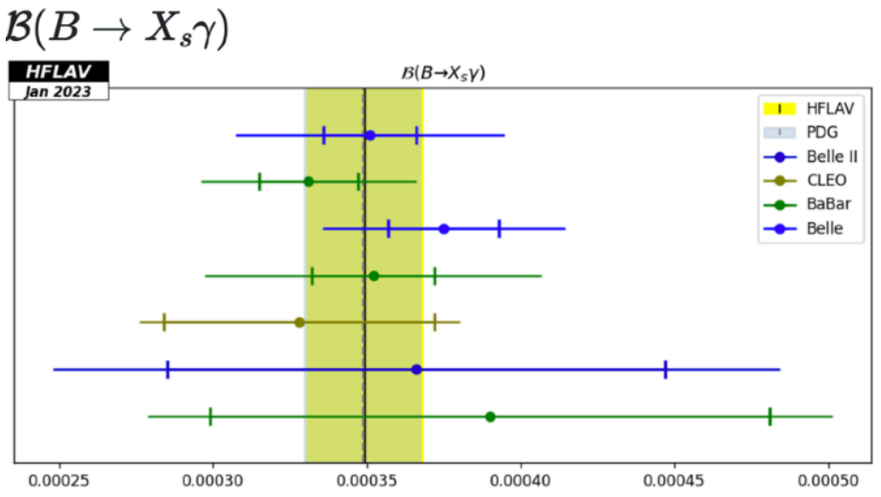

Experiment	Measurement [10^{-4}]	$\Delta\chi^2$	Reference	Comments
Average	3.49 ± 0.19	1.03	$p = 0.98$ (ndf=6)	
PDG	3.49 ± 0.19		pdgLive	
Belle	$3.51 \pm 0.15 \pm 0.41$	0.00	Phys.Rev.Lett. **103**,241801 (2009)	Measurement extrapolated to $E_\gamma > 1.6$ GeV using the m The systematic error includes a shape-function systematic
BaBar	$3.31 \pm 0.16 \pm 0.31$	0.28	Phys.Rev.Lett. **109**,191801 (2012)	Measurement extrapolated to $E_\gamma > 1.6$ GeV using the m The systematic error includes a shape-function systematic
Belle	$3.75 \pm 0.18 \pm 0.35$	0.43	Phys.Rev.D **91**,052004 (2015)	Measurement extrapolated to $E_\gamma > 1.6$ GeV using the m The systematic error includes a shape-function systematic
BaBar	$3.52 \pm 0.20 \pm 0.51$	0.00	Phys.Rev.D **86**,052012 (2012)	Measurement extrapolated to $E_\gamma > 1.6$ GeV using the m The systematic error includes a shape-function systematic
CLEO	$3.28 \pm 0.44 \pm 0.28$	0.17	Phys.Rev.Lett. **87**,251807 (2001)	Measurement extrapolated to $E_\gamma > 1.6$ GeV using the m The systematic error includes a shape-function systematic
Belle II	$3.66 \pm 0.81 \pm 0.86$	0.02	arXiv:2210.10220	Measurement extrapolated to $E_\gamma > 1.6$ GeV using the m The systematic error includes a shape-function systematic
BaBar	$3.90 \pm 0.91 \pm 0.64$	0.13	Phys.Rev.D **77**,051103 (2008)	Measurement extrapolated to $E_\gamma > 1.6$ GeV using the m The systematic error includes a shape-function systematic

input values in blue correspond to yet unpublished results.

TABLE I: Results of the partial branching fraction measurements. The right-hand part of the table shows the main contributions to the systematic uncertainty. Signal efficiency and background modelling uncertainties are correlated (see Sections 9.2 and 9.3).

E_γ^B [GeV]	$\frac{1}{\Gamma_B}\frac{d\Gamma_i}{dE_\gamma^B}(10^{-4})$	Statistical	Systematic	Fit procedure	Signal efficiency	Background modelling	Other
$1.8 - 2.0$	0.48	0.54	0.64	0.42	0.03	0.49	0.09
$2.0 - 2.1$	0.57	0.31	0.25	0.17	0.06	0.17	0.07
$2.1 - 2.2$	0.13	0.26	0.16	0.13	0.01	0.11	0.01
$2.2 - 2.3$	0.41	0.22	0.10	0.07	0.05	0.04	0.02
$2.3 - 2.4$	0.48	0.22	0.10	0.06	0.06	0.02	0.05
$2.4 - 2.5$	0.75	0.19	0.14	0.04	0.09	0.02	0.09
$2.5 - 2.6$	0.71	0.13	0.10	0.02	0.09	0.00	0.04

$B \to K\nu\nu$ - BACKGROUND SUPPRESSION

PRL.127(2021)18,181802

51 features are used to train 2 consecutive binary classifiers (FastBDT) called BDT_1 and BDT_2:

– Event shape

– Kinematics of the K^+ candidate

– variables related to the ROE

– variables related to the $D^{0/+}$suppression

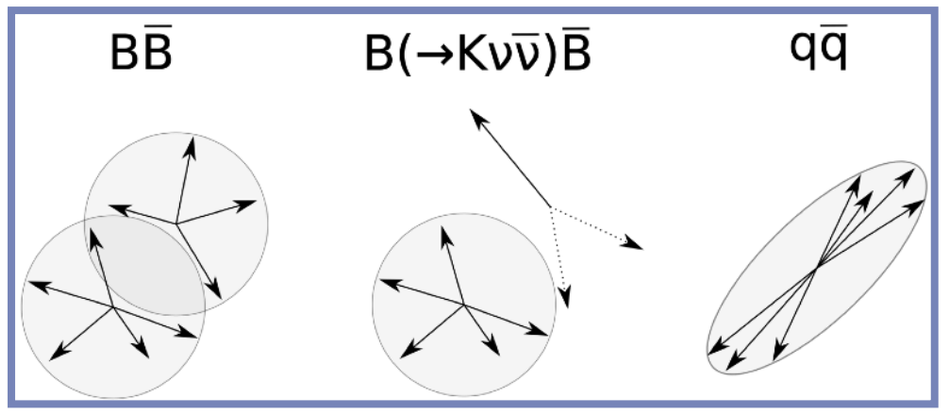

The BDT_2 is trained with the same features on the events with $BDT_1 > 0.9$

Signal region and control regions (used for background estimation) are defined in the $BDT_2 \times p_T(K^+)$ space

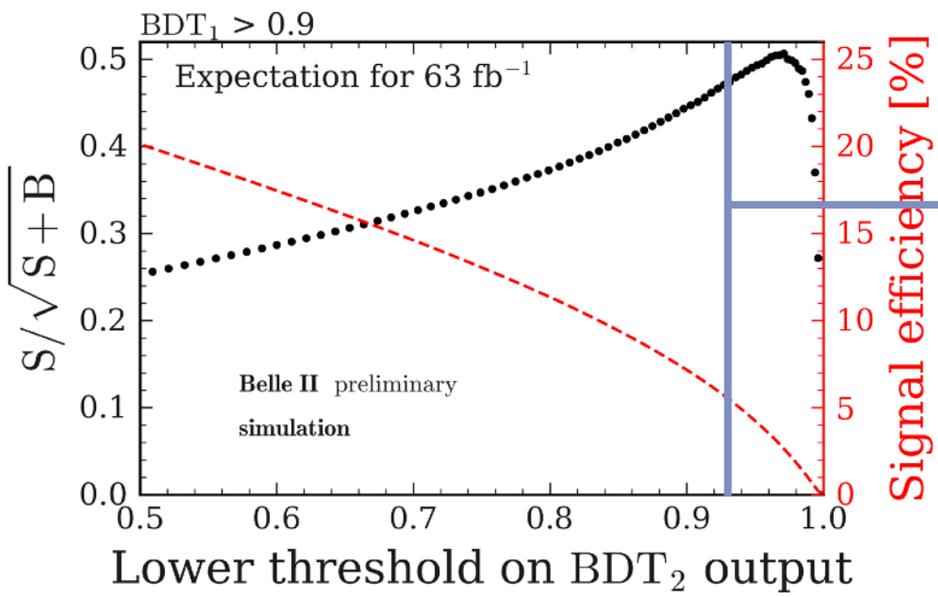

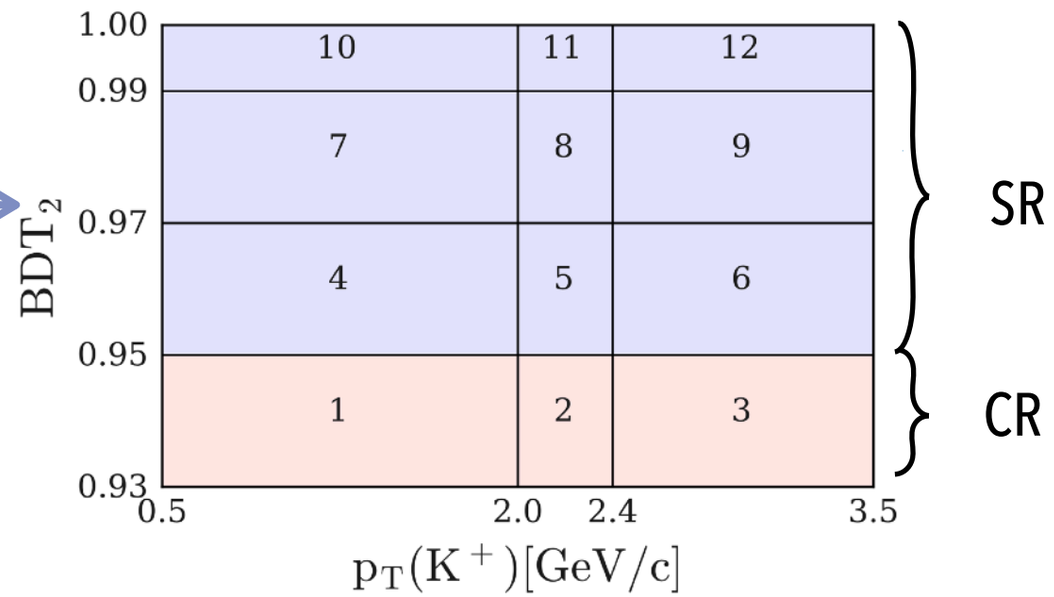

$B \to K\nu\nu$ - VALIDATION

PRL.127(2021)18,181802

The analysis procedure is validated using $B^+ \to K^+ J/\psi(\mu^+\mu^-)$ events. The momentum of the signal kaon (2-body) is corrected to match the spectrum of 3-body $B^+ \to K^+\nu\bar{\nu}$ events

$\mu\mu$'s from the selected J/ψ decays are ignored and the modified events are reconstructed with the inclusive tagging

An excellent Data-MC agreement for the $BDT_{1,2}$ outputs is observed

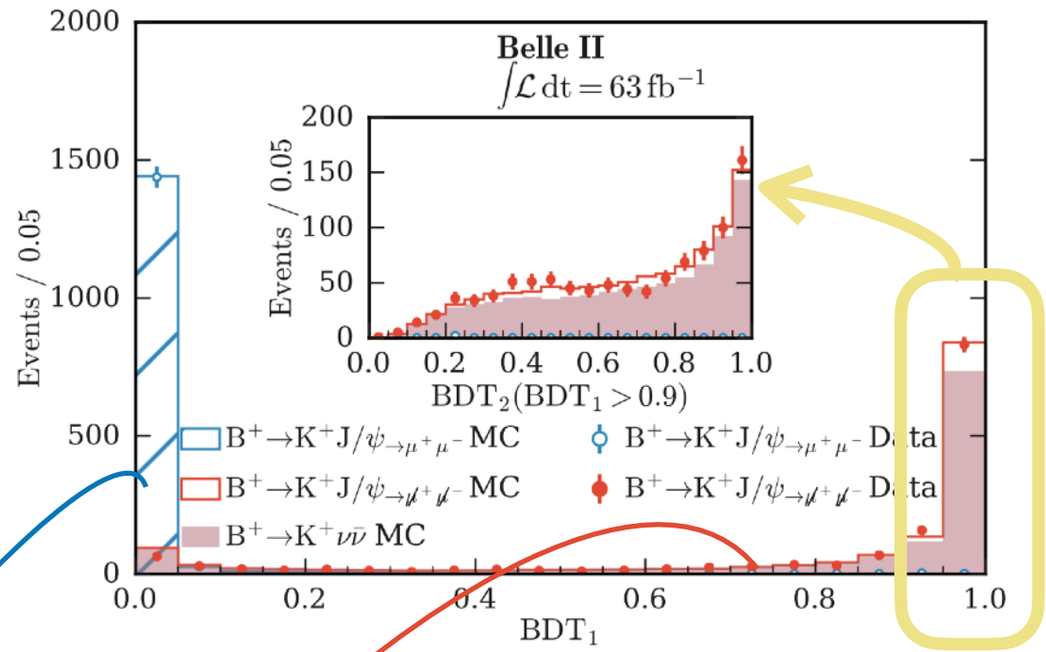

$B^+ \to K^+ J/\psi(\to \mu^+\mu^-)$ events

$B^+ \to K^+ J/\psi(\to \mu^+\mu^-)$ events where $\mu\mu$ are ignored and K^+ kinematics updated.

The Data-MC agreement is also checked with off-resonance data (9 fb^{-1})

A very good Data-MC shape agreement is found but with discrepancy in yields (factor 1.4 ± 0.1)

A 50% normalisation uncertainty in the fit is used

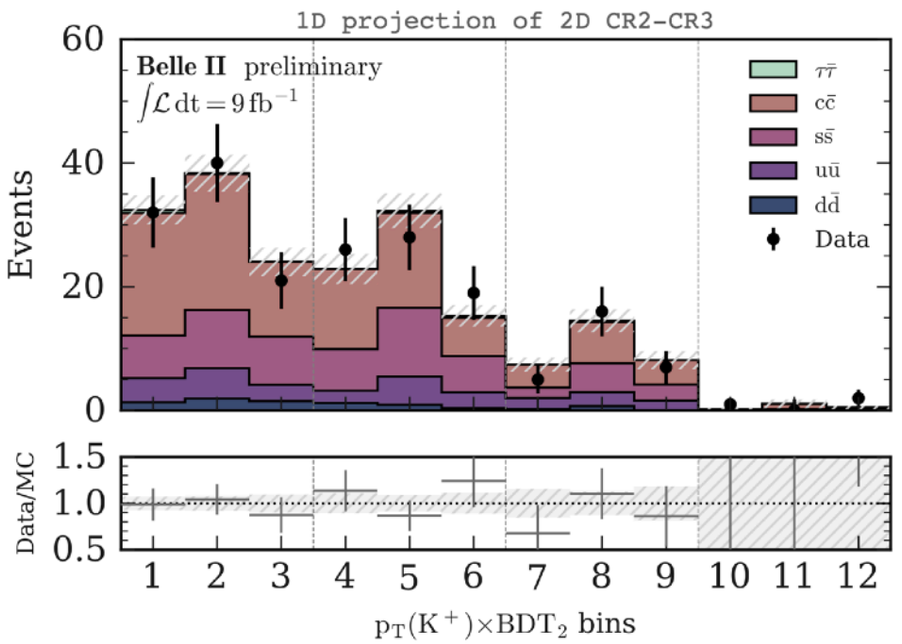

LEPTONIC DECAYS

B⁺→	BF	B-tagging	
τν	[1.25±0.28(stat.)±0.27(syst.)]×10⁻⁴	Semileptonic	Phys.Rev.D 92 (2015) 5, 051102
μν	<8.6×10-7	Inclusive	Phys.Rev.D 101 (2020) 3, 032007
eν	<9.8 x 10^-7	Inclusive	Phys.Lett.B 647 (2007) 67-73

Prospects

2207.06307

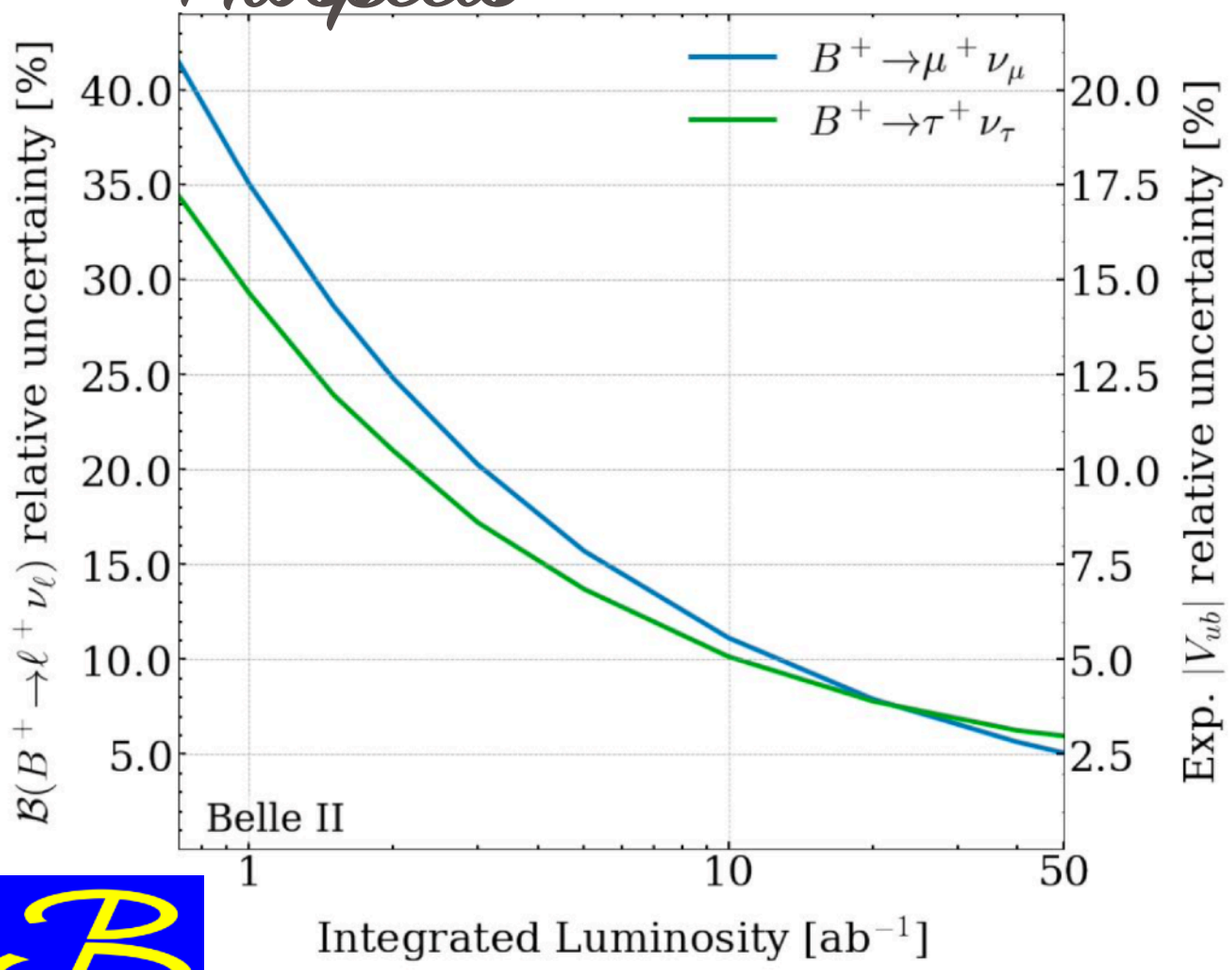

- Leptonic decays $B^+ \to l^+\nu$ are suppressed by $|V_{ub}|$ and helicity factor.
- Small theoretical uncertainty of 0.7%: clean probe of $|V_{ub}|$
- Currently, $B(B^+ \to \tau^+\nu)$ is determined to about 20% accuracy.
- Belle II should observe $B^+ \to \mu^+\nu$ with 5 ab^{-1}, measure $|V_{ub}|$ with 2.5% accuracy for the 50 ab-1 dataset.

S. Glazov, ECFA workshop, DESY, Hamburg, 5 Oct 2022

$B_{(s)} \to \tau\tau$ AT LHC*b*

- $\tau^- \to \pi^-\pi^+\pi^-\nu_\tau$
- Neural network fit performed on events with **both tau's in central box** of pseudo-Dalitz
- Background from **data in control region**: one tau in boxes 4, 5 or 8 and the other in boxes 4 or 8
- Contamination from **residual signal in control region** taken into account

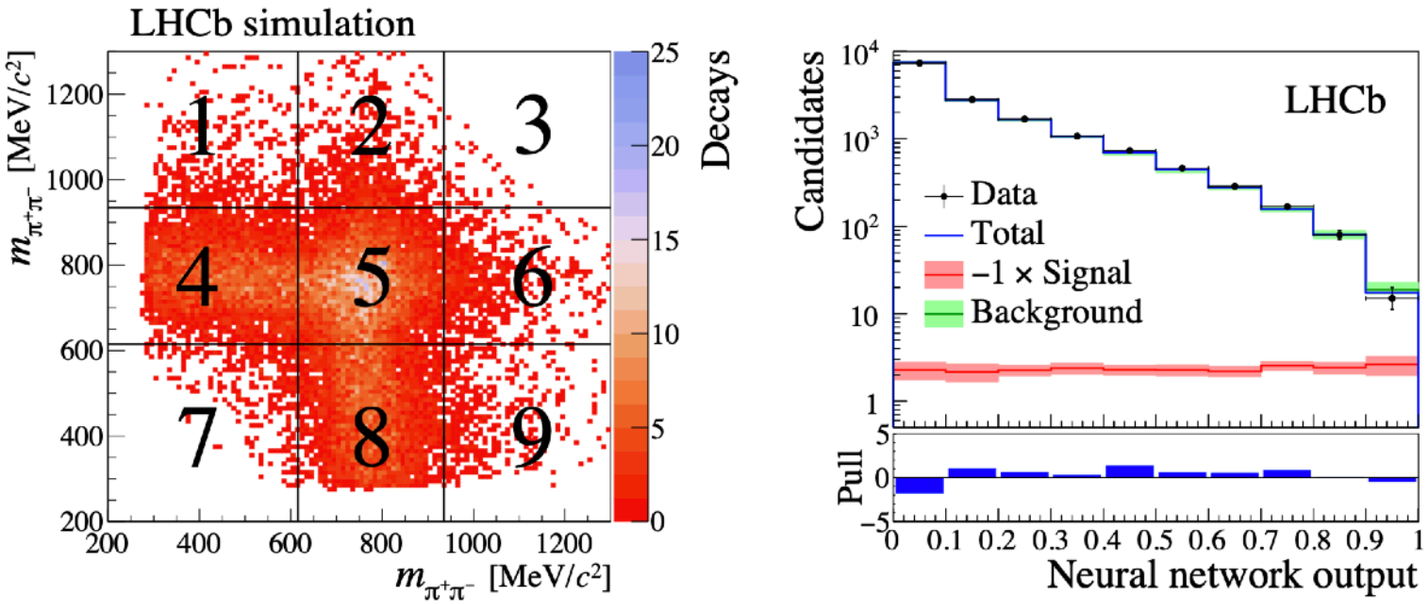

$\mathcal{B}(B^0 \to \tau^+\tau^-) < 2.1 \cdot 10^{-3}$ $\mathcal{B}(B_s^0 \to \tau^+\tau^-) < 6.8 \cdot 10^{-3}$ @ 95 % CL

THEORY

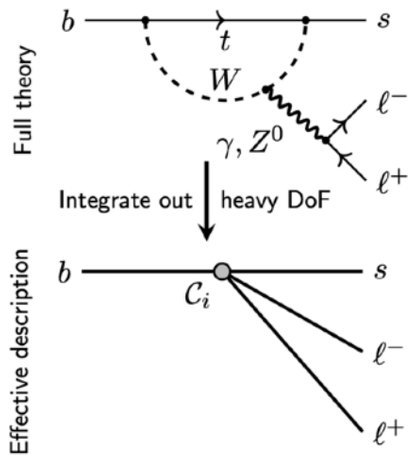

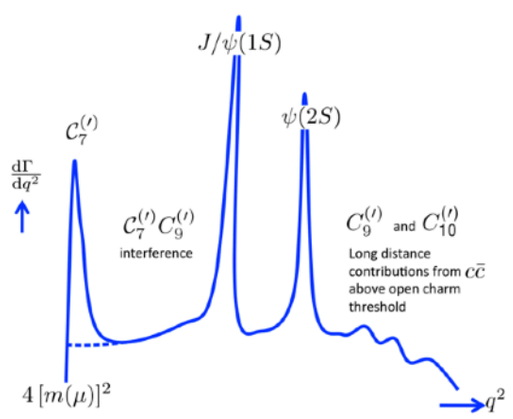

- $b \to s\ell\ell$ transitions described model-independently in effective theory

$$\mathcal{H}_{\text{eff}} = -\frac{4G_F}{\sqrt{2}} V_{\text{tb}} V_{\text{ts}}^* \frac{e^2}{16\pi^2} \sum_i \mathcal{C}_i \mathcal{O}_i$$

Local operator

Wilson coefficient ("effective coupling")

Effective couplings in $b \to s\ell\ell$ transitions

Wilson coefficient		Operator
γ-penguin	$\mathcal{C}_7^{(\prime)}$	$\frac{e}{g^2} m_b (\bar{s}\sigma_{\mu\nu} P_{R(L)} b) F^{\mu\nu}$
ew. penguin	$\mathcal{C}_9^{(\prime)}$	$\frac{e^2}{g^2} (\bar{s}\gamma_\mu P_{L(R)} b)(\bar{\mu}\gamma^\mu \mu)$
	$\mathcal{C}_{10}^{(\prime)}$	$\frac{e^2}{g^2} (\bar{s}\gamma_\mu P_{L(R)} b)(\bar{\mu}\gamma^\mu \gamma_5 \mu)$
scalar	$\mathcal{C}_S^{(\prime)}$	$\frac{e^2}{16\pi^2} m_b (\bar{s} P_{R(L)} b)(\bar{\mu}\mu)$
pseudoscalar	$\mathcal{C}_P^{(\prime)}$	$\frac{e^2}{16\pi^2} m_b (\bar{s} P_{R(L)} b)(\bar{\mu}\gamma_5 \mu)$

For completeness

- Different $q^2 = m^2(\ell^+\ell^-)$ regions probe different operator combinations

U_1 LQ

$$\mathcal{L} = x_L^{ij}\, \bar{Q}_i \gamma_\mu U_1^\mu L_j + x_R^{ij}\, \bar{d}_{Ri} \gamma_\mu U_1^\mu \ell_{Rj} + \text{h.c.}\,,$$

Angelescu et al , 2018

- $b \to c\tau\bar{\nu}$:

$$\mathcal{L}_{\text{eff}} \supset -\frac{\left(x_L^{b\tau}\right)^* \left(V x_L\right)^{c\tau}}{m_{U_1}^2} (\bar{c}_L \gamma^\mu b_L)(\bar{\tau}_L \gamma_\mu \nu_L)$$

- $b \to s\mu\mu$:

$$\mathcal{L}_{\text{eff}} \supset -\frac{\left(x_L\right)^{s\mu} \left(x_L^{b\mu}\right)^*}{m_{U_1}^2} (\bar{s}_L \gamma^\mu b_L)(\bar{\mu}_L \gamma_\mu \mu_L)$$

$$x_L = \begin{pmatrix} 0 & 0 & 0 \\ 0 & x_L^{s\mu} & x_L^{s\tau} \\ 0 & x_L^{b\mu} & x_L^{b\tau} \end{pmatrix}$$

$B^+ \to K^+ \tau \ell$ BACKGROUND NATURE

- After reconstruction the $B\bar{B}$ background is enhanced compared to $q\bar{q}$ because of the *B*-tagging and the presence of a kaon and (at least one) lepton for B_{sig}
- The background composition depends on the charge configuration

$M(K^+X^-)$ with

$$X^-: \begin{cases} \ell^- & \textbf{OS}_\ell \\ t_\tau^- & \textbf{SS}_\ell \end{cases}$$

Signal

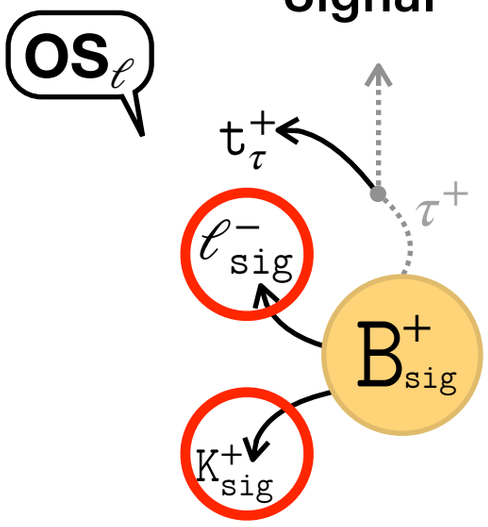

B^+B^- background

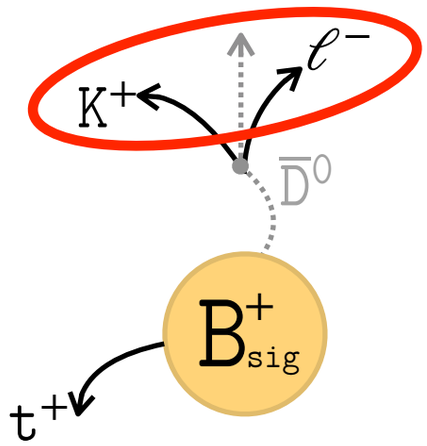

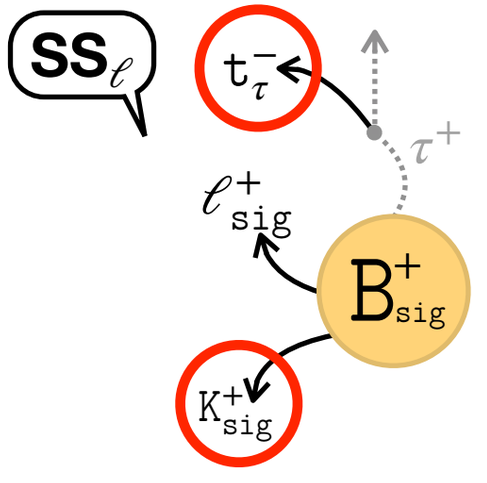

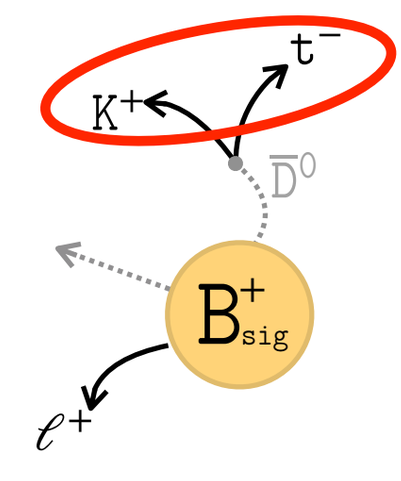

From PDG

$$\Gamma(B^+ \to \bar{D}^0 X) = (79 \pm 4)\,\%$$
$$\Gamma(\bar{D}^0 \to K^+ X) = (54.7 \pm 2.8)\,\%$$

Most important variable for BB background suppression

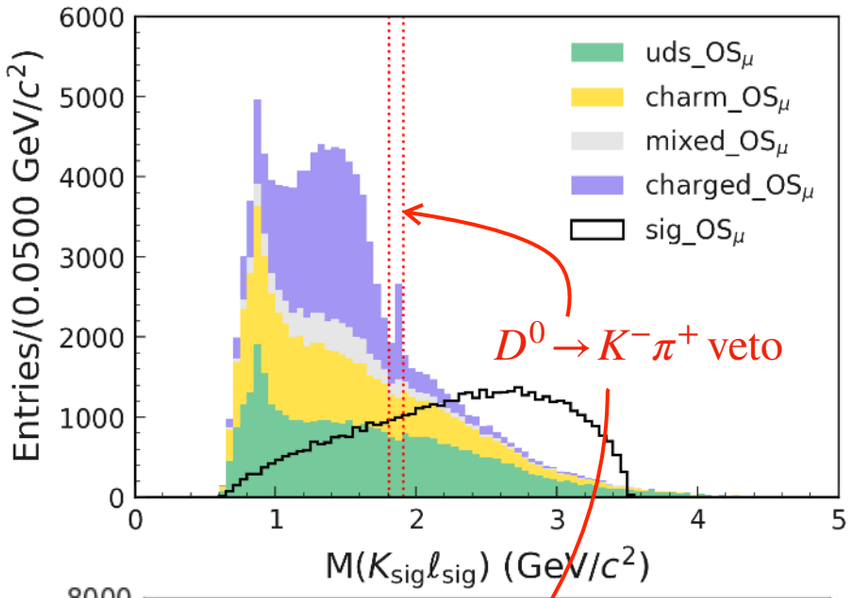

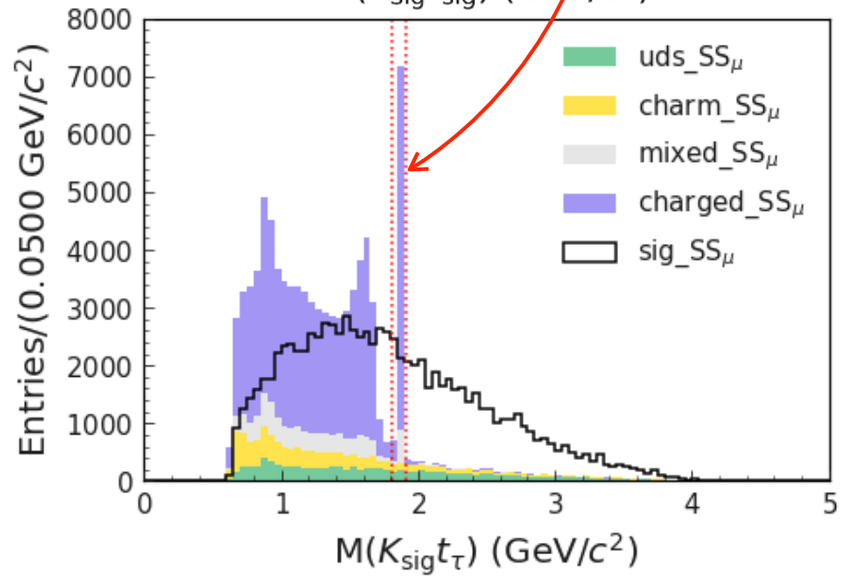

SYSTEMATIC UNCERTAINTIES

Mult. uncertainties:
⇔ number of reco. events

$$\mathcal{B}^{(UL)} = \frac{N_{sig}^{(UL)}}{\varepsilon \times 2N_{B\bar{B}} \times f^{+-}}$$

Data/MC discrepancies affecting the BR measurement are evaluated with ad-hoc control samples

Source	$K^+\tau^+\mu^-$	$K^+\tau^+e^-$	$K^+\tau^-\mu^+$	$K^+\tau^-e^+$
Additive (events)				
PDF shape (mean)	0.09	0.01	0.08	0.08
PDF shape (width)	0.02	0.08	0.04	0.07
PDF shape (f_{sig})	0.28	0.16	0.11	0.16
Linearity	0.03	0.04	0.02	0.04
Total	0.30	0.18	0.14	0.20
Multiplicative (%)				
B_{tag} calibration	5.9	5.9	5.9	5.9
Track reconstruction	1.1	1.1	1.1	1.1
Kaon id.	1.3	1.4	1.3	1.3
Lepton id.	0.3	0.4	0.3	0.4
τ daughter id.	0.7	0.7	0.6	0.6
MC statistics	1.0	1.5	1.2	1.0
Number of $B\bar{B}$ pairs	1.4	1.4	1.4	1.4
BDT $B\bar{B}$ selection	10.6	10.0	12.7	12.6
BDT $q\bar{q}$ selection	8.8	8.6	9.2	6.6
f^{+-}	1.2	1.2	1.2	1.2
Total	15.3	14.8	17.0	15.7

From PDG

$\Gamma(B^+ \to D^- \pi^+ \pi^+) \sim 10^{-3}$

$\Gamma(D^- \to K^+ \pi^+ \pi^+) \sim 10\,\%$

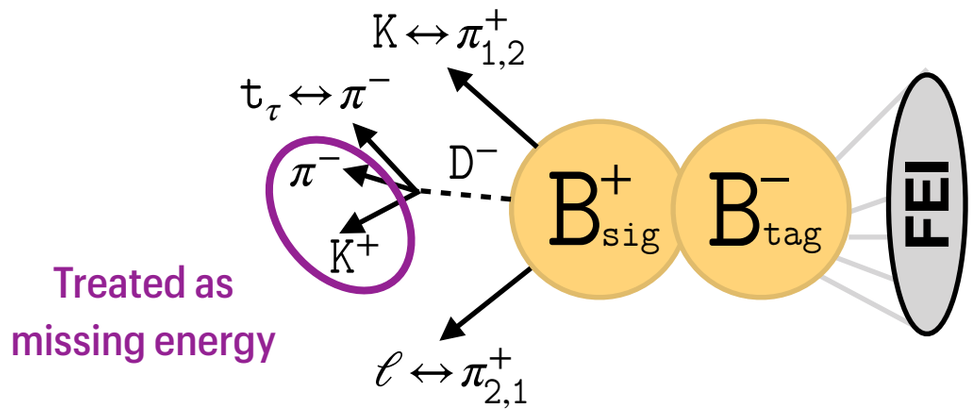

Treated as missing energy

Generated as result of two resonant decays [Belle, BaBar]

$B^+ \to \bar{D}^{**0}(D^-\pi_1^+)\pi_2^+, \quad \bar{D}^{**0} \equiv \{\bar{D}_0^{*0}, \bar{D}_2^{*0}\}$

with randomised assignment of $\{\pi_1, \pi_2\}$ to $\{K, \ell\}$ for $M(Kt_\tau)$ variable (SS mode)

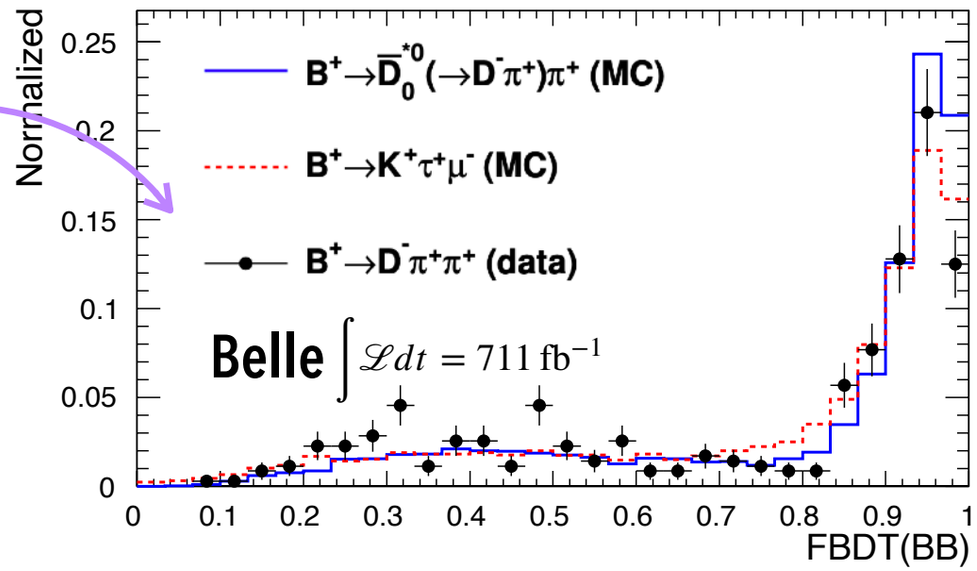

SYSTEMATIC UNCERTAINTIES

Mult. uncertainties:
⇔ number of reco. events

$$\mathcal{B}^{(UL)} = \frac{N_{sig}^{(UL)}}{\varepsilon \times 2N_{B\bar{B}} \times f^{+-}}$$

Data/MC discrepancies affecting the BR measurement are evaluated with ad-hoc control samples

Source	$K^+\tau^+\mu^-$	$K^+\tau^+e^-$	$K^+\tau^-\mu^+$	$K^+\tau^-e^+$
Additive (events)				
PDF shape (mean)	0.09	0.01	0.08	0.08
PDF shape (width)	0.02	0.08	0.04	0.07
PDF shape (f_{sig})	0.28	0.16	0.11	0.16
Linearity	0.03	0.04	0.02	0.04
Total	0.30	0.18	0.14	0.20
Multiplicative (%)				
B_{tag} calibration	5.9	5.9	5.9	5.9
Track reconstruction	1.1	1.1	1.1	1.1
Kaon id.	1.3	1.4	1.3	1.3
Lepton id.	0.3	0.4	0.3	0.4
τ daughter id.	0.7	0.7	0.6	0.6
MC statistics	1.0	1.5	1.2	1.0
Number of $B\bar{B}$ pairs	1.4	1.4	1.4	1.4
BDT $B\bar{B}$ selection	10.6	10.0	12.7	12.6
BDT $q\bar{q}$ selection	8.8	8.6	9.2	6.6
f^{+-}	1.2	1.2	1.2	1.2
Total	15.3	14.8	17.0	15.7

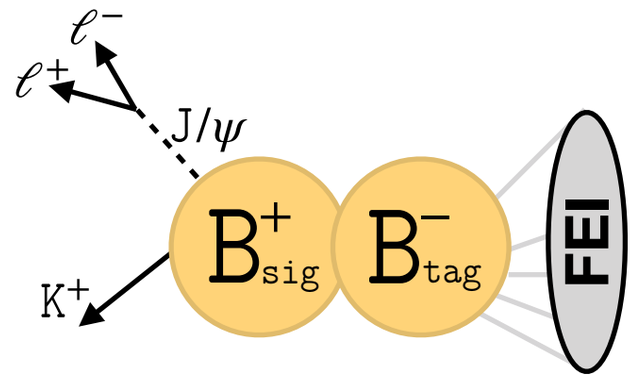

- No need of same decay kinematics
- Good agreement between MC and data

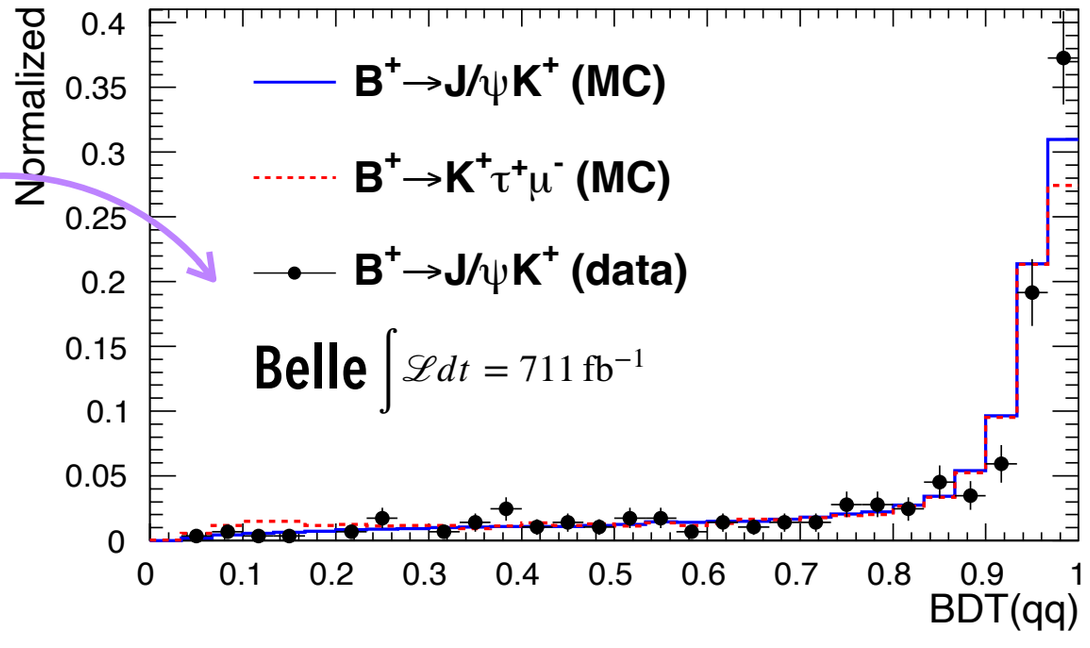

SYSTEMATIC UNCERTAINTIES

Mult. uncertainties:
⇔ number of reco. events

$$\mathcal{B}^{(UL)} = \frac{N_{sig}^{(UL)}}{\varepsilon \times 2N_{B\bar{B}} \times f^{+-}}$$

Data/MC discrepancies affecting the BR measurement are evaluated with ad-hoc control samples

Source	$K^+\tau^+\mu^-$	$K^+\tau^+e^-$	$K^+\tau^-\mu^+$	$K^+\tau^-e^+$
Additive (events)				
PDF shape (mean)	0.09	0.01	0.08	0.08
PDF shape (width)	0.02	0.08	0.04	0.07
PDF shape (f_{sig})	0.28	0.16	0.11	0.16
Linearity	0.03	0.04	0.02	0.04
Total	0.30	0.18	0.14	0.20
Multiplicative (%)				
B_{tag} calibration	5.9	5.9	5.9	5.9
Track reconstruction	1.1	1.1	1.1	1.1
Kaon id.	1.3	1.4	1.3	1.3
Lepton id.	0.3	0.4	0.3	0.4
τ daughter id.	0.7	0.7	0.6	0.6
MC statistics	1.0	1.5	1.2	1.0
Number of $B\bar{B}$ pairs	1.4	1.4	1.4	1.4
BDT $B\bar{B}$ selection	10.6	10.0	12.7	12.6
BDT $q\bar{q}$ selection	8.8	8.6	9.2	6.6
f^{+-}	1.2	1.2	1.2	1.2
Total	15.3	14.8	17.0	15.7

Data/MC FEI efficiency discrepancy

Used efficiency corrections obtained with $B^- \to D^0(K^-\pi^+)\ell^-\bar{\nu}_\ell$ sample.
The overall correction is
$\varepsilon_{D\ell\nu}$: **(86.3 ± 1.4(stat) ± 5.0 (syst))%**
Our average is obtained by re-weighting the calibration factors for each FEI B_{tag} mode, obtaining

$\bar{\varepsilon}$ **: (85 ± 5)% (stat⊕syst)**

Completely consistent with other estimations (with $J/\psi K^+$, $\bar{D}^{(*)0}\pi^+$ samples)

SYSTEMATIC UNCERTAINTIES

Additive uncertainties:
⇔ signal yield fit

$$\mathcal{B}^{(\mathrm{UL})} = \frac{\mathrm{N}_{\mathrm{sig}}^{(\mathrm{UL})}}{\varepsilon \times 2\mathrm{N}_{\mathrm{B\bar{B}}} \times \mathrm{f}^{+-}}$$

Signal shape PDF is fixed from MC and needs calibration

Source	$K^+\tau^+\mu^-$	$K^+\tau^+e^-$	$K^+\tau^-\mu^+$	$K^+\tau^-e^+$
Additive (events)				
PDF shape (mean)	0.09	0.01	0.08	0.08
PDF shape (width)	0.02	0.08	0.04	0.07
PDF shape (f_{sig}) *	0.28	0.16	0.11	0.16
Linearity	0.03	0.04	0.02	0.04
Total	0.30	0.18	0.14	0.20
Multiplicative (%)				
B_{tag} calibration	5.9	5.9	5.9	5.9
Track reconstruction	1.1	1.1	1.1	1.1
Kaon id.	1.3	1.4	1.3	1.3
Lepton id.	0.3	0.4	0.3	0.4
τ daughter id.	0.7	0.7	0.6	0.6
MC statistics	1.0	1.5	1.2	1.0
Number of $B\bar{B}$ pairs	1.4	1.4	1.4	1.4
BDT $B\bar{B}$ selection	10.6	10.0	12.7	12.6
BDT $q\bar{q}$ selection	8.8	8.6	9.2	6.6
f^{+-}	1.2	1.2	1.2	1.2
Total	15.3	14.8	17.0	15.7

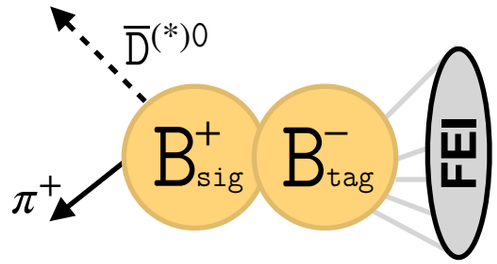

Mean and width of PDF are calibrated with **inclusive** $B^+ \to \overline{D}^{(*)0}\pi^+$ **sample**

Signal PDF
right-sided Crystal Ball (CB) + Gaussian (G)

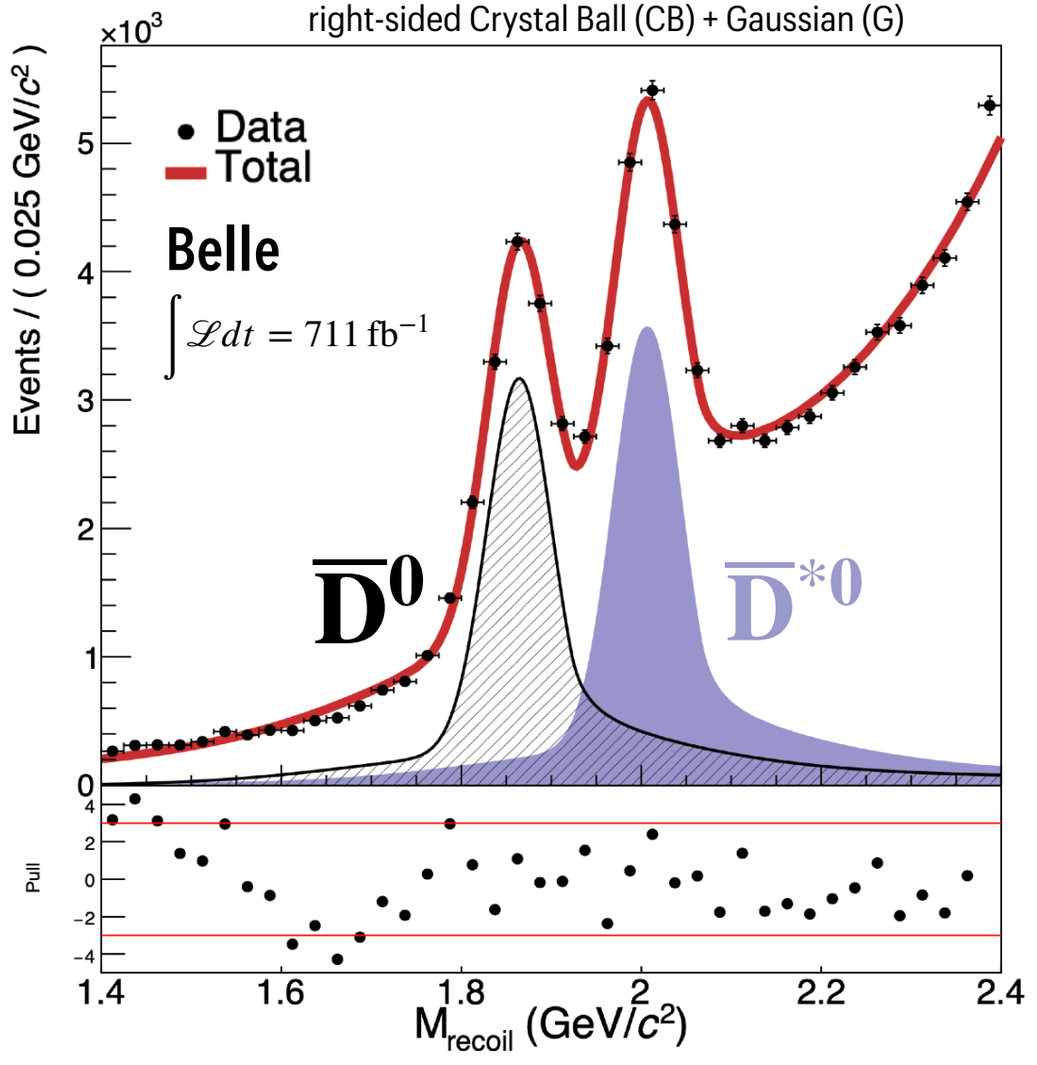

* We vary $f_{sig}(\leftrightarrow f_{\mathrm{CB}})$ by $\pm 10\,\%$ to assess the syst. uncertainty on the fixed value from MC

B-ANOMALIES OBSERVABLES

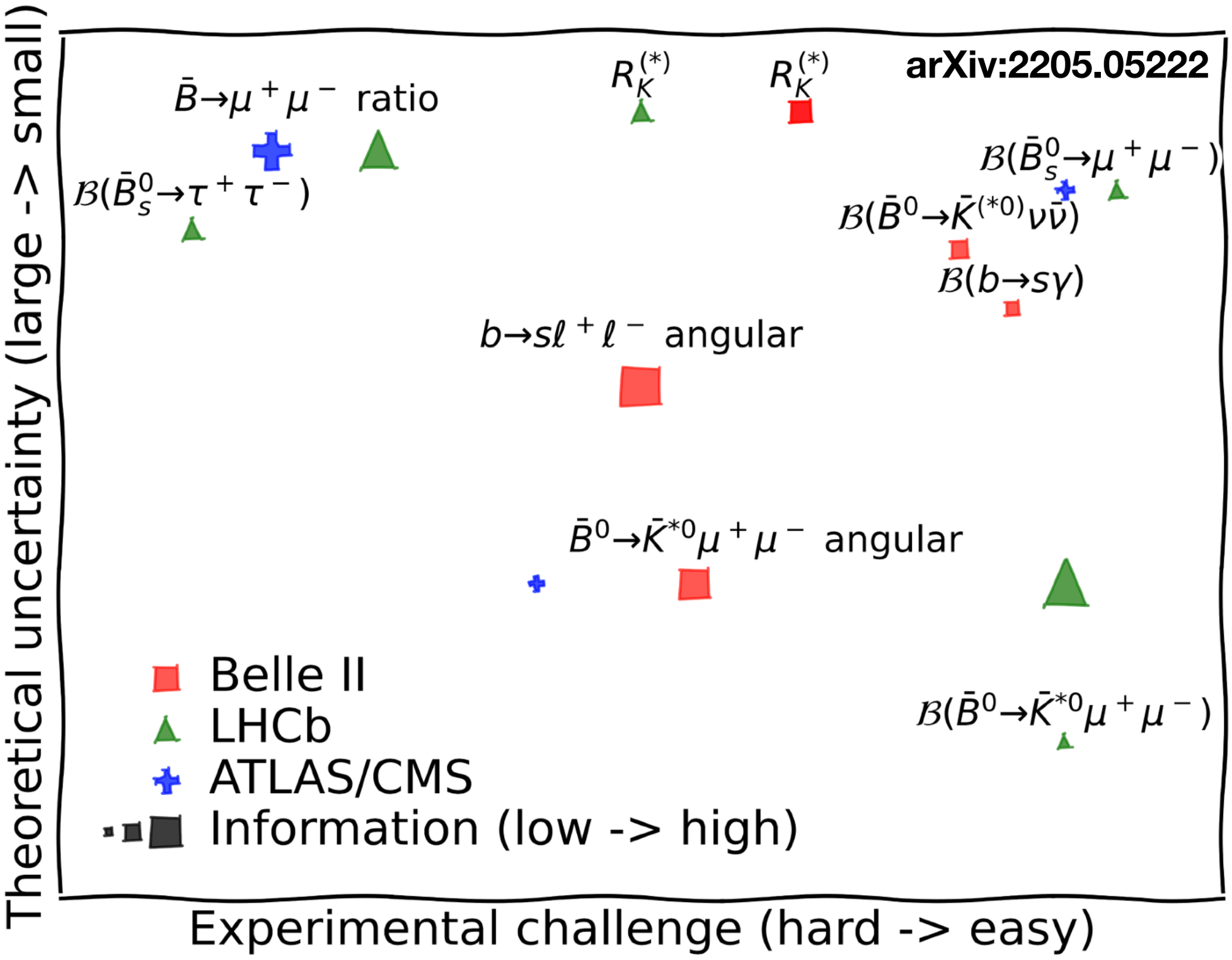

MC PHYSICS MODEL BEYOND PHASE-SPACE

LFV in $\mathrm{b} \to \mathrm{s}\ell\ell$ transitions can be encoded in the $\mathscr{H}_{\mathrm{eff}}$ by effective operators producing different $\mathrm{q}^2 \equiv \mathrm{m}^2_{\ell\tau}$ ($\varepsilon^{\mathrm{NP}}_{\mathrm{sig}}$) from that obtained with the 'baseline' PHSP model ($\varepsilon_{\mathrm{sig}}$)

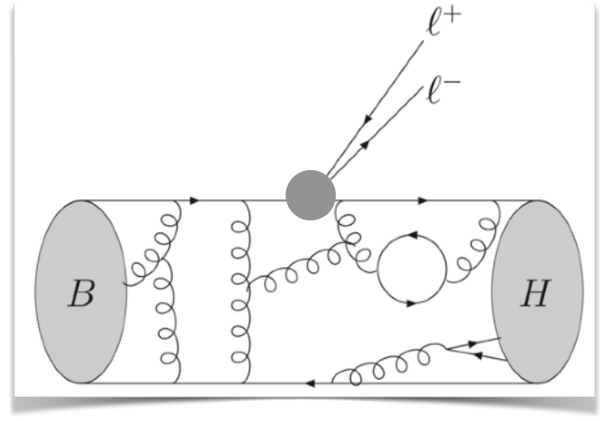

[arXiv:1809.06229]

Wilson Coefficients (effective couplings)

$$\mathscr{H}_{eff}(\mathrm{b} \to \mathrm{s}\ell_1^-\ell_2^+) = -\frac{4\mathrm{G_F}}{\sqrt{2}}\mathrm{V_{tb}V_{ts}^*} \sum_{\mathrm{i=1..9,10,S,P}} \left(\mathrm{C_i^{12}(\mu)O_i^{12}(\mu) + C_i'^{12}(\mu)O_i'^{12}(\mu)}\right)$$

LH RH

At the energy scale $\mu \sim m_b$

Important role for LFUV

Effective operators

$$d\Gamma/dq^2 = \sum_{k=V,S,I} \phi_k(q^2) f_k(C_k)$$

$k = 9(10)$: (axial) **vector**
$k = S(P)$: (pseudo) **scalar**
$k = 9S, 10P$: **interference**

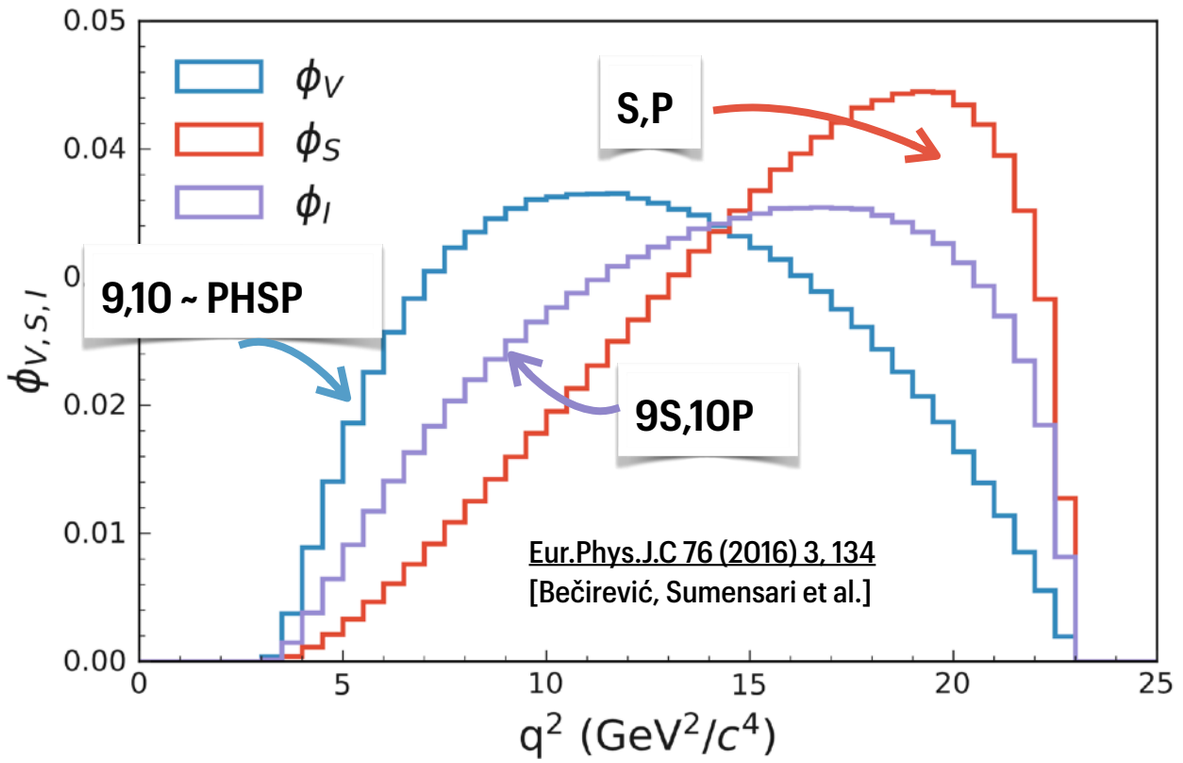

Weight factors assuming the `extreme' BSM scenario (S term) are applied to estimate the lowest $\varepsilon^{\mathrm{NP}}_{\mathrm{sig}}$

TABLES

Decay Mode	$N_{B\overline{B}}$ (10^6)	$\mathcal{B}$ upper limit (90% C.L.)
Lepton flavor violating modes (light flavors):		
$B^0 \to \mu^\pm e^\mp$	85	17×10^{-8}
$B^0 \to \mu^\pm e^\mp$	384	9.2×10^{-8}
$B^+ \to \pi^+ \mu^\pm e^\mp$	230	17×10^{-8}
$B^0 \to \pi^0 \mu^\pm e^\mp$		14×10^{-8}
$B \to \pi \mu^\pm e^\mp$		9.2×10^{-8}
$B^+ \to K^+ \mu^- e^+$	229	9.1×10^{-8}
$B^+ \to K^+ \mu^+ e^-$		13×10^{-8}
$B^+ \to K^+ \mu^\mp e^\pm$		9.1×10^{-8}
$B^0 \to K^0 \mu^\mp e^\pm$		27×10^{-8}
$B \to K \mu^\mp e^\pm$		3.8×10^{-8}
$B^+ \to K^{*0} \mu^- e^+$		53×10^{-8}
$B^+ \to K^{*0} \mu^+ e^-$		34×10^{-8}
$B^+ \to K^{*0} \mu^\mp e^\pm$		58×10^{-8}
$B^+ \to K^{*+} \mu^- e^+$		130×10^{-8}
$B^+ \to K^{*+} \mu^+ e^-$		99×10^{-8}
$B^+ \to K^{*+} \mu^\mp e^\pm$		140×10^{-8}
$B \to K^* \mu^\mp e^\pm$		51×10^{-8}

Decay Mode	$N_{B\overline{B}}$ (10^6)	$\mathcal{B}$ upper limit (90% C.L.)
Lepton flavor violating modes (including τ):		
$B^0 \to \tau^\pm e^\mp$	378	2.8×10^{-5}
$B^0 \to \tau^\pm \mu^\mp$		2.2×10^{-5}
$B^+ \to K^+ \tau^- \mu^+$	472	4.5×10^{-5}
$B^+ \to K^+ \tau^+ \mu^-$		2.8×10^{-5}
$B^+ \to K^+ \tau^\mp \mu^\pm$		4.8×10^{-5}
$B^+ \to K^+ \tau^- e^+$		4.3×10^{-5}
$B^+ \to K^+ \tau^+ e^-$		1.5×10^{-5}
$B^+ \to K^+ \tau^\mp e^\pm$		3.0×10^{-5}
$B^+ \to \pi^+ \tau^- \mu^+$		6.2×10^{-5}
$B^+ \to \pi^+ \tau^+ \mu^-$		4.5×10^{-5}
$B^+ \to \pi^+ \tau^\mp \mu^\pm$		7.2×10^{-5}
$B^+ \to \pi^+ \tau^- e^+$		7.4×10^{-5}
$B^+ \to \pi^+ \tau^+ e^-$		2.0×10^{-5}
$B^+ \to \pi^+ \tau^\mp e^\pm$		7.5×10^{-5}

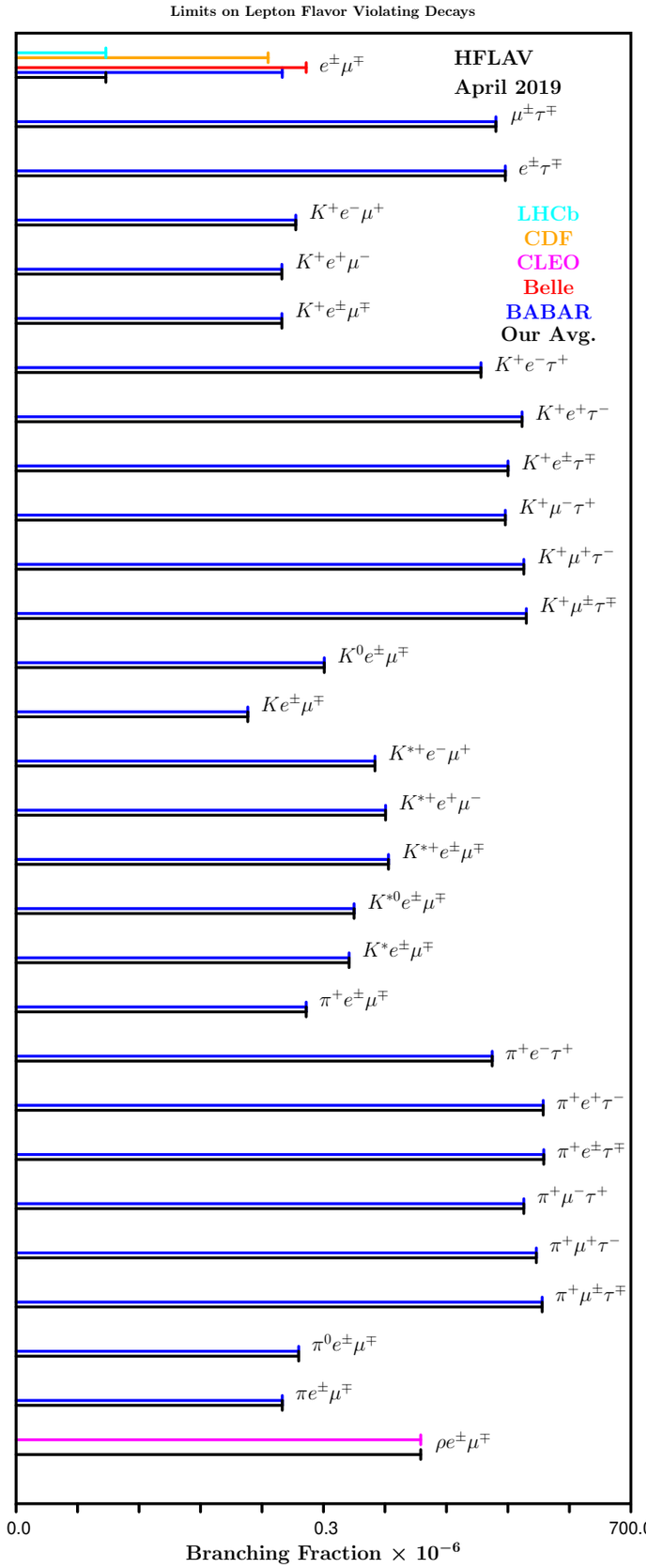

TABLES

Branching fractions of charmless semileptonic B^+ decays to LFV and LNV final states (part 1)

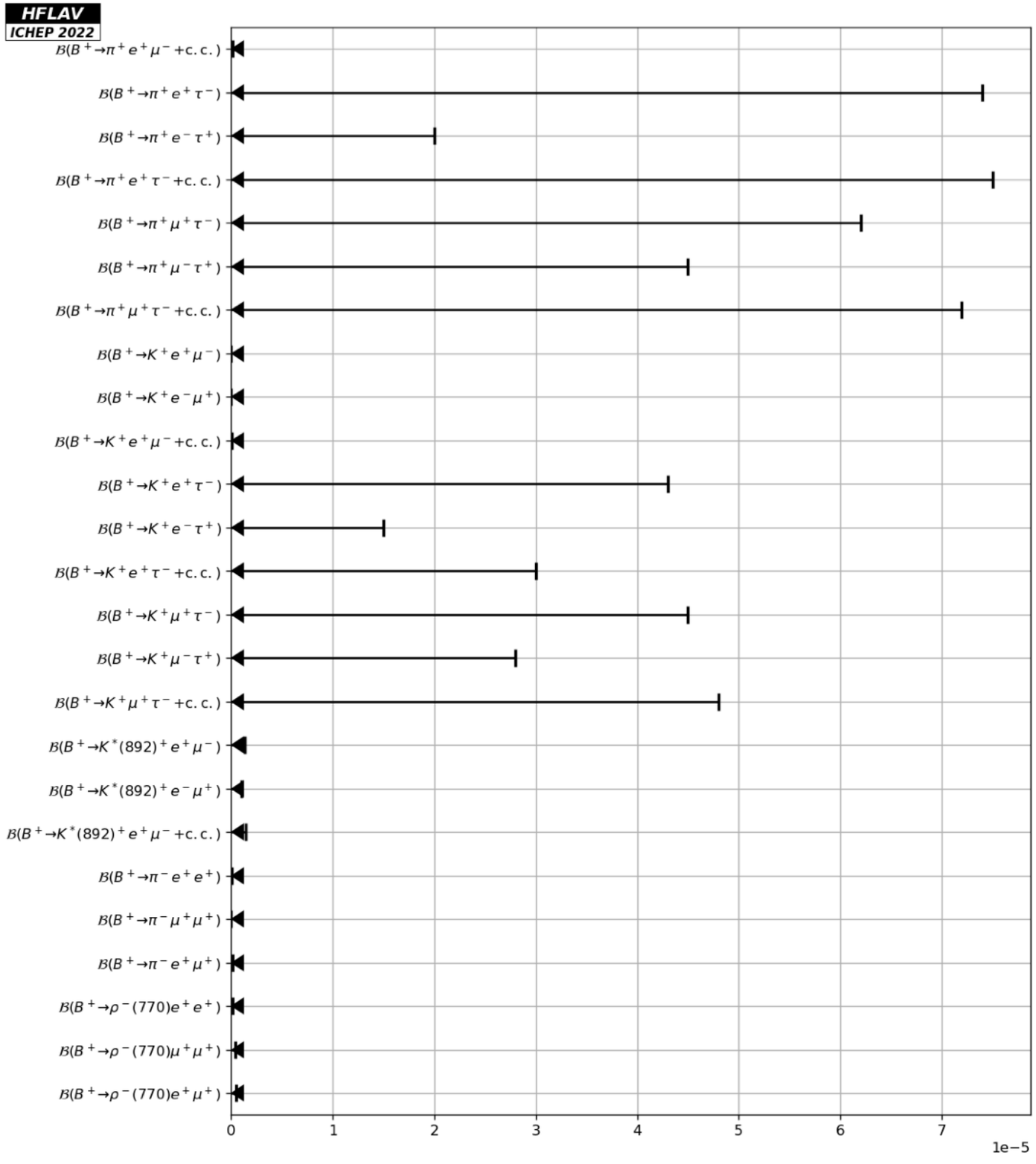

TABLES

Branching fractions of charmless semileptonic B^+ decays to LFV and LNV final states (part 2)

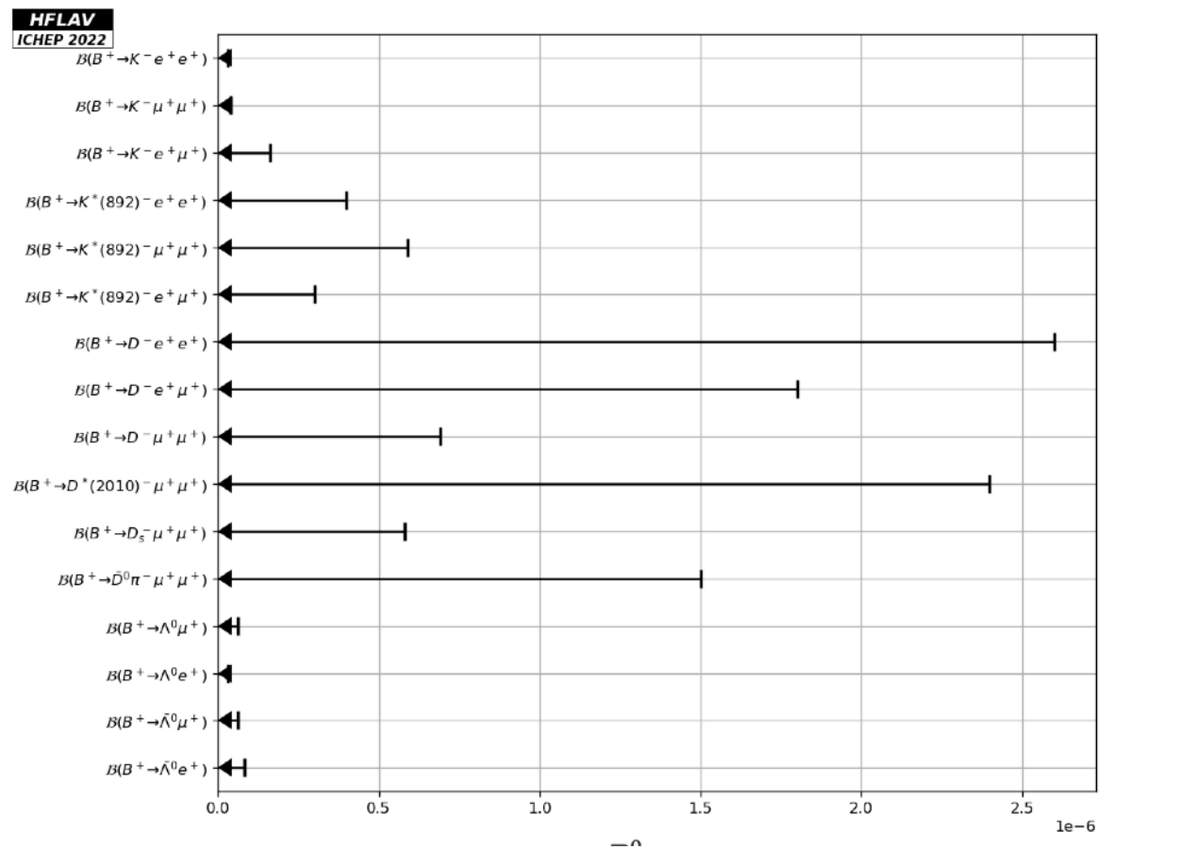

Branching fractions of charmless semileptonic B^0 decays to LFV and LNV final states

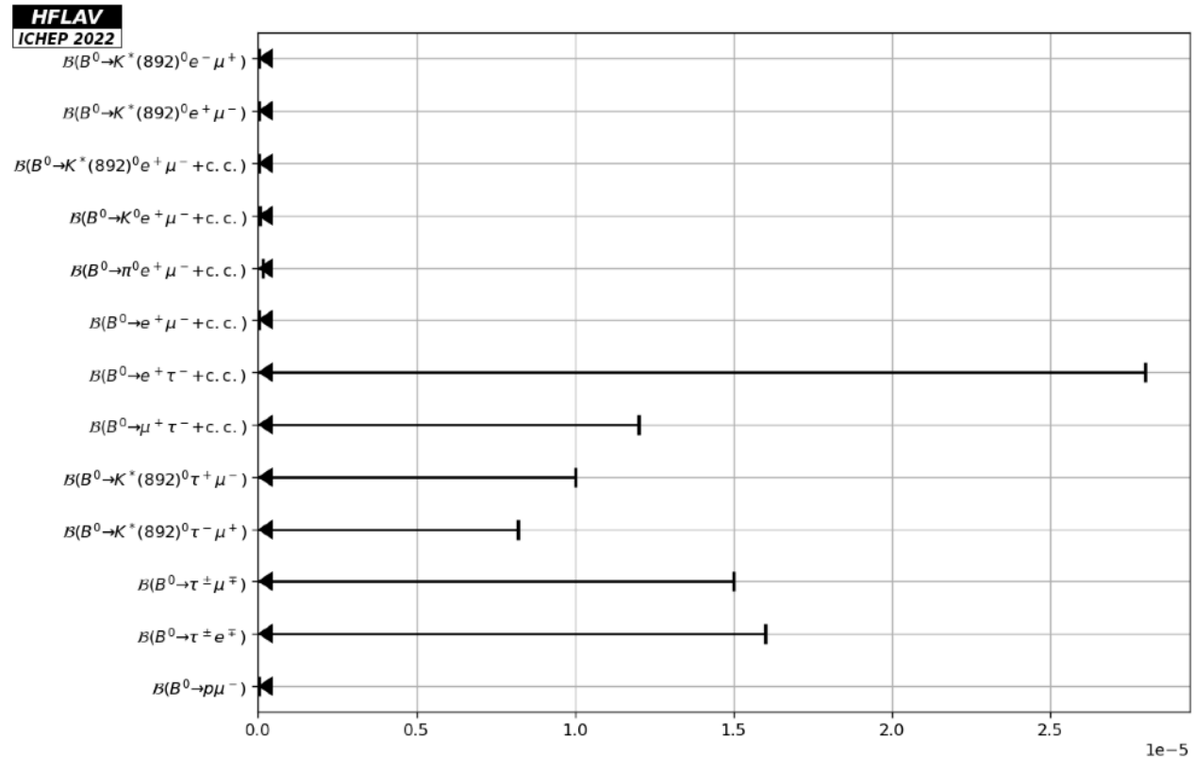

SHAPE VARIABLES FOR CONTINUUM SUPPRESSION

Variables related to the B meson direction: the spin-1 $\Upsilon(4S)$ decaying into two spin-0 B mesons results in a $\sin^2\theta_B$ angular distribution with respect to the beam axis; in contrast for $e^+e^- \to f\bar{f}$ events, the spin-1/2 fermions f, and its two resulting jets, are distributed following a $1 + \cos^2\theta_B$ distribution. Using the angle θ_B between the reconstructed momentum of the B candidate (computed in the Υ (4S) reference frame) and the beam axis, the variable $\mathbf{|\cos\theta_B|}$ allows one to discriminate between signal B decays and the B candidates from continuum background.

The **Fox-Wolfram moments**: for a collection of N particles with momenta p_i, the k-th order Fox-Wolfram moment H_k is defined as

$$H_k = \sum_{i,j}^{n} |\vec{p}_i||\vec{p}_j| P_k(\cos\theta_{ij})$$

where θ_{ij} is the angle between p_i and p_j, and P_k is the k-th order Legendre polynomial. Notice that in the limit of vanishing particle masses, $H_0 = 1$; that is why the normalized ratio $R_k = H_k/H_0$ is often used, so that for events with two strongly collimated jets, R_k takes values close to zero (one) for odd (even) values of k. These sharp signatures provide a convenient discrimination between events with different topologies.

$$R_n = \frac{H_n}{H_0}$$

Thrust: for a collection of N momenta p_i ($i = 1,\cdots N$), the thrust axis T is defined as the unit vector along which their total projection is maximal; the thrust scalar T (or thrust) is a derived quantity defined as

$$T = \frac{\sum_{i=1}^{N} |\vec{T} \cdot \vec{p}_i|}{\sum_{i=1}^{N} |\vec{p}_i|}$$

For a BB event, both B mesons are produced almost at rest in the $\Upsilon(4S)$ rest frame, so their decay particles are isotropically distributed, their thrust axes are randomly distributed, and thus $|\cos\theta_T|$ follows a uniform distribution in the range [0,1]. In contrast for $q\bar{q}$ events, the momenta of particles follow the direction of the jets in the event, and as a consequence the thrusts of both the B candidate and the ROE are strongly directional and collimated, yielding a $|\cos\theta_T|$ distribution strongly peaked at large values.

Cleo Cones: Set of nine variables corresponding to the momentum flow around the thrust axis of the B candidate, binned in nine cones of 10° around the thrust axis as illustrated

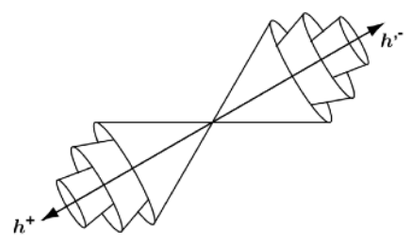

EXCLUSIVE $b \to d\gamma$: $B^0 \to K^0_S K^0_S \gamma$

PhysRevD.106.012006

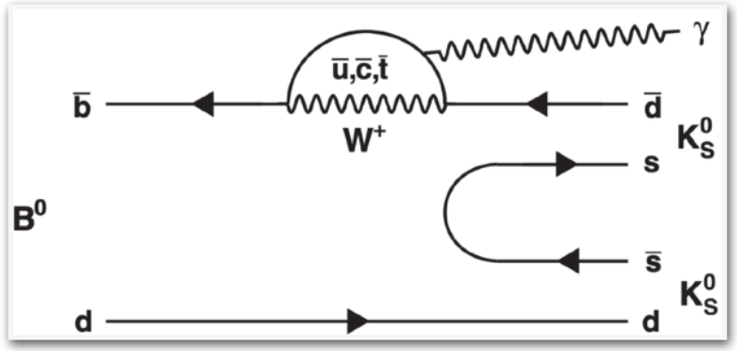

- First search, $b \to d\gamma$ only probed through $B \to \rho/\omega\gamma$
- $K^0_S K^0_S$ production can occur via tensor states
- Yields extracted with M_{bc} fit
- Total BF and 'partial' BF in 10 m_{KK} bins

5.8×10^{-7} @ 90 % CL

$m_{KK} \in (1.0, 3.0)\,\mathrm{GeV}/c^2$

Mass bin (GeV/c^2)	ϵ_S (%)	N_{bkg}	σ_{sys} (%)	N_{obs}	S_{90}	U.L. (10^{-7})
1.0–1.2	3.3	0.8 ± 0.3	3.2	0	1.8	0.7
1.2–1.4	3.0	0.9 ± 0.3	3.2	3	6.5	2.8
1.4–1.6	2.7	0.8 ± 0.3	3.2	1	3.6	1.7
1.6–1.8	2.5	0.3 ± 0.1	3.2	0	2.1	1.1
1.8–2.0	2.3	0.8 ± 0.3	3.2	2	5.1	2.9
2.0–2.2	2.2	0.2 ± 0.1	3.2	1	4.2	2.5
2.2–2.4	2.2	0.4 ± 0.2	3.2	1	3.9	2.4
2.4–2.6	2.2	0.2 ± 0.2	3.2	0	2.2	1.3
2.6–2.8	2.3	0.0 ± 0.0	3.2	1	4.2	2.3
2.8–3.0	2.4	0.1 ± 0.0	3.2	0	2.3	1.2

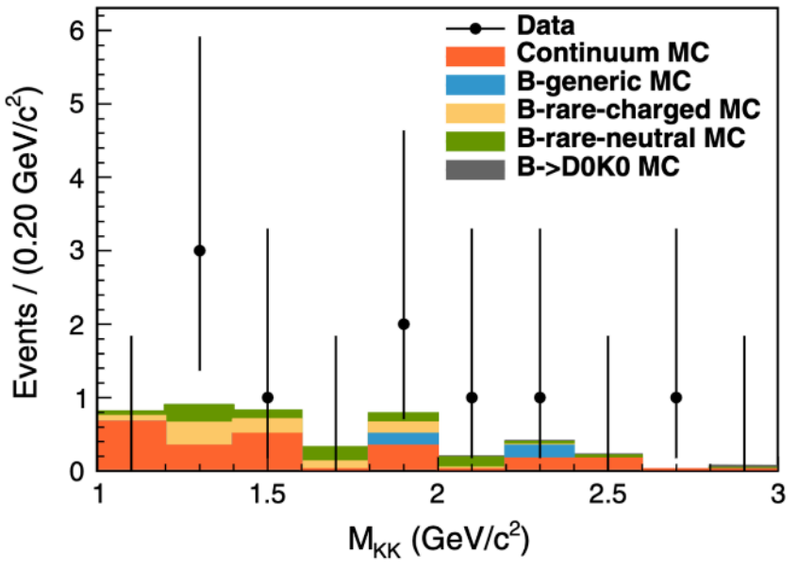

Branching fraction product	$\epsilon_S(\%)$	N_{bkg}	$\sigma_{sys}(\%)$	N_{obs}	S_{90}	U.L.(10^{-7})
$B^0 \to f_2(1270)(\to K^0_S K^0_S)\gamma$	2.3	1.8 ± 0.4	3.1	3	5.7	3.1
$B^0 \to f'_2(1525)(\to K^0_S K^0_S)\gamma$	2.2	0.8 ± 0.3	3.1	1	3.6	2.1

$m_{KK} \in (1.00, 1.44)\,\mathrm{GeV}/c^2$

$m_{KK} \in (1.44, 1.63)\,\mathrm{GeV}/c^2$